COMPUTER-ASSISTED GENERATION AND CURATION OF GENOME-SCALE METABOLIC MODELS WITH CASE STUDIES IN THE METHANOGEN GENUS METHANOSARCINA

BY

MATTHEW NICHOLAS BENEDICT

DISSERTATION

Submitted in partial fulfillment of the requirements
for the degree of Doctor of Philosophy in Chemical Engineering
in the Graduate College of the
University of Illinois at Urbana-Champaign, 2014

Urbana, Illinois

Doctoral Committee:

Associate Professor Nathan D. Price, Chair, Institute for Systems Biology
Professor William W. Metcalf
Professor Huimin Zhao
Associate Professor Christopher V. Rao

Abstract

Methanogenic archaea, organisms that make methane as a byproduct of their metabolism, play a critical role in the global carbon cycle and have potential as a source of renewable biofuels. As a result, there has been a great deal of interest in understanding how methanogenesis works. A wide array of tools has been developed for studying methanogen metabolism, including genetic manipulation tools and efficient culturing techniques. These tools are especially well developed in model methanogens such as *Methanococcus maripaludis*, *Methanosarcina acetivorans* and *Methanosarcina barkeri*. *Methanosarcina* species are particularly attractive model organisms for methanogenesis due to their wide substrate utilization capabilities (compared to other methanogens): the diversity in metabolic capabilities for these organisms enables manipulations of methanogenesis pathways that would be lethal in other methanogens. Genetic manipulation tools have been valuable for identifying functions of individual enzymes and pathways in these organisms, but more holistic methods are needed in order to understand how these work together to accomplish observed phenotypes.

Genome-scale metabolic networks allow researchers to put information on individual parts of metabolism together in a way that is useful for making novel insights. For my first Ph.D. project, I built and carefully curated a genome-scale metabolic network for *Methanosarcina acetivorans* and used constraint-based analysis tools to build a quantitative model based on that network. I then used the model to make predictions about how *M. acetivorans* utilizes carbon monoxide and the impact of the soluble heterodisulfide reductase HdrABC on its metabolic activity.

While highly-curated metabolic networks are useful for studying metabolic phenotypes, the process of building them is not scalable. A genome-scale metabolic network for a single organism can take months to years to curate using the established protocols. One key reason for the lack of scalability of this process is a dearth of adequate tools to aid users in evaluating annotations and gene calls that form a bedrock for the automated generation of draft networks. The main focus of my Ph.D. has been the development of two software packages to improve the scalability of generating and curating genome-scale metabolic networks. One of these software packages, likelihood-based gap filling, uses annotation likelihood estimates for alternative gene annotations to identify pathways to fill gaps in metabolic networks that are maximally consistent with available genomic data. The other package, ITEP (Integrated Toolkit for Exploration of metabolic Pan-genomes), is a set of tools for curating and studying

patterns in gains and losses of genes across groups of related organisms. In this dissertation, I describe how these tools can be used to build and to assess the quality of different parts of metabolic networks.

As my final project, I have developed a new method of combining comparative genomics (using ITEP) with metabolic modeling to expose errors in both genomes and metabolic networks. I applied this method to 30 species in the genus *Methanosarcina*, 27 of which were newly sequenced, and demonstrated specific examples of these errors and possible ways to address them. The approach I developed makes certain classes of errors readily apparent that are not obvious when only examining individual organisms.

Acknowledgements

I would first and foremost like to thank all of the members of my family for their consistent support of my decision to pursue a Ph.D. and continuing encouragement throughout the process. Thanks also to my wonderful girlfriend Meng Sun (孙梦) for showing me the meaning of devotion, opening my eyes to a whole new world, and always keeping a positive perspective even when my own has wavered. I couldn't have done this without you.

I am deeply indebted to a lot of friends here at UIUC for too many things to list. Special thanks for Nicholas Chia for working closely with me and teaching me most of what I know about Linux and bioinformatics and for being incredibly supportive. Special thanks also to Ahmet Badur for always believing in me and for lots of good times. Thanks also to my prior roommates for many memories in the old house on Illinois street: Shuyi Ma, Kristine Pangan-okimoto, Josh and Ritika Tice, and Samantha Weiss. Thanks to Dawn Eriksen for convincing me to come here ☺. Thanks to my Chinese and Taiwanese friends for your support and putting up with (and even encouraging!) my 不好中文: Wan-ting Chen, Mei-hsiu Lai, Qidi Sun, Chunjing Wang, Yuliang Wang, Su Xiao, Wanwan Yang, Yuanchang Zhou, Peiyun Zhou, and others who have moved on to greener pastures or taller cities.

Thanks also go out to my friends back in Connecticut, especially Katie Bowers, without whose encouragement I would certainly not have applied to graduate school, and Bryne Botticelli, who has been a lifelong friend.

Thank you to Nathan Price, William Metcalf, Christopher Rao and Huimin Zhao for taking the time to serve on my prelim and defense committee. Your time investment is greatly appreciated.

Thank you to Nathan Price for being a very patient and understanding advisor. Thanks to him, I have had the opportunity to interact with a truly world-class body of scientists. In addition to Nathan, I am deeply indebted to numerous collaborators for help with scoping, implementing and interpreting the results of the projects in this dissertation. In no particular order, thanks to James Henriksen, Petra Kohler, Judy Luke, William Metcalf, Sarah Reinhart, Rachel Whitaker, and Nick Youngblut for working with me on methanogens and comparative genomics. Thanks to Scott Devoid and Chris Henry at Argonne National Labs and to Mike Mundy and Nicholas Chia at the Mayo Clinic for working with me on the KBase-related

projects and for many interesting discussions on modeling. Thanks to Gary Olsen at UIUC and to Jim Davis, Ross Overbeek, and Fangfang Xia at Argonne National Labs for inviting me to join in on numerous interesting discussions on annotation improvement and software development. Thanks to John Cole and Zan Luthey-Schulten for help with visualization efforts and scientific discussions.

Thanks to the entire Price lab for being such an awesome group of people. I am especially indebted to Caroline Milne, James Eddy, Matt Gonnerman, Matt Richards, and Shuyi Ma for working with me on the projects in this dissertation, putting up with my badgering over Gchat, and reading over and editing manuscripts, proposals, posters and presentations. Additional special thanks go to Chunjing Wang and Caroline Milne for extensive moral support.

I'm truly grateful to the staff of the Department of Chemical and Biomolecular Engineering and the Institute for Genomic Biology at UIUC, who have consistently supported me despite having plenty of opportunity not to in the last few years of my time here. I especially want to thank Christine Bowser, Kay Moran , Cathy Paceley, and Debbie Piper for helping with countless administrative issues over the years. Thanks also to Theresa Fitzgerald at ISB for her help with similar issues there.

Last and certainly not least, thank you to Carl Woese for highly enlightening discussions on the nature of evolution and for being an awesome person. We all miss you.

Table of contents

Chapter 1: Introduction

Methanogenesis and methanogens

Methanogens are strictly anaerobic archaea that generate methane as their primary metabolic byproduct. It has been estimated that $5x10^{14}$ g of methane is released into the atmosphere each year by the action of methanogenesis [1], which represents about 4% of the total annual global carbon circulation [2]. Methane is a potent greenhouse gas with 25 times the potency of carbon dioxide [3], contributing about 20% of the annual radiative forces of anthropomorphically-sourced greenhouse gasses in the atmosphere [4], and methanogenesis is the chief mechanism by which this methane is emitted into the atmosphere [5]. Therefore, it is of great interest to understand methanogenesis and the potential responses of methanogens to global warming. Methanogens play a critical role in the global carbon cycle, metabolizing the waste products of other organisms such as acetogenic bacteria. The metabolism of these waste products keeps their concentration low, allowing the metabolic pathways of these other organisms to remain thermodynamically feasible [6].

Methanogens are a metabolically, physiologically, and phylogenetically diverse collection of organisms, all of which fall into the domain Archaea. Methanogens have adapted to life in a wide range of temperatures, salt concentrations, and levels of substrate availability [2] in which they coexist with other organisms such as sulfate reducers [7, 8], nitrate reducers and iron reducing organisms [9]. Different groups of methanogens have adapted to utilize different substrates [10] and have vastly different pathways for utilization of the same substrates [2]. These pathway differences have implications for the survival strategies and ecological roles of these groups: some organisms grow more slowly but require less substrate for survival, while others grow more quickly but have greater growth requirements [2] .

There are at least three major phylogenetically coherent classes of methanogens: the group I methanogens, the group II methanogens (Methanomicrobiales) and the group III methanogens (Methanosarcinales) [11]. Each of these classes has divergent energy conservation pathways and substrate utilization capabilities [11].

The group I methanogens include *Methanococcus maripalidus* and *Methanocaldococcus jannaschii*, two key model methanogens from which genetic manipulation techniques have been developed and from which many archaeal-specific pathways have been deduced [12]. Most group I methanogens grow by reducing CO_2 with molecular hydrogen, although some (such as *M. maripalidus*) can also grow using formate as an electron donor instead of hydrogen [13]. The *Methanosphaera* are an exception: they are only capable of growing by reducing methanol with H_2 to make ATP and assimilating acetate as a source of carbon for anabolic functions [14].

The group II methanogens (Methanomicrobiales) are relatively poorly studied but they include *Methanofollis ethanolicus* [15], which grows by using ethanol as an electron donor, *Methanogenium organiphilum* [16], which grows on 2-propanol and other secondary alcohols as electron donors, and several other species that can grow on $H_2\backslash CO_2$ or formate.

The group III methanogens (Methanosarcinales) contain the only organisms in the methanogens that are capable of growth on acetate as a sole carbon and energy source and the only ones that use cytochromes in their energy conservation pathways [2]. It has been argued that the use of cytochromes has enabled the Methanosarcinales to occupy ecological niches separate from the group I and group II methanogens, even when growing on the same substrates (e.g. H_2/CO_2 or methanol+H_2) because the energy conservation mechanisms are more efficient [2]. The Methanosarcinales contain the genus *Methanosarcina*, whose members have the greatest substrate utilization diversity of any known methanogens. The *Methanosarcina* genus has members that are capable of growth on acetate, methanol, methylamines, methylsulfides, or H_2. However, not all of the *Methanosarcina* are capable of growth on hydrogen [17] and at least one has been experimentally proven to lack hydrogenase activity [18].

Genetic manipulation techniques have been developed for several model methanogen species, including *Methanosarcina acetivorans* [19-21], *Methanosarcina barkeri* [21, 22], and *Methanococcus maripalidus* [23]. The ability to delete, insert, and manipulate the expression of targeted genes in these organisms has enabled researchers to determine the function of many novel genes in methanogenesis and has helped elucidate the interactions between them [21]. In addition, genetic manipulation has been and will continue to be instrumental in engineering novel methanogen strains. In the first published example of an effort to rationally engineer a novel methanogenic pathway, Lessner *et al.* developed novel

Methanosarcina strains that are able to grow on methyl acetate and methyl propionate, two substrates which are not utilized by wild-type strains [24].

Genome-scale modeling

Genome-scale network modeling has emerged as a powerful tool for integration and interpretation of diverse data sets such as genetic, proteomic, and transcriptomic data [25]. Genome-scale models have been applied to understand disease mechanisms [26], discover novel drug targets [27-29], and guide the design of robust strains that optimize production of industrially useful compounds such as ethanol and butanol [30, 31]. Genome-scale network models are especially useful for strain design when combined with genetic manipulation tools such as the ability to add and delete genes.

Genome-scale network models are dependent on the generation of interaction networks between cellular components such as metabolites, proteins, and RNAs. Such networks can be generated using a variety of approaches, including by statistical inference from high-throughput data ("top-down"), and by collection of individually supported nodes and edges into a cohesive whole ("bottom-up") [32]. Many successful approaches have combined data of different types, using the well-supported metabolic networks (which are reconstructed from the bottom up) as a scaffold on which to interpret other data such as transcription data [27, 33, 34], proteomic data [35] or metabolomics data [36].

Constraint-based analysis techniques such as flux balance analysis (FBA) [37] are one way to make quantitative predictions based on the physical and physiological constraints implied by reconstructed metabolic networks and experimental data. FBA is an optimization technique that seeks to identify sets of reaction rates (or "fluxes") that maximize a presumed cellular objective, such as maximization of growth rate. The objective is maximized subject to physical constraints - such as mass and energy conservation - and constraints imposed by the cell upon itself such as regulatory constraints. Additional constraints can be imposed on reaction rates based on biochemical knowledge such as measurements of metabolite concentrations, transcript abundance, or protein abundance, which allows one to draw conclusions about the implied effects of differences in these quantities on cellular metabolism.

There are many different choices for cellular objectives, and it has been found that the most accurate objective function varies depending on the growth conditions [38]. In order to ensure sufficient

completeness of the network and to simulate conditions of maximum growth potential, it is common to construct a "biomass equation" which is a sink of essential metabolites generated by the cell in pre-defined proportions, and then maximize that subject to physical and biological constraints [39]. Other common objectives include maximization of ATP yield or minimization of total flux through all reactions in the cell [38].

The existence of such tools and of whole-genome sequences for model *Methanosarcina* species and the usefulness of these organisms as models of methanogenesis has motivated the generation of genome-scale metabolic models for these species. In **Chapter 2** of this thesis, I describe the development, curation and applications of a genome-scale metabolic network model for the methanogen *Methanosarcina acetivorans* [40]**,** a *Methanosarcina* species that lacks hydrogenases. A second model was concurrently developed for *M. barkeri* [41]*,* a hydrogenase-dependent *Methanosarcina* species. Therefore, there are now highly-accurate genome-scale metabolic networks and models for both of the major metabolic subtypes in the *Methanosarcina* genus.

Automated reconstruction of genome-scale metabolic networks

Genome-scale metabolic models have been constructed and manually curated for over 50 organisms [42]. Manual curation is used to check and correct gene functional annotations, to ensure that the resulting metabolic network reflects available biochemical knowledge as accurately as possible, and to reconcile differences between simulations and experimental data (**Figure 1.1**) [43]. Extensive manual curation is necessary to obtain accurate models, in part because of the prevalence of missing, inaccurate, or ambiguous functional annotations for genes [43]. As a result, the model-building process is time- and labor-intensive, often taking months or even years to complete [43]. Clearly, at the current pace, model building cannot keep up with the recent surge in availability of whole genome sequences.

To accelerate the rate of discoveries possible using these models and to keep pace with the rapid proliferation of available whole-genome sequences, it is necessary to improve the quality of the automatically generated basis models used as a starting point for manual reconstruction and also to improve metrics for the quality of reconstructed networks. Important advances towards the former goal have included the development of curated databases of biochemical and genetic information [44] and

the design of algorithms to improve network structure and suggest resolutions for discrepancies between predicted and experimental data [45]. Importantly, frameworks have been designed to integrate biochemical data with network-building algorithms, automating the process of building a draft metabolic network [46]. Towards the latter goal, methods have been developed to estimate the likelihood that an annotation is correct given the level of sequence homology to other genes with similar function, conservation of gene neighborhoods and consistency of regulatory patterns, among other lines of evidence [47].

In **Chapter 3** of this thesis, I describe an algorithm that ties together these two approaches, linking likelihood estimates for gene function with the automated generation of network models from a high-quality biochemical database. My method both provides solutions that maximize the consistency of gap filling solutions with available genetic evidence and presents users with an interpretable metric of the quality of evidence for inclusion of each gap filled reaction. The algorithm has been implemented as part of the DOE KnowledgeBase framework, permitting ready access to users anywhere in the world.

High-throughput genomics and pan-genomes

Due to the advancement of nucleotide sequencing technology, the cost of whole-genome sequencing has fallen substantially since the advent of the genomic era, to the point where it will soon be possible to sequence a human genome for less than a thousand dollars [48]. Complete genome sequences are now publicly available for thousands of bacteria and archaea, including at least 50 methanogens across all three classes[1]. Complementing the increased accessibility of whole-genome sequencing, there has been increased interest in the study of collections of closely-related organisms and the analysis of the full complement of genes in a species, the sum of which is called a "pan-genome". A pan-genome analysis typically includes an assessment of the portions of the species' genomes that are well-conserved ("core") and those that are not conserved ("variable") [49]. Studying patterns in the distribution of variable genes has led to insight on potential genetic underpinnings of observed differences in the biology of different strains. For example, studying variable gene sets in *Escherichia coli* [50], *Salmonella enterica* [51] and the genus *Yersinia* [52] has led to the discovery of pathovar-specific pathogenicity islands and virulence factors. Similar studies in species *Lactobacillus delbrueckii* have

[1] There were 50 complete genome sequences for methanogens in Genbank as of 01-03-2014

identified unique genetic features of the industrial strain *L. delbrueckii* subsp. *bulgaricus* that could be responsible for its exceptional usefulness in yogurt production [53].

With an expansion of available pan-genomic datasets has come a corresponding increase in the available software tools with which to analyze these datasets. Numerous web interfaces [47, 54-56] and desktop software tools [57-59] have been developed for comparative genomics. Software tools have also been developed to tackle the specific problems related to analysis of pan-genomes, such as the identification and functional analysis of core and variable gene sets [60-63] phylogenetic analysis [59, 64], curation of genomes and gene calls [65], and comparison of different orthologous group prediction methods [66]. Unfortunately, no tool was yet available to tie these aspects together these in a flexible way. I designed a software suite, ITEP (Integrated Toolkit for Exploration of microbial Pan-genomes), with these goals in mind. ITEP is described in **Chapter 4** of this thesis.

To tie these efforts back to the methanogen work, I have used ITEP to identify differences in metabolic genes between *Methanosarcina acetivorans*, *M. barkeri* (two strains which have genome-scale metabolic models) and 28 other strains of *Methanosarcina*. By combining comparative genomics and predictions from metabolic modeling, I was able to identify and in some cases fix errors in either the models or in gene calls (missing genes). This work is described in **Chapter 5**.

Research objectives and dissertation overview

The overarching objectives of my thesis were: 1) to build an accurate genome-scale model of a model methanogen, 2) to build tools for comparative genomics and automatic generation of high-quality genome-scale metabolic models, and 3) to apply these tools to study the metabolic capabilities of relatives of the reference methanogens and improve the quality of the metabolic network reconstruction. The chapters in this thesis, addressing these objectives, are organized as follows:

- **Chapter 2** discusses the reconstruction and manual curation of the model methanogen *Methanosarcina acetivorans* C2A and the use of this model to make novel metabolic insights.
- **Chapter 3** discusses the design and implementation of an algorithm to estimate annotation likelihoods and use these estimates to optimally fill gaps in draft metabolic models.

- **Chapter 4** discusses the design and applications of a new software toolkit, ITEP (Integrated Toolkit for the Exploration of Pan-genomes), that makes it easy to perform pan-genomic analysis such as the study of gene gain and loss patterns, compare and contrast results of different clustering methods, and design pipelines for further analysis and curation of these results.

- **Chapter 5** discusses the use of ITEP's comparative genomics capabilities to find and suggest fixes for inconsistencies between gene gain and loss patterns and metabolic model predictions in the genus *Methanosarcina*.

- Finally, **Chapter 6** discusses how this work fits into the greater scheme of metabolic modeling and where I believe both this work and the field in general are heading.

Figures and tables

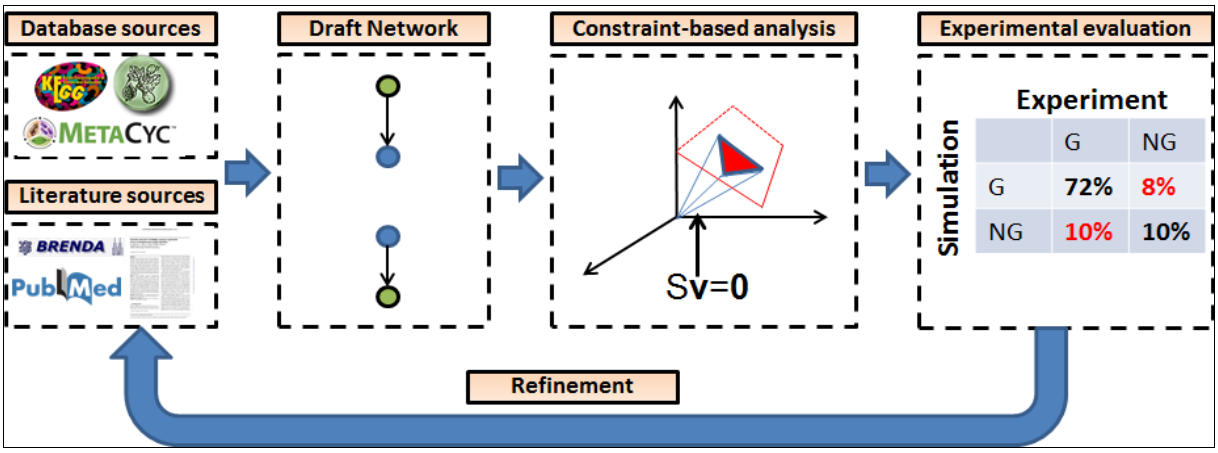

Figure 1.1. General schematic of the metabolic reconstruction process. Metabolic reconstruction generally involves five major steps which are performed iteratively to maximize consistency with known physiology. A draft network is first generated using automated methods from online biochemical and genetic databases. Then, simulation techniques such as flux balance analysis are used to test the consistency with experimental data. In general, the draft network will be too incomplete to perform effective simulations, so it is necessary to iteratively identify and fill gaps in the network using automated tools and literature searches as a guide. The network is refined until it reflects available experimental data as well as possible (such as growth/no growth data under various perturbations, as shown here).

Chapter 2: Genome-scale metabolic reconstruction and hypothesis testing in the methanogenic archaeon *Methanosarcina acetivorans* C2A[2]

Abstract

Methanosarcina acetivorans strain C2A is a marine methanogenic archaeon notable for its substrate utilization, genetic tractability, and novel energy conservation mechanisms. To help probe the phenotypic implications of this organism's unique metabolism, we have constructed and manually curated a genome-scale metabolic model of *M. acetivorans*, iMB745, which accounts for 745 of the 4540 predicted protein coding genes (16%) in the *M. acetivorans* genome. The reconstruction effort has identified key knowledge gaps and differences in peripheral and central metabolism between methanogenic species. Using flux balance analysis, the model quantitatively predicts wild type phenotypes and is 96% accurate in knockout lethality predictions compared to currently available experimental data. The model was used to probe the mechanisms and energetics of byproduct formation and growth on carbon monoxide, and the nature of the reaction catalyzed by the soluble heterodisulfide reductase HdrABC in *M. acetivorans.* The genome-scale model provides quantitative and qualitative hypotheses that can be used to help iteratively guide additional experiments to further the state of knowledge about methanogenesis.

Introduction

Methanogenic archaea are unique in their ability to grow on low energy substrates such as acetic acid by converting them into methane and other byproducts. Methanogens are a critical part of the global carbon cycle, consuming byproducts of other natural bioprocesses that would otherwise be recalcitrant in sulfate poor, anaerobic environments [67]. They also play an important role in global warming, since methane is a greenhouse gas twenty times as potent as carbon dioxide [68] and methanogenesis is the primary mechanism for methane emission into the atmosphere [5].

[2] This chapter uses previously published material and is reprinted with the permission of the publisher. The citation is as follows:

Benedict MN, Gonnerman MC, Metcalf WW, Price ND: **Genome-Scale Metabolic Reconstruction and Hypothesis Testing in the Methanogenic Archaeon *Methanosarcina acetivorans* C2A**. *J Bacteriol* 2012, **194**(4):855-865.

Methanosarcina is the only known genus of methanogens with members that can utilize all of the known methanogenic pathways (acetoclastic, methylotrophic, hydrogenotrophic, and methyl reduction) [69]. This metabolic diversity makes these species relatively permissive to metabolic and genetic manipulations compared to other methanogens. To help capitalize on this, the genomes of three *Methanosarcina* species have been sequenced [70-72]. In addition, genetic tools have been developed for several of these species, including methods for directed mutagenesis and regulated expression of specific genes [19, 24, 73, 74].

The constraint-based reconstruction and analysis (COBRA) strategy is a powerful paradigm for consolidating large amounts of metabolic knowledge and synthesizing that knowledge into quantitative phenotypic predictions [32, 75]. To perform constraint-based analysis on an individual organism, its metabolic network is reconstructed from the bottom up, beginning with a sequenced and annotated genome and ending with a network of reactions and reaction-gene associations that directly link genotype and phenotype. Many metabolic reconstructions have been curated by hand and used to make useful predictions such as identification of putative drug targets and the design of novel strains for enhanced biofuel production [43, 75].

In recent years, there have been major advances towards automating much of the reconstruction process [46]. Automation is needed to continue the exponential increase in the number of genome-scale metabolic models [30, 75]. However, automated reconstructions for methanogens are still particularly problematic for three major reasons: 1) automated predictions tend to be overly homogenized due to their strong reliance on homology-based methods; 2) reaction and gene databases have a more limited coverage of archaea than the other domains of life, and 3) the energy conservation mechanisms of methanogens are highly specialized [10]. Hence, manual curation is necessary to obtain reliable predictions from metabolic models of these organisms.

Amongst methanogens, *M. acetivorans* is notable for its substrate utilization. It can grow and produce methane using methylated substrates, carbon monoxide or acetate, but it cannot grow with hydrogen as its primary energy source [17]. Also, unlike most methanogens, *M. acetivorans* is genetically tractable. Therefore, this organism offers opportunities to learn about novel energy conservation mechanisms.

An independent reconstruction for *M. acetivorans* strain C2A has recently been reported [76]. The previously reported reconstruction was primarily curated using an automated curation pipeline including the GapFind, GapFill, and GrowMatch algorithms [77, 78]. Herein we present iMB745, an extensively curated manual reconstruction that differs significantly from the other published model. As many literature sources as available were integrated to generate a highly accurate list of metabolic reactions, making this reconstruction a valuable knowledge base for this organism. In addition, curation has enabled us to make quantitative phenotypic predictions using constraint-based modeling. We demonstrate the usefulness of this model to probe hypotheses for the workings of incompletely understood parts of the *M. acetivorans* metabolic network. The analysis thus represents a successful application of the hypothesis-driven modeling approach.

Methods

Model Reconstruction

An initial list of potential reaction-gene associations in *Methanosarcina acetivorans* str. C2A was generated based on a union of data in the Kyoto Encyclopedia of Genes and Genomes (KEGG) [79], MetaCyc [80], the Model SEED reconstruction [46], the Transport Protein Analysis Database (TransportDB) [81], and UniProt [82]. Reactions from the existing *Methanosarcina barkeri* str. Fusaro reconstruction [83] and the BiGG database [84] were added if there was sufficient evidence for their inclusion, based on sequence homology and/or literature-based curation, or to fill gaps in the annotation. Some gene suggestions from EFICAZ, which includes evidence from other bioinformatics tools like PFAM, were also incorporated [85]. Gene associations were verified whenever possible using bidirectional BLASTP against archaeal protein products with experimentally verified functions [86]. In case of conflicts, metabolic functions suggested from literature were chosen over those suggested in the databases, and inconsistent reactions were removed from the model (see supplemental material for a comprehensive list).

Reaction and metabolite nomenclature consistent with the BiGG database was utilized whenever possible to facilitate comparison to existing manually curated metabolic models [84]. Reactions and metabolites without BiGG identifiers were assigned abbreviations in a similar manner to those present in the database (see supplemental material for a complete list).

Logical gene protein reaction (GPR) relationships were constructed manually based on literature or database evidence. For example, genes annotated or characterized to be separate subunits of a complex were given an "AND" relationship. If there was no evidence of a protein complex catalyzing a reaction with multiple genes, the genes were all assigned an OR relationship.

All intracellular and transport reactions were computationally mass and charge balanced at a pH of 7 based on charges and formulas computed with ACD/Labs software (Version 12; Advanced Chemistry Development, Inc.). Charges and formulas are available in the supplemental material.

Construction of the Biomass Reaction

The biomass reaction is a sink on essential cell components that represents the consumption of molecular building blocks (such as amino acids and nucleotides) required for cell division. The biomass reaction for *Methanosarcina acetivorans* str. C2A was modified from the closest relative for which a biomass reaction had previously been built, *Methanosarcina barkeri* str. Fusaro [83]. This biomass objective function was first expanded by incorporating more detailed carbohydrate data from *M. barkeri* [87] and adding methanofuran-B to the list of required cofactors [88] . Then, coefficients for lipids were modified based on available data on the unique lipid composition of *M. acetivorans* [89]. Nucleotide and amino acid coefficients specific to *M. acetivorans* were calculated based the published genome sequence according to established procedures [43]. The coefficients of compounds in the soluble pool were assumed to be the same as those in the *M. barkeri* biomass equation.

Flux Balance Analysis (FBA)

Exponential growth phenotypes were predicted using flux balance analysis (FBA), which has been previously reviewed [37]. Briefly, all reactions in the model were represented in a stoichiometric matrix, **S**, in which each column represented a reaction and each row a metabolite. Hence, the entry (*i,j*) of **S** contained the stoichiometric coefficient of metabolite *i* in reaction *j*. If metabolite concentrations are assumed to be constant (steady state), conservation of mass requires that:

$$\mathbf{S}v = 0$$

where v is the vector of reaction fluxes (reaction rates). Because there were more reactions than metabolites in the model (as is typical), multiple possible flux distributions were possible that all satisfied the mass balance.

Reaction fluxes were also constrained by setting minimum and maximum fluxes. In the current study, the reversibility of each reaction was determined based on literature, database evidence, and thermodynamic calculations. The flux through reversible reactions was unconstrained, while that of irreversible reactions was set to have a $\mathbf{v}_{min}$=0. Substrate uptake rates were set to experimentally measured values for purposes of simulations (see supplemental material for values and references). The reaction rate through the non-growth associated ATP maintenance reaction (ATPM) was set to 2.5 mmol/gDW/hr to account for upkeep energy costs. This value is somewhat lower than the experimental value of 8.39 mmol/gDW/hr used in the current *E. coli* model, and larger than that in the published *M. barkeri* model [83]. Growth-associated ATP maintenance was included in the biomass equation and was set to 65 mmol/gDW, similar to the *M. barkeri* and *E. coli* FBA models [83, 90], to account for energy costs for growth (such as production of macromolecules from biomass components. Both growth associated maintenance (GAM) and non-growth associated maintenance (NGAM) costs were chosen to best match experimentally measured growth and secretion rates. The NGAM is about 1.5 mmol/gDW/hr more than that of the previously published *M. barkeri* model [83], primarily because ion pumping inefficiencies for membrane-bound pumps such as Fpo were lumped into the NGAM rather than explicitly stated in the reaction stoichiometry. Detailed calculations and references related to the biomass equation are available in the supplemental material.

Under the assumption that the cell seeks to maximize its growth potential, the specific growth rate was predicted by maximizing the flux through the biomass reaction subject to the aforementioned constraints:

$$\text{Max } v_{biomass}$$

Subject to:

$$\mathbf{S}v = 0$$

$$\mathbf{v}_{min} \leq \mathbf{v} \leq \mathbf{v}_{max}$$

Reaction fluxes were predicted in mmol/gDW/hr, and growth rates were predicted in hr^{-1}. FBA problems were solved using the COBRA toolbox in MATLAB [91] linked to the GLPK linear program solver. Simulations were also repeated using the CPLEX package via the TOMLAB 7.0 interface, with identical results. Defined high salt (HS) media without vitamin supplement was used for all simulations. The complete media composition is listed in the supplemental material and was defined from Sowers *et al.* [92].

Flux Variability Analysis

Flux balance analysis (FBA) does not necessarily yield a unique flux distribution, although it will yield a unique optimal value for the objective function. Flux variability analysis (FVA) was thus used to calculate the possible range of each flux under optimal growth conditions. Mathematically, the possible range of flux through each reaction *i* was calculated by maximizing and minimizing its flux v_i while constraining the objective to be larger than a certain threshold [93]:

$$\text{Min/Max } v_i$$

$$\text{Subject to:}$$

$$\mathbf{S}v = 0$$

$$\mathbf{v}_{min} \leq \mathbf{v} \leq \mathbf{v}_{max}$$

$$v_{biomass} \geq pct * v_{biomass,MAX}$$

All flux variability analyses in this paper were performed with pct = 100% (the biomass objective function was fixed to its maximum value, within rounding error). Flux variability analysis was performed using the fluxVariability function in the COBRA toolbox [91].

Knockout lethality studies

To perform knockout lethality studies, knocked out genes were assigned a value of 0 (FALSE) and other genes were assigned a value of 1 (TRUE). The Boolean GPRs were evaluated for every reaction, and reactions with a GPR evaluating to FALSE were removed from the model. After modifying the network in this way, FBA was used to make a growth-no growth prediction (growth was defined as a predicted $v_{biomass} > 10^{-5}\ hr^{-1}$) for all knockouts of metabolic genes. Lethality predictions were compared to published

gene knockout phenotype data (see supplemental material for references). For substrates with an unknown uptake rate (such as monomethylamine), the uptake rate was assumed to be 15 mmol/gDW/hr, similar to the calculated rate for growth on methanol [94], for purposes of FBA simulations.

Calculation of Theoretical ATP Yield and Thermodynamic Efficiency

To calculate theoretical (maximum possible) ATP yield under various conditions, a flux balance analysis problem was solved, but the flux through the non-growth associated maintenance (ATPM) reaction was maximized instead of flux through of the biomass equation. If necessary, the model was forced to carry flux through a specific ATP generating pathways (such as acetogenesis) by adding constraints on other ATP-generating pathways (such as methanogenesis). The theoretical ATP yield was calculated by dividing the maximum flux through the ATP maintenance reaction by the CO uptake rate. Thermodynamic efficiency was calculated as the ratio of the theoretical ATP yield predicted by the model and the ATP yield if the entire Gibbs energy available from the production of methane and CO_2 from a given substrate (under standard conditions) was used to generate ATP [95].

Thermodynamics

Experimental standard Gibbs free energy change of reactions were unavailable for most of the reactions in the network, but they were available and included for some methanogenesis reactions [2, 95] and reactions involved in central metabolism [96] based on experimental Gibbs free energies of formation. When available, the free energy changes were used to help make decisions about reaction reversibility (in combination with direct experimental or modeling evidence).

To estimate the standard Gibbs free energy change of reactions for which no experimental data was available, Mol files were generated to represent all compounds in the model, containing charged structures at a pH of 7. The mol files contain the structures and location of charged moieties in each compound in the model. Charges were computed and charged mol files were exported using ACD/Labs software (Version 12; Advanced Chemistry Development, Inc.). The Gibbs energy of each compound was estimated using a previously published group contribution method [97]. Standard Gibbs free energies of formation and reaction are reported in the supplemental material under the following conditions:

temperature of 25^0C, pH of 7, an ionic strength of 0, water in the liquid phase, and all other compounds in aqueous phase at a concentration of 1M.

Results

Model Reconstruction

The metabolic network of *Methanosarcina acetivorans* was curated and validated as described in the methods. The final network accounts for the activity of 745 metabolic genes and contains 715 intracellular metabolites and 756 reactions (excluding exchange and biomass reactions). The network is considerably larger than that in the manually curated model of *M. barkeri* [83] and is comparable in size to that found in other genome-scale metabolic reconstructions [98]. In addition to reactions included in the model, reactions that were specifically excluded from the model due to literature or modeling evidence were also recorded. Complete lists of reactions included, GPR relationships, and excluded reactions may be found in the supplemental material.

The metabolic network of *M. acetivorans* consists mostly of reactions required for synthesis of amino acids, nucleotides, and cofactors (**Figure 2.1 A**). This was not surprising given the relatively small number of growth factors required for the growth of this organism. The reconstructed network includes pathways for synthesizing most of the cofactors required for methanogenesis in *Methanosarcina* species. The exception is methanophenazine, which to the authors' knowledge has no complete synthesis pathway proposed in any organism. Synthesis pathways were also included for several other cofactors such as NAD, biotin, flavins and folate.

There are still significant gaps in the knowledge of central metabolic pathways. For example, no homologues to currently known IMP dehydrogenase genes could be found in the genome of *M. acetivorans*, but the reaction catalyzed by this enzyme is predicted to be essential for nucleic acid synthesis. In addition, several of the methanogenic cofactor synthesis pathways that are completely or partially characterized in *Methanocaldococcus jannaschii* seem to have diverged in *Methanosarcina*. Although this is perhaps not surprising given the great evolutionary distance between *Methanocaldococcus* and *Methanosarcina*, the identification of these differences could provide

motivation for further investigation into the evolution of these species. A detailed discussion of these differences and other identified gaps in metabolic pathways is provided in the supplemental text..

Comparison to Existing Genome-Scale Reconstructions of *Methanosarcina* Species

The iMB745 model is the third model of members of *Methanosarcina* to be published. The first was iAF692, a manually curated model of *M. barkeri* str. Fusaro [83]. The iAF692 model was used to estimate the ion-pumping stoichiometry of the Ech hydrogenase and the ATP requirements of nitrogenase in that organism. The second was iVS941, a genome-scale model of *M. acetivorans* C2A based heavily on automated approaches [76]. The iVS941 model was used to study the essentiality of methanogenesis pathways during growth on CO, acetate, and methanol and to predict ways to reconcile simulated knockout lethality predictions with available data.

Many of the differences between iMB745 and each of the previously published models are due to new literature sources for novel metabolic paths unique to the archaea. For example, both of the previously published models include the non-oxidative portion of the pentose phosphate pathway for synthesis of five-carbon sugars. However, the genes encoding for reactions in that pathway are apparently absent in many methanogens, including both *M. acetivorans* and *M. barkeri*. An alternative pathway for synthesis of ribulose-5-phosphate was recently characterized in *Methanocaldococcus jannaschii* [99], which unlike the pentose phosphate pathway generates formaldehyde as a byproduct. The genes involved in that pathway had strong homology to genes in *M. acetivorans*. Therefore, the reactions in the pentose phosphate pathway were excluded from the iMB745 model and the new pathway was added to the model. Other gaps in the previously existing models were also filled based on recent literature; see supplemental text for details.

The iMB745 model accounts for key differences in methanogenesis pathways between *M. acetivorans* and *M. barkeri* (**Figure 2.1 B-D**). Critically, the Fpo and Vht hydrogenases are not functional in *M. acetivorans*, as has been shown experimentally [18], even though sequence homology suggests that both are present. Due to the strong sequence identity between the *M. acetivorans* and *M. barkeri* homologues, the automated reconstruction approach from the previous *M. acetivorans* reconstruction incorrectly included these reactions in the model. The automated model also did not include the

recently-characterized soluble heterodisulfide reductase (HdrABC), which plays an important role in methanogenesis during growth on methylated substrates [100].

Other important differences also are found between existing models. For example, *M. acetivorans* cannot grow on H_2 and CO_2 and grows on CO using a completely different pathway that involves secretion of acetate, methylsulfides and formate [101, 102]. M*. acetivorans* is also able to grow on dimethylsulfide, whereas *M. barkeri* can only perform methanogenesis from that substrate [103]. The iMB745 network includes pathways and genes necessary to perform these functions which are not found in either of the previously-existing reconstructions. The iMB745 network also includes novel pathways for synthesis of methanofuran and cell wall polymers that were newly added to the biomass equation (see methods), and accounts for experimentally determined differences in lipid composition compared to *M. barkeri* [89]. Therefore, the description of essential biochemistry is more complete in this model than in the previously published ones.

Estimation of Rnf and Mrp Ion-pumping Stoichiometry

The stoichiometry of ion pumps in the electron transport chain can have a significant effect on the quantitative predictions of metabolic models [90]. In lieu of experimental data, it becomes necessary to estimate the stoichiometry by simulation. In the *M. acetivorans* model, flux balance analysis was used to estimate the stoichiometry of ion exchange due to the H^+/Na^+ exchanging complex Mrp and the Rnf complex, two methanogenesis enzymes found in *M. acetivorans* but not *M. barkeri* [104]. The Rnf complex is thought to catalyze the reduction of methanophenazine by ferredoxin, and generate either a proton or sodium motive force [105]. The specific ion pumped by Rnf is unknown, but Mrp is strongly up-regulated on acetate compared to methyltrophic substrates, suggesting an increased importance for H^+/Na^+ exchange across the membrane on that substrate [104]. Since the ion pumping activity of Rnf is essential for growth on acetate and Mrp and Rnf are co-regulated [104], it was assumed for modeling purposes that Rnf pumps sodium ions.

The ATP yield of methanogenesis on substrates that utilize Rnf is strongly dependent on both the number of sodium ions pumped by Rnf and the H^+/Na^+ exchange ratio of Mrp, neither of which has been determined experimentally. H^+/Na^+ exchange proteins are known in other organisms that pump protons and sodium ions in 2:1 [106], 3:2 [107], or 1:1 ratios [108]. To find which combination was most likely in

light of experimental growth data, a sensitivity study was performed, varying the number of sodium ions pumped by Rnf as well as the H^+/Na^+ ratio of Mrp. The closest match between the predicted and experimental growth yields occurred when Rnf was set to pump 3 Na^+/2 e^- and Mrp to 1 H^+/Na^+ (**Figure 2.2**). Changes in these ratios had minimal effect on predicted product secretion rates. Due to the close match with experimental growth yields, these ratios were chosen for all further simulations.

The calculated ratios are consistent with thermodynamic data. The Rnf complex utilizes the same electron acceptor (methanophenazine) as the F_{420} dehydrogenase (Fpo), but uses ferredoxin instead of F_{420} as the electron donor. The reaction catalyzed by Fpo is coupled to the pumping of two protons across the membrane [109]. Since ferredoxin has a lower redox potential than F_{420}, it is reasonable to expect that Rnf can pump more proton equivalents across the membrane than Fpo.

F_{420} Regeneration during Growth on Carbon Monoxide

Both *M. acetivorans* and *M. barkeri* grow on carbon monoxide by oxidizing it to CO_2 and subsequently reducing CO_2 to methane [110]. In methanogens, the reduction of carbon dioxide to methane requires oxidation of two equivalents of reduced coenzyme F_{420}. Therefore, to achieve growth on carbon monoxide, a mechanism for generating reduced coenzyme F_{420} must be present in the cell. In CO-grown *M. barkeri,* reduced F_{420} is probably regenerated by generation of molecular hydrogen via the reverse action of Ech hydrogenase, followed by H_2-dependent reduction of F_{420} via the F_{420}-reducing hydrogenase, Frh [111, 112]. Ech hydrogenase is not present in the *M. acetivorans* genome, and although an *frh* operon is present, it does not encode a functional enzyme [18]. Thus, the mechanism for F_{420} regeneration in *M. acetivorans* during growth on CO remains unknown [110].

Our model suggests that F_{420} is regenerated by the combined action of F_{420} dehydrogenase (Fpo) and the Rnf complex (**Figure 2.3 A**). In the proposed pathway, Rnf would reduce methanophenazine with ferredoxin, and subsequently, reverse electron transport via Fpo would be used to generate reduced F_{420}. Reverse electron transport by Fpo has not been observed experimentally, but it is thermodynamically feasible in an environment containing excesses of oxidized F_{420} and reduced methanophenazine. In addition, this hypothesis is consistent with the high levels of Fpo protein and transcript measured during growth on CO [113]. Finally, the estimated proton pumping stoichiometries for Rnf and Fpo (3 and 2 proton equivalents, respectively) suggest that *M. acetivorans* would conserve one proton for each unit

of F_{420} reduced. This is consistent with the level of conservation in *M. barkeri,* in which the Ech hydrogenase pumps at least one proton out of the cell [114].

As an alternative hypothesis, we also tried to implement a F_{420}-ferredoxin oxioreductase reaction for the purposes of regenerating coenzyme F_{420} during growth on CO [100]:

FFRED: f420-2(*aq*) + 2 fdred(*aq*) + h(*aq*) → f420-2h2(*aq*) + 2 fdox(*aq*)

Growth on CO was predicted to be possible if reaction FFRED was added to the model (data not shown). However, the presence of FFRED was also predicted to make a Δ*rnf* mutant viable on acetate, contrary to experimental evidence (N.R. Baun, A.M. Guss, G. Kulkarni, and W. W. Metcalf, Unpublished Results), and therefore the reaction was not included in the model. According to the model, a Δ*rnf* mutant growing on acetate could survive with a lower growth rate by reducing coenzyme F_{420} with FFRED and then generating a proton gradient with Fpo and heterodisulfide reductase (Hdr).

It is possible that an enzyme catalyzing a reaction like FFRED really exists, but that the ATP yield of this alternative path is insufficient to make the cell viable for growth on acetate. According to the model, the theoretical maximum wild type ATP yield of methanogenesis from acetate (utilizing Rnf) is only about 0.75 ATP/acetate, corresponding to about a 65% thermodynamic efficiency (at pH 7) or 30% efficiency (at pH 0) [95]. The efficiency is considerably higher than that of methanogenesis from carbon monoxide (0.56 ATP/CO, 34%) or methanol (0.75 ATP/methanol, 27%), possibly because the cell is not viable with less efficient ATP production from this substrate.

Model Consistency with Knockout Lethality Data

Comparison of knockout lethality predictions to available data indicates that the model correctly predicts the growth/no growth phenotypes of 60/63 knockout mutants correctly (Table 1). All of the incorrect predictions were cases in which genes were experimentally shown to be lethal but predicted to be nonlethal. Two of the incorrect lethality predictions involved acetogenesis during growth on carbon monoxide. The genes encoding Pta and Ack are essential for growth on CO [102]. However, flux balance analysis incorrectly predicts that a Δ*pta*Δ*ack* mutant can grow by producing methane and carbon dioxide as sole byproducts. Although inhibition of Mtr and (if the Mtr bypass indeed exists)

another reaction in methanogenesis would cause the Δ*pta*Δ*ack* mutation to be lethal, we cannot rule out the possibility that other mechanisms such as regulatory constraints are responsible for the essentiality of these genes. Physiological evidence exists both supporting [102] and refuting [101] inhibition of methanogenesis reactions by carbon monoxide.

A Δ*mch* mutant was predicted to be viable on acetate (**Table 2.1**), but this knockout is known to be lethal on that substrate [115]. The *mch* gene was hypothesized to be essential for growth on acetate because it generates reduced F_{420}, which *M. acetivorans* requires for use in anabolic reactions such as the F_{420}-dependent glutamate synthase [116]. However, when growing on CO, Mch cannot be used to generate reduced F_{420}, because it is required to carry flux in the direction of F_{420} oxidation. Therefore, to achieve growth on CO, another enzyme (in the model, this is predicted to be Fpo) must be present that is able to reduce F_{420}. Flux balance analysis predicts that this other enzyme could also be used to reduce F_{420} during growth on acetate, therefore making *mch* nonessential for growth on acetate. However, the incorrect prediction depended on the ability of *M. acetivorans* to secrete methyl sulfides during growth on acetate, which is unlikely given that the Mts methyltransferase required for methyl-sulfide synthesis is down-regulated during growth on acetate [113, 117]. Hence, including the regulatory constraint would fix the phenotype prediction.

Knockout data was useful for refining the model and finding gene annotations in the *M. acetivorans* genome that are inconsistent with experimental data. For example, *M. acetivorans* uses Ack and Pta to activate acetate to acetyl-CoA during acetoclastic methanogenesis, and cannot grow on acetate without the encoding genes [102]. However, the *M. acetivorans* genome also encodes genes (MA3168 and MA3602) with high sequence identity to the ADP-forming acetyl-CoA synthase of *Methanocaldococcus jannaschii* that catalyzes an alternative pathway for activating acetate [118]. Including this reaction would make Pta and Ack nonessential for growth on acetate. On this basis, the reactions in the alternative pathway were excluded from the model.

Model Consistency with Growth Phenotype Data

The iMB745 model was used to predict growth phenotypes for wild type strains of *Methanosarcina acetivorans* growing on acetate, methanol, and carbon monoxide, the three substrates for which growth and substrate uptake data are available [94, 102, 119]. Predicted growth rates were highly dependent

on substrate uptake rates, which varied up to two-fold depending on the data set used to perform the calculation (see supplemental material). It was possible to pick uptake rates within the experimentally feasible ranges for each substrate that matched the observed growth rates and growth yields within 20% (**Table 2.2**).

Both growth and secretion rates closely matched the experimental values during growth on acetate. On methanol, the rate of methanogenesis was predicted to be much lower than experiment, but the ratios of products are consistent with experimental data. When maximizing ATP yield during growth on methanol, the predicted ratio of methane to CO_2 produced was exactly 3:1, as would be expected to balance redox potentials in the cell [100]. When optimizing for growth, the actual ratio of methane to CO_2 secreted was predicted in the model to be 3.8:1, because the carbon dioxide-fixing activity of carbon monoxide dehydrogenase/acetyl CoA synthase reduced the net secretion of carbon dioxide. The actual ratio in *M. barkeri* has been measured as 3.4:1 or 4.4:1 [120].

M. acetivorans produces acetate, formate, methane, and methylsulfides as byproducts when grown on carbon monoxide (in addition to CO_2) [101, 102]., but the mechanisms of formate and methylsulfide formation are unclear. Therefore, to make predictions about the necessary conditions to produce these byproducts, it was necessary to hypothesize mechanisms for how they are produced.

It is currently unknown how or why *M. acetivorans* generates formate during growth on CO, although it is probably not coupled to methanogenesis [101]. It is possible that formate is produced as a byproduct of carbon monoxide dehydrogenase during growth on CO to prevent toxic CO accumulation in the cell [101, 121]**.** The CO dehydrogenase enzyme from *Rhodospirillum rubrum* has been shown to create formate as a byproduct, and formate may formed by a similar mechanism in *M. acetivorans* [122], although the physiological substrate for the reaction is still unknown [121]. In order to investigate formate production, the following reaction was tentatively included in the model:

CODH3_SIDERXN: co(*g*) + h2o(*l*) → for(*aq*) + h(*aq*)

This reaction implies that formate production from CO does not yield ATP, which is likely to be true since this reaction is endergonic ($\Delta G^{0'}$=+24 kJ/mol, or +6 kJ/mol if CO is treated in aqueous phase) under standard conditions [96].

The recently-characterized Mts enzymes are necessary for production of dimethylsulfide (DMS) in *M. acetivorans,* although due to the very low ratio of dimethylsulfide production rate to the transcription level of these enzymes, the *in vivo* function of these enzymes remains unclear [123]. The source of methylsulfide needed as a substrate for Mts to make dimethylsulfide is unknown. However, due to the similar structure of sulfide (HS^-) and methylsulfide, one could reasonably hypothesize that methylsulfide is formed by the same Mts enzyme that produces dimethylsulfide:

MSS: m5hbc(*aq*) + h2s(*aq*) + h(*aq*) → ch4s(*aq*) + 5hbc_red(*aq*)

Here, m5hbc is the methylated form of a cobalamide cofactor utilized in methyltransferases in *Methanosarcina* [124] and 5hbc_red is the unmethylated form.

Despite inclusion of reactions to make the observed byproducts acetate, formate, and methylsulfides, FBA predicted that only methane and CO_2 would be produced as byproducts during growth on CO. Consequently, the methane secretion rate was significantly higher than that observed in experiments (Table 2). To investigate the reason for this incorrect prediction, the theoretical ATP yield was calculated for production of each byproduct per mole of CO consumed, as described in the methods. The theoretical ATP yield from methanogenesis was significantly higher than acetogenesis, methylsulfide production, or formate generation (**Figure 2.3 B**). Because most biosynthesis reactions were unconstrained in the direction necessary for biosynthesis, FBA predicted utilization of pathways with greater ATP production efficiency, because if less substrate is needed to satisfy the ATP requirements of the cell, then more is available to produce biomass. We subsequently examined possible conditions under which these byproducts could be produced in an FBA model.

Formate Production and Regulation of CO Levels in *M. acetivorans*

M. acetivorans encodes at least two complete carbon monoxide dehydrogenase (CODH) operons, and their relative expression during growth on CO may depend on the concentration of CO in the media [121]**.** Since formate production may be a result of a side reaction of CODH [122], it is tempting to speculate that the level of carbon monoxide in the cell is regulated by the balance of the levels of these proteins, one of which produces formate as a byproduct and one which does not. FBA predicts that if

the proposed mechanism for formate production is correct, reducing the flux through the primary reaction catalyzed by CODH leads to production of formate (**Figure 2.3 C**). This indicates that CO toxicity could be controlled by balancing the rates of the side reaction and the primary reaction of CODH enzymes.

CO Inhibition of the Methyltransferase Mtr and its Possible Role in Acetogenesis

The sodium-pumping methyltransferrase Mtr catalyzes the reversible transfer of methyl from methyl-tetrahydrosarcinopterin to methyl-Coenzyme M via a cobalamide intermediate. This enzyme is strongly down-regulated during growth on CO compared to other substrates [121]. It has been hypothesized that methanogenesis is kinetically limited during growth on CO [102], possibly including Mtr, although this hypothesis is controversial [101]. Flux balance analysis predicted that if Mtr was *not* inhibited, the cell could still survive without methanogenesis or acetogenesis by producing methylsulfides. The theoretical ATP yield of methylsulfide production, including ATP generation due to the sodium gradient created by Mtr (0.33 ATP/CO), is sufficient to overcome the ATP maintenance requirement (0.22 ATP/CO; see **Figure 2.3 B**). Since acetogenesis is actually essential for growth on carbon monoxide [102], and methylsulfide production is actually very low, this prediction suggests that either Mtr activity is strongly limited during growth on carbon monoxide, or that production of methylsulfides is kinetically limited.

Despite the down-regulation and possible inhibition of Mtr during growth on CO, significant methanogenesis is still observed during growth on this substrate [101, 102]. The combination of these observations has inspired the hypothesis that a Mtr bypass reaction exists that performs the same reaction but does not generate a sodium gradient [110]:

MTR_BYPASS: mh4spt(*aq*) + 5hbc_red(*aq*) + h(*aq*) → h4spt(*aq*) + m5hbc(*aq*)

This reaction, when coupled with methyl transfer to coenzyme M, would be strongly thermodynamically favored in the direction of methyl-CoM formation (ΔG^0=-30 kJ/mol) [2]. The presence of the bypass reaction could permit tolerance for a wider range of environmental CO concentrations by permitting the cell to balance the increased ATP potential of Mtr with a possible greater kinetic capacity of the Mtr bypass reaction [110].

To test the effects of the Mtr bypass reaction on metabolism, the bypass reaction was added to the metabolic network, and the sodium-pumping Mtr was removed from the model. The modified model was still predicted only to perform methanogenesis and not acetogenesis, because theoretical ATP yield of methanogenesis was still higher than that of acetogenesis (0.44 ATP/CO and 0.38 ATP/CO, respectively, see also **Figure 2.3 B**). In addition, flux variability analysis indicated that no alternative optimal solutions led to acetate secretion. As a result, Mtr inhibition is probably not the sole reason for acetogenesis during growth on CO.

Exploration of an Alternate Heterodisulfide Reductase (HdrABC) on Methanol

HdrABC is a soluble heterodisulfide reductase typically found in methanogens without cytochromes [125]. Most methanogens with cytochromes, including *Methanosarcina* species, use a membrane-bound heterodisulfide reductase HdrDE instead of the soluble HdrABC to couple methanogenesis to ATP production [2]. Surprisingly, *M. acetivorans* was found to utilize both types of heterodisulfide reductase during growth on methyltrophic substrates [100].

Since the HdrABC complex is not a sodium or proton pump, it is unclear if the activity of this complex is coupled to ATP synthesis in *M. acetivorans*. In *Methanothermobacter marburgensis,* a methanogen without cytochromes, HdrABC is coupled to ATP synthesis through its interaction with the MvhADG hydrogenase complex [125]. The HdrABC/MvhADG complex in *M. marburgensis* uses an electron bifurcation mechanism, in which the electrons from two equivalents of molecular hydrogen are donated to ferredoxin and to the heterodisulfide [125]. *M. acetivorans* lacks the genes encoding the MvhADG complex, but the similarity of the Hdr enzymes suggests that *M. acetivorans* HdrABC may also use an electron bifurcation mechanism (**Figure 2.4 A**), splitting the electrons of two fully-reduced ferredoxins between heterodisulfide and coenzyme F_{420} [100]. Alternatively, the HdrABC may simply reduce heterodisulfide with ferredoxin, acting as a sink for excess ferredoxin produced during oxidation of methanol to CO_2.

To test the electron bifurcation hypothesis in a genome-scale context, the phenotype of *M. acetivorans* was simulated with and without electron bifurcation in HdrABC. The addition of two additional constraints was necessary to obtain reasonable predictions. Reactions catalyzed by Pta and Ack were disabled to prevent acetate secretion, which has not been observed during growth on methanol [126],

and the flux through pyruvate-acetyl CoA oxioreductase was set to be equal to the wild-type value to prevent secretion of formate and other unobserved byproducts during growth on methanol [119]. In the presence of Rnf, flux variability analysis did not predict utilization of HdrABC regardless of mechanism. However, a Δ*rnf* mutant was predicted to utilize HdrABC to oxidize ferredoxin using any optimal flux distribution (**Figure 2.4 B**). The Δ*rnf* mutant was predicted to grow 35% slower than the wild type without bifurcation and 20% slower with bifurcation. A Δ*rnf* mutant actually grew about 25% slower on methanol than the wild type (William Metcalf, unpublished data), so within experimental error it is difficult to tell which mechanism is correct. Further experiments could help elucidate the true mechanism.

Discussion

We have built and manually curated a computable genome-scale model of metabolism in *M. acetivorans*, only the third methanogen species to be reconstructed (after *M. barkeri* [83] and *M. jannaschii* [127]) and the second in the genus *Methanosarcina*. We have focused on three approaches to model-guided discovery using the *Methanosarcina acetivorans* model: 1) identification of knowledge gaps and "missing" reactions in metabolic pathways, 2) detailed study of metabolic differences between closely related methanogenic species, and 3) use of constraint-based modeling to study alternative hypotheses about the workings of the metabolic network and the implications of those hypotheses on predicted phenotypes.

The reconstruction endeavor has helped pinpoint gaps in our knowledge of the metabolic networks, both due to unknown differences between different archaeal species and differences between archaea and other domains of life. Interestingly, even some pathways for synthesis of specialized methanogenic cofactors, such as those for tetrahydrosarcinopterin and coenzyme M, seem to have diverged from those observed in other methanogens such as *Methanocaldococcus jannaschii*. However, the synthesis pathways for other methanogenic cofactors (such as coenzyme B synthesis) are conserved across these genera. This observation raises interesting questions about the evolution of these ecologically important organisms and the role of the environment in the selection of metabolic pathways.

Constraint-based modeling proved useful for integrating experimental data from different sources and identifying tensions between data sets. Some of these tensions, such as the disparity between the ability

of *M. acetivorans* to grow on CO and the lethality of a *mch* knockout, may have been difficult to identify without a genome-scale model and its accompanying predictions. These findings highlight the usefulness of an integrative, genome-scale modeling approach for both validating model predictions and identifying gaps in our knowledge of methanogen biology.

One of the strengths of genome-scale metabolic modeling is the ability to continually update the model as additional experimental data becomes available [128]. Our investigations of alternative hypotheses for the mechanism of F_{420} regeneration during growth on carbon monoxide, pathways for synthesis of byproducts observed during growth on CO, and the precise reaction catalyzed by the soluble heterodisulfide reductase HdrABC have yielded predictions that can be tested in the laboratory. As additional data becomes available, improved models may be constructed and used to provide further novel hypotheses in an iterative process that lies at the heart of systems biology.

Supplemental material

Supplemental material related to this chapter is located online at:

http://jb.asm.org/content/194/4/855/suppl/DC1

List of Abbreviations

Metabolites (as in model): 5hbc_red: 5-Hydroxybenzimidazolylcob(I)amide; ch4s: Methyl sulfide; co: Carbon monoxide; co2: Carbon dioxide; com: Coenzyme m; cob: Coenzyme b; f420-2: Oxidized F_{420}; f420-2h2: Reduced F_{420}; fdox: Reduced ferredoxin; fdred: Reduced ferredoxin; for: Formate; formmfr(b): Formylmethanofuran(b); h: H^+; h2o: Water; hsfd: Heterodisulfide; mh4spt: Methyl-tetrahydrosarcinopterin; mphen: Oxidized methanophenazine; mphenh2: Reduced methanophenazine; m5hbc: Co-Methyl-Co-5-hydroxybenzimidazolylcobamide; na1: Na^+;

Genes and proteins: *ack*: Acetate kinase; *cdh*: CO dehydrogenase/acetyl CoA synthase; *ech*: Ech hydrogenase; *fpo*: F_{420} dehydrogenase; *frh*: F_{420}-reducing hydrogenase; *hdr*: Heterodisulfide reductase; *mch*: Methenyl-H4SPt cyclohydrolase; *mrp*: Multiple resistance protein (Na^+/H^+ exchange pump); *mtr*: Sodium-pumping h4spt-coenzyme M methyltransferase; *mts*: Dimethylsulfide-coenzyme M methyltransferase; *pta*: Phosphotransacetylase; *rnf*: Putative ferredoxin-methanophenazine oxioreductase

Modeling: COBRA: Constraint-based reconstruction and analysis; FBA: Flux balance analysis; FVA: Flux variability analysis; GAM: Growth-associated maintenance cost; NGAM: Non-growth associated maintenance cost.

Figures and Tables

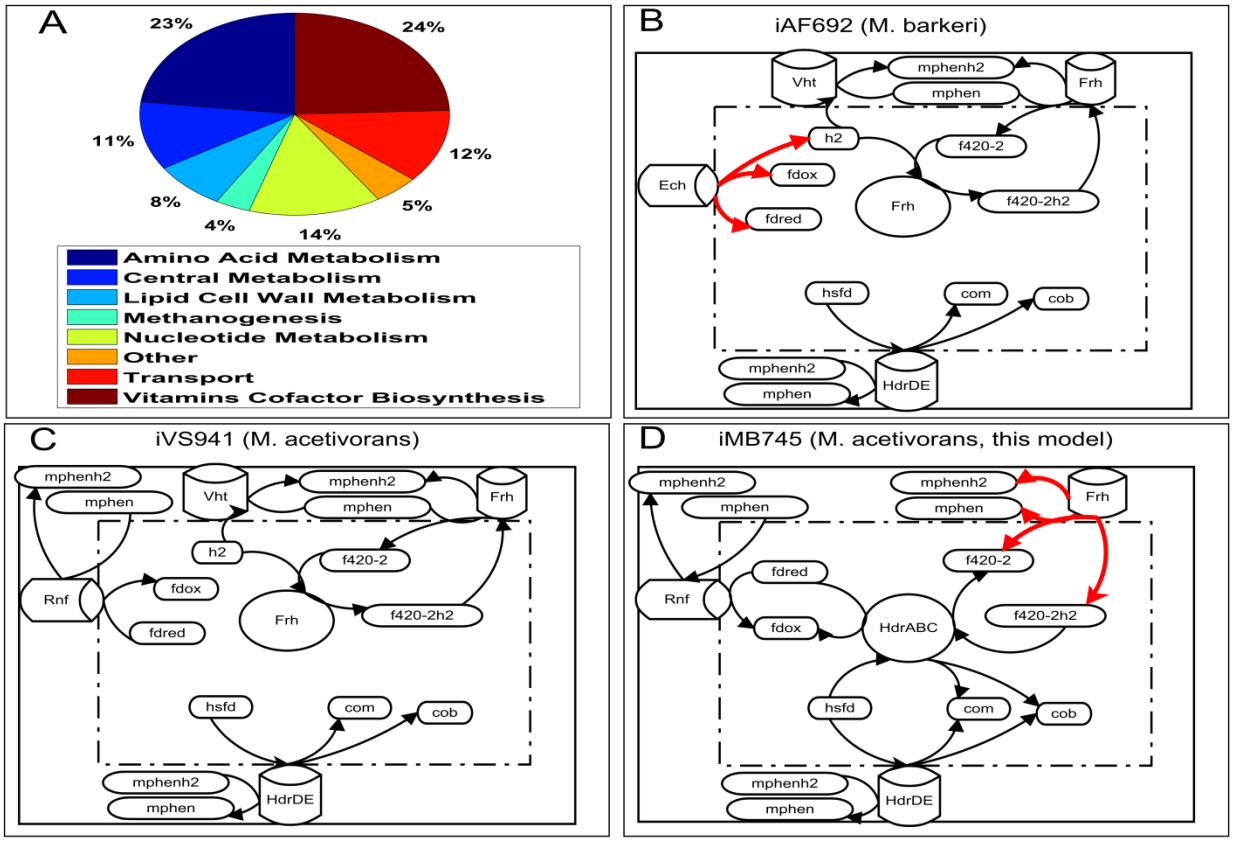

Figure 2.1. Properties of the model of *Methanosarcina acetivorans* and comparison to other existing *Methanosarcina* models. (A): After curation, the metabolic model contained reactions related to synthesis of essential biomass components, cell wall components, and methanogenesis, among others. (B-D): Comparison of the electron transport chains in the three available *Methanosarcina* models. Red reactions are reversible in that model. Note that the curated *M. acetivorans* model includes the Rnf complex and the soluble heterodisulfide reductase (HdrABC) and excludes Frh and Vht, two hydrogenases known to be inactive in *M. acetivorans* but present and active in *M. barkeri*.

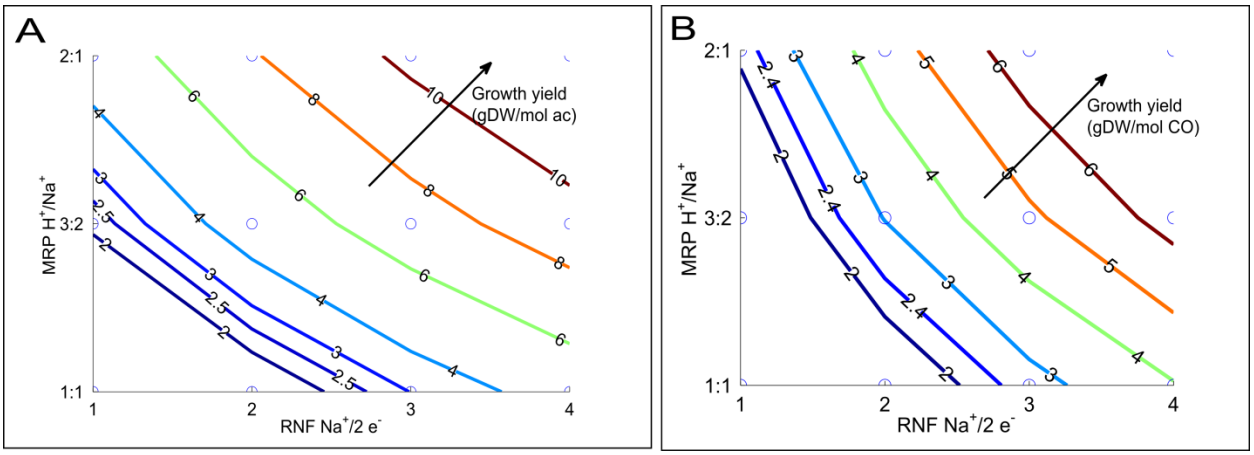

Figure 2.2 Analysis of the ion-pumping stoichiometry of Rnf and Mrp during growth on acetate (A) and carbon monoxide (B). Circles represent simulated combinations of ion pumping stoichiometries for the two pumps. The experimental growth yield during growth on acetate is 2.4 gDW/mmol and on CO is 2.5 gDW/mol. Only the combination of a 3 $Na/2e^-$ stoichiometry for Rnf and a 1 $Na^+/1\ H^+$ stoichiometry for Mrp was consistent with experimental data. See supplemental for the analogous simulation of growth on methanol.

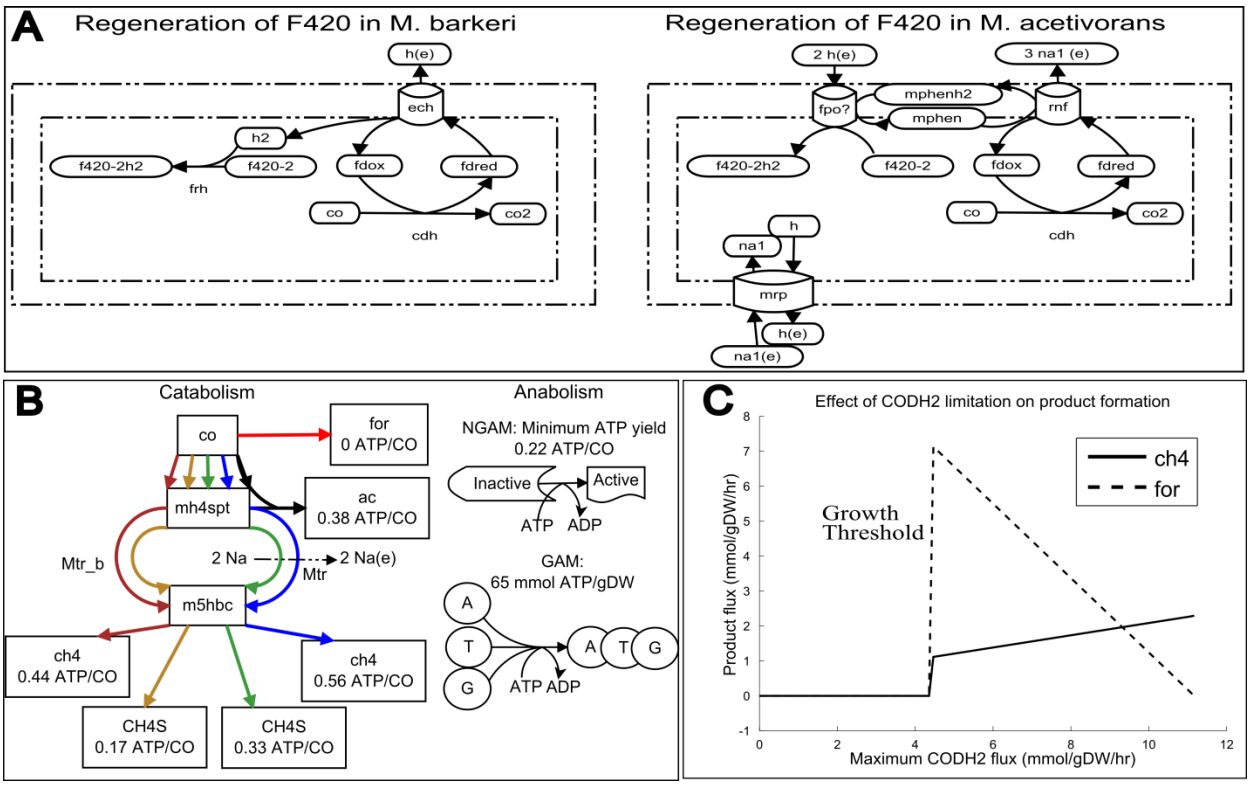

Figure 2.3 Analysis of growth of *M. acetivorans* on carbon monoxide. (A) Regeneration of coenzyme F_{420} during growth on carbon monoxide for both *M. barkeri* (left) and proposed pathway for *M. acetivorans* (right). (B) Theoretical ATP yields during growth on CO varied depending on the byproduct produced and whether sodium-pumping Mtr or its non-pumping bypass reaction (Mtr_b) is active. Red: formate generation; black: acetogenesis; blue: methanogenesis (with Mtr), green: methylsulfide production (with Mtr), gold: methylsulfide production (with Mtr_b), dark red: methanogenesis (with Mtr_b). At least 0.22 ATP/CO is required to overcome the non-growth associated maintenance requirement and an additional 65 mmol ATP/gDW is required for growth. (C) FBA predicts that limitation of CO dehydrogenase activity leads to formate production.

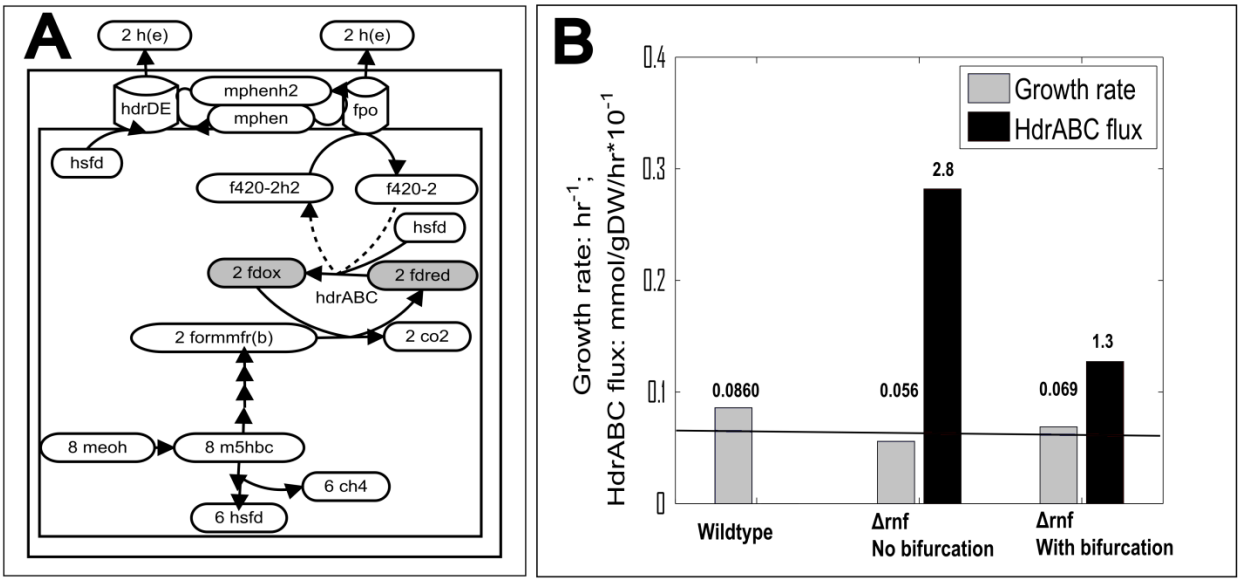

Figure 2.4 Studies on the soluble heterodisulfide reductase HdrABC during growth on methanol. (A) Hypothesized bifurcation mechanism of the soluble heterodisulfide reductase HdrABC during growth on methylotrophic substrates in *M. acetivorans*. The alternative hypothesis is that the reaction does not involve F_{420} (dashed lines). (B) Flux balance analysis predicts that, during growth on methyltrophic substrates (methanol shown), HdrABC is not used when Rnf is available, but a Δ*rnf* mutant is predicted to carry flux through HdrABC. The growth rate for the Δ*rnf* was predicted to be about 20% less with bifurcation and 35% less without.

Table 2.1 Knockout lethality predictions from FBA (L = lethal and N = nonlethal) and agreement with experimental results. Green boxes: correct prediction; Red boxes: incorrect prediction. No color means no experimental data is available for that knockout under those conditions. AC: acetate; DMA: dimethylamine; DMS: dimethylsulfide; MeOH: Methanol; MMA: monomethylamine; TMA: trimethylamine**.** See supplemental material for knockout data references.

Genotype	AC	CO	DMA	DMS	MeOH	MMA	TMA
ΔackΔpta	L	N	N	N	N	N	N
ΔatpDCIXBEFAG	N	N	N	N	N	N	N
ΔcooS1F	N	N	N	N	N	N	N
ΔcooS2	N	N	N	N	N	N	N
ΔhdrABC	N	N	N	N	N	N	N
ΔhdrED	L	N	L	L	L	L	L
Δmch	N	L	L	L	L	L	L
ΔmtaA1	N	N	N	N	L	N	N
ΔmtaB1C1ΔmtaB2C2ΔmtaB3C3	N	N	N	N	L	N	N
ΔmtaA1ΔmtaB1C1ΔmtaB2C2ΔmtaB3C3	N	N	N	N	L	N	N
ΔmtbA	N	N	L	N	N	L	N
ΔmtsDΔmtsFΔmtsH	N	N	N	L	N	N	N
ΔmtsXΔmtsY, X and Y two mts genes	N	N	N	N	N	N	N
ΔrnfHCDGEABF	L	L	N	N	N	N	N
ΔlysK	N	N	N	N	N	N	N
ΔlysS	N	N	N	N	N	N	N
Δmtr	L	N	L	L	L	L	L
TOTAL CORRECT	11/13	5/6	7/7	3/3	15/15	8/8	11/11

Table 2.2 Growth and secretion rates and yields of *M. acetivorans* on methanol, acetate, and carbon monoxide using experimentally feasible uptake rates [94, 102, 119]. For simulations on CO, no additional constraints to Hdr or Cdh were assigned. All measured values are averaged across literature sources (see supplemental material for a complete list of references). Note that due to experimental variability, the measured methanol uptake rate and secretion of methane on that substrate are inconsistent with mass balance constraints.

		Growth (hr^{-1})		Growth yield (gDW/mmol)		CH4 rate (mmol/gDW/hr)	
Substrate	**Measured**	**Measured**	**Predicted**	**Measured**	**Predicted**	**Measured**	**Predicted**
Acetate	7	0.023	0.021	2.4	3.0	4.9	6.6
Methanol	20	0.098	0.086	5.2	4	22	13.3
CO	11.6	0.029	0.030	2.5	2.6	0.4	2.3

Chapter 3: Likelihood-based gene annotations for gap filling and quality assessment in genome-scale metabolic models[3]

Abstract

Genome-scale metabolic models provide a powerful means to harness information from genomes to predict cellular phenotypes and deepen biological insights. With exponentially increasing sequencing capacity, there is an enormous need for automated reconstruction techniques that can provide more accurate models in a short time frame. Current methods for automated metabolic network reconstruction rely on gene and reaction annotations to build draft metabolic networks and algorithms to fill gaps in these networks. However, automated reconstruction is hampered by database inconsistencies, incorrect annotations, and gap filling largely without considering genomic information. Here we develop a metric for applying genomic information to predict alternative functions for genes and estimate their likelihoods from sequence homology. We show that computed likelihood values were significantly higher for annotations found in manually curated metabolic networks than those that were not. We then apply these alternative functional predictions to estimate reaction likelihoods, which are used in a new gap filling approach called *likelihood-based gap filling* to predict more genomically consistent solutions. To validate the likelihood-based gap filling approach, we applied it to models where essential pathways were removed, finding that likelihood-based gap filling identified more biologically relevant solutions than network-based gap filling approaches. We also demonstrate that models gap filled using likelihood-based gap filling provide greater coverage and genomic consistency with metabolic gene functions compared to network-based approaches. Interestingly, despite these findings, we found that likelihoods did not significantly affect consistency of gap filled models with Biolog and knockout lethality data. This indicates that the phenotype data alone cannot necessarily be used to discriminate between alternative solutions for gap filling and therefore, that the use of other information is necessary to obtain a more accurate network. All described workflows are implemented as part of the DOE Systems Biology Knowledgebase (KBase) and are publicly available via API or command-line web interface.

Author summary

[3] This chapter has been submitted as a manuscript to PLOS Computational Biology. Thanks go to my co-authors: Michael Mundy, Christopher Henry, Nicholas Chia and Nathan Price.

Genome-scale metabolic modeling is a powerful approach that allows one to computationally simulate a variety of metabolic phenotypes. However, manually constructing accurate metabolic networks is extremely time intensive and it is thus desirable to have automated computational methods for providing high-quality metabolic networks. Incomplete knowledge of biological chemistries leads to missing, ambiguous, or inaccurate gene annotations, and thus gives rise to incomplete metabolic networks. Computational algorithms for filling these gaps in a metabolic model rely on network topology based approaches that can result in solutions that are inconsistent with existing genomic data. We developed an algorithm that directly incorporates genomic evidence into the decision-making process for gap filling reactions. This algorithm both maximizes the consistency of gap filled reactions with available genomic data and identifies candidate genes for gap filled reactions. The algorithm has been integrated into KBase's metabolic modeling service, an automated metabolic network reconstruction framework that includes the ModelSEED automated metabolic reconstruction tools.

Introduction

Genome-scale metabolic models (GEMs) integrate available information about metabolism to provide a basis for holistic modeling and prediction of metabolic phenotypes [129]. GEMs have been utilized broadly [30, 40, 130, 131] across all three domains of life [132] to accelerate research in such areas as network evolution [133-135], synthetic biology [31, 136], and the discovery of novel drug targets [137]. However, achieving a sufficiently accurate metabolic model to enable high utility currently requires a very time-intensive manual reconstruction process, often taking many months or even years to complete [43]. As the throughput of sequencing technologies continues to increase and as research on microbial populations produces more and more genomes [138], there is a growing need for methods that automate high-quality metabolic model reconstruction.

Since the advent of genome-scale metabolic modeling, protocols [43], databases [80, 84, 139], algorithms [46, 77, 140] and toolboxes [46, 141, 142] have been developed to help systematize the lengthy and iterative process of collecting, curating, and integrating large volumes of biochemical knowledge. There have also been previous efforts to fully automate this process, including, notably, the Department of Energy's ModelSEED [46]. Despite these important advances, significant barriers to high-quality automated metabolic reconstructions still persist. Even with human curation, ambiguous or

incorrect annotations are still pervasive [143]. Incomplete annotations leave gaps in the metabolic networks that need to be filled in order to make simulation possible [43, 144]. Inaccurate annotations also give rise to the need to identify and assess the merits of alternative annotations for genes, a process that typically done manually as part of the model curation process [43]. An automated approach to model building that accounts for alternative annotations would help expedite manual curation and ensure that the draft models maximally account for alternatives that can be identified based on available data.

Existing algorithms for filling gaps, or dead-end reactions, in metabolic networks broadly fall into approaches based on network topology [77, 145], pre-defined pathways [146], or phenotype data [78, 147, 148]. Network topology-based algorithms such as GapFill identify dead-end reactions in a metabolic network and identify the minimum number of modifications to the network that can be made to activate those reactions [77]. Variations of GapFill have been developed that assign specific penalties based on thermodynamics or database incompleteness [145]. Pathway-based algorithms, such as that implemented in the PathwayTools [146], automatically complete pre-defined pathways that have sufficient representation in the draft model. Finally, several algorithms use phenotype data to help choose gap filling pathways, including OMNI, which maximizes model consistency with reaction rate data [147], GrowMatch, which maximizes consistency with experimental growth/no growth results [78], and MIRAGE, which maximizes the co-occurrence and co-expression of connected reactions [148]. Uniquely among these methods, MIRAGE also automatically identifies gene candidates for optimal gap fill solutions.

While existing methods capably activate the necessary reactions to allow growth simulations, they often do so by over fitting, resulting in the inclusion of spurious pathways. This is epitomized by a recent article that showed that in some cases, pruning these spurious pathways can lead to significant improvements in simulation accuracy [149]. Although genomic evidence may be incorporated after gap filling through human curation of potential solutions [150], these solutions are unlikely to fully reflect all the available knowledge of the genome. Methods that addresses both the resolution of dead-end metabolites and the identification of gene-reaction pairings for the reactions added to the model during the resolution of the gaps in the reaction network help researchers identify poorly-supported solutions when building models, thus helping to reduce over-fitting.

The goal of our work is to improve the quality of automatically generated metabolic reconstructions and models by explicitly incorporating alternative potential gene annotations and their estimated likelihoods into the gap filling process. We have developed a likelihood-based gap filling workflow that (1) assigns likelihood scores based on sequence homology to multiple annotations per gene and, from these, likelihoods for reactions in a network and (2) identifies maximum-likelihood pathways for gap filling using a mixed-integer linear programming (MILP) formulation. We have also developed a workflow to iteratively identify pathways that activates gene-associated orphaned reactions in a network and assesses the likelihood of these pathways. Critically, the likelihood-based approach makes the gap filling solution genome-specific and provides users with putative gene-protein-reaction relationships and confidence metrics for each result. We show that our likelihood-based approach improves the quantity and quality of new gene annotations compared to the existing gap filling algorithm, while the resulting models have comparable accuracy when simulating high-throughput growth phenotype data, when compared with previous network-based gap filling algorithms. The workflow tools are fully integrated within the Department of Energy's System Biology Knowledgebase (KBase), and are publicly available via both a web-based command line interface (available at http://kbase.us) and a web service API.

Results

Gap filling workflows using likelihood and network-based approaches

Confidence scores are useful for building models and assessing the quality of the annotations, reactions and pathways therein [43]. We have developed a quantitative likelihood measurement for the evidence that a gene carries a specific annotated function and a technique by which these likelihood estimates can be converted into the likelihood of existence of a reaction in a cell's metabolic network (see Methods). Importantly, we simultaneously compute the likelihoods of multiple annotations for a single gene, which both broadens the space of testable annotation hypotheses in gap filling solutions and helps mitigate possible errors in the most likely annotation.

The conversion from annotation to reaction likelihood scores is performed based on the reaction-role links in the SEED reaction database [46]. We have implemented four gap filling workflows (**Figure 3.1** and **Appendix B**) that use these reaction likelihoods (*likelihood-based gap filling*) or rely only on network context (*network-based gap filling*), in conjunction with two distinct gap filling strategies.

In the first strategy, which is the most commonly used in the field, gap filling is used to activate one particular reaction in a model such as the biomass reaction [77]. We call this approach *targeted gap filling* because it seeks to activate a single target reaction in the network. A successful application of targeted gap filling enables simulations to be performed on the resulting model using an increasingly large suite of constraint-based analysis algorithms [32, 151].

In the second strategy, which we call *iterative gap filling*, gap filling is used to activate the maximum number of orphaned reactions in a model in an iterative fashion, activating high-priority reactions first (see Methods). One could imagine such an approach would sacrifice specificity for sensitivity (while targeted gap filling would do the opposite). In the iterative gap filling workflow, a post-processing step is also used to reduce the redundancy resulting from attempting to activate every gene-associated reaction, to assess the value of each gap filled pathway in terms of how much of the original annotated network is corrected by the pathway, and optionally, to apply a cutoff to the cost of pathways added to the model (see Methods and **Appendices B and C**).

Likelihoods reflect a measure of confidence in predicted function

As part of the model curation process, it is necessary to evaluate the quality of each annotation and fix those which are found to be problematic [43]. We have implemented a simple method to estimate annotation likelihoods accounting for two sources of ambiguity: (1) sequence divergence between query genes and the genes in the reference database, and (2) inconsistencies in annotation within the reference database (see Methods). We characterized the utility of our reaction likelihoods by comparing the gene-reaction links created using our automated likelihood-based approach to those present in manually curated metabolic networks of *Escherichia coli* K12 [130] and *Bacillus subtilis* str. 168 [145]. We found that highly likely gene-reaction links were significantly enriched in the models compared to less-likely gene-reaction links (**Figure 3.2**) indicating that a higher likelihood score reflects higher confidence in the predicted function. We also identified large numbers of high-likelihood gene annotations that are not in the comparison models, which reflect promising candidates for further investigation and possible inclusion in the models.

Proof of principle for likelihood-based gap filling

Unlike the network-based gap filling approach, the likelihood-based approach is able to produce different solutions for different organisms, even if the starting network is identical, based on the organisms' genetic content. To demonstrate the utility of this approach in improving model quality, we identified a set of 32 reactions from the iBsu1103 genome-scale metabolic model of *B. subtilis* [145] that were predicted to be essential for growth and whose existence in the model was supported by literature evidence[152]. This set of reactions represented a gold standard set of reactions that should be incorporated into gap filling solutions if they were missing. We then removed all 32 gold standard reactions from the iBsu1103 model and applied the targeted network-based gap filling and likelihood-based gap filling algorithms to restore biomass production in the knockout model.

In order to evaluate the effects of parameterizing each algorithm, we modified the chosen penalties for transporters and for thermodynamically unfavorable reversibility changes. The optimal penalty for transporters was higher for network-based gap filling (55 or greater - equivalent to adding about 7 intracellular reactions on average) than for likelihood-based gap filling (25 or greater). Optimal penalties for thermodynamically unfavorable reversibility changes were also higher for network-based than likelihood-based gap fill (40 and 12, respectively). Despite the same number of tuning parameters available for each method, likelihood-based gap filling successfully outperformed the network-based method by replacing a maximum of 31 of the 32 gold-standard reactions. Network-based gap filling only replaced only a maximum of 24 reactions, even with extremely high penalties for transporters and unfavorable reversibility changes. Given that no transporters or reversibility changes were part of this test, the parameters chosen to be optimal for network-based gap filling were unreasonably high. Therefore we used the optimal penalties for likelihood-based gap filling for the remainder of the results in this manuscript (**Appendix A**).

The failures in network-based gap filling were a result of picking shorter pathways to fill certain gaps for which longer pathways are the correct choice. For example, the synthesis of isopentyl diphosphate (IPDP), a primary precursor for lipid synthesis, can occur by one of two routes, the mevalonate pathway and the non-mevalonate pathway [153]. *B. subtilis* uses the non-mevalonate pathway for IPDP synthesis [154, 155]. The mevalonate pathway contains fewer reactions than the non-mevalonate pathway, and thus the network-based gap filling approach incorrectly used the mevalonate pathway to restore IPDP

production (**Figure 3.3**). However, all of the knocked out reactions in the non-mevalonate pathway had high estimated likelihoods. Hence, likelihood-based gap filling correctly chose this pathway to restore production of IPDP.

Annotation of likelihood-based gap filling reactions

Mapping between genes and reactions allows for a useful connection to genetic manipulations, drug targets, and experimental validation. One important step in curating gap filling solutions is identifying genes in the genome that could be responsible for catalyzing the gap filled reactions and assessing the quality of the genomic evidence behind these assignments[150]. We have compared the ability to do identify these genes with likelihood-based and network-based gap filling by using the estimated Gene-Protein-Reaction relationships (GPR) from our likelihood computations to assign genes to reactions that are gap filled using each approach. We found that likelihood-based gap filling produced significantly more links between genes and reactions and more gene-associated reactions than post-processing of network-based gap filling results (i.e. seeking for gene homology after reactions were gap filled). This was true for both the targeted gap filling and iterative gap filling approaches ($p < 0.05$, Wilcoxon signed-rank test; **Figure 3.4**). The result suggests that the likelihood-based approach typically yields more and better-supported candidate annotations and associations that are not apparent when using the common post-processing procedure.

In addition to improved quantity, the likelihood-based approach also improved the average quality of annotation hypotheses generated from gap filling. In particular, the average likelihood of gene associations added using likelihood-based gap filling was significantly greater than that using network-based gap filling ($p < 0.05$, Wilcoxon signed-rank test; **Figure 3.5**). The effect of using reaction likelihoods on the number and likelihood of added genes was more pronounced for iterative gap filling, indicating that likelihood-based gap filling was able to find more likely pathways to activate peripheral model reactions in addition to the biomass reaction.

Consistency of automatically generated models with experimental phenotypes

One commonly-used method to verify the integrity of genome-scale metabolic models is to compare their predictions with high-throughput phenotyping data, such as knockout lethality screens [43]. To test

the impact of each of our workflows on the accuracy of model phenotype predictions, we applied our workflows to construct and fill gaps in genome-scale models for 22 organisms for which either Biolog or gene knockout lethality data was available. We then compared the predictions of these models to the phenotype data, without fitting to the data (**Table 3.1**). There were many differences in the pathways identified using likelihood-based gap filling compared to network-based gap filling: between 5% and 30% of the reactions in a likelihood-based gap filling solution were not found in the network-based solution, despite using the same parameters for each (see **Appendix A**). However, the use of likelihoods did not significantly affect the phenotype predictions. For Biolog data, iterative gap filling increased the sensitivity by 11% compared to targeted gap fill, but decreased specificity (more false positives) by 13%-15%. The overall accuracy (total correct/total experiments) decreased by about 5% for iterative compared to targeted gap filling.

Since gap filling only adds a small number of genes to the model compared to the number in the draft model (about a 7% increase for iterative gap filling), the sensitivity and specificity of knockout lethality predictions were very similar for all four workflows. The sensitivity varied from 84-86% and specificity from 64-67%. We also examined the lethality predictions specifically for genes added in gap filling (**Figure 3.6**). The negative predictive value was essentially identical for all four workflows at 40%. However, there was a notable improvement in the positive predictive value in the iterative gap filling workflows (80%) compared to network-based workflows (40%). Taken together, these results indicate that iterative gap filling mostly adds genes predicted to be nonlethal knockouts, and that most of these predictions are correct.

Discussion

We have used genomic evidence-based likelihood metrics for annotations and reactions to increase the consistency of gap filled pathways with available genomic data compared to the common procedure of post-processing network-based solutions. This approach increases the quantity of hypothesized gene-associated reactions compared to post-processing network-based gap filling solutions. However, despite the significantly increased level of evidence for gap filling solutions resulting from likelihood-based gap filling, there was not a significant difference in knockout lethality or growth (Biolog) predictions. This result suggests that using phenotype data to filter gap-filling solutions may not result in a more accurate metabolic network (that is, one that better reflects biological evidence for the specific components

included). Indeed, validation metrics such as consistency with knockout lethality predictions have a large number of ways in which they could be fit to become consistent with phenotype data, which can lead to decreases in observed accuracy when the model is tested on new data not available during its construction [149]. Therefore, alternative methods such as quantification of quality of individual reactions or pathways in the network are important metrics for validation.

An important feature of the likelihood-based gap filling algorithm is that it can differentiate between genomes by assigning organism-specific likelihoods for each reaction in a network. As a direct result, the gap filling solutions resulting from this algorithm are also organism-specific. This direct link back to evidence in the genome directly enables the identification of pathways that are not parsimonious, but that are most consistent with genomic data. We have shown that the likelihood-based approach increases both the quality and the quantity of hypothesized gene associations from gap filling, especially when using the iterative approach to maximize the number of activated reactions subject to evidence constraints. Of course, when building a high-quality network model, gap filled pathways should be evaluated by experts to evaluate the evidence cited in the algorithm, to search for existing experimental evidence in favor of or refuting the suggested solutions, or to design new experiments to test the existence of the hypothesized functions in the modeled organism [43, 141]. The reported confidence metrics for annotations and for reactions will help curators target these curation efforts.

Our implementations of the likelihood-based, network-based, network-based iterative, and likelihood-based iterative gap filling workflows are available in KBase via a web service API or web-based command line interface. The integration of our implementation in KBase's infrastructure captures the provenance of modeling data and enables users to readily build new, functioning models (**Appendices B and C**). In addition to gap filling, KBase includes implementations of many other modeling and reconstruction tools such as tools for the automatic generation of compartmentalized community models [156] and phenotype reconciliation tools.

The proposed integration of likelihoods into gap filling can also serve as a tool for hypothesis generation in biology. An initial pool of potential annotations with associated likelihoods can be generated using many different methods such as protein co-localization or co-occurrence [47, 157] or from high-throughput '-omics' datasets such as metabolomics. This initial pool can be quite broad (many alternative functions for each gene). The likelihood-based gap filling approach we have outlined is

sufficiently general to incorporate likelihoods based on any type of evidence. The gap filling algorithm then selects from this broad pool of hypotheses for the new annotations that best explain a complex combination of biological observations, providing insights into enzyme promiscuity, adaptation, and evolution. Importantly, KBase is a unified platform across multiple databases and data types; the integration of likelihood-based gap filling in this platform provides a roadmap for the integration of these diverse data sets. As systems biology expands to incorporate a greater number of high-throughput biological measures, the utility of a computational framework for leveraging this vast knowledge *in toto* grows rapidly.

Methods

The likelihood-based gap filling method consists of three major steps: (1) the calculation of annotation likelihoods for each individual gene, (2) the calculation of reaction likelihoods for the cell as a whole, and (3) the use of reaction likelihoods to inform the gap filling process. Each of these steps is detailed below. The iterative gap filling approach consists of two major steps: (1) iteratively integrating gap filling solutions into a model, and (2) performing reaction sensitivity analysis to prune redundant or poorly supported reactions. We have included as part of the Supporting Information detailed tutorials on the use of the KBase web-based interface (**Appendix B**) or the web service API (**Appendix C**) to perform this analysis.

Likelihood-based and iterative gap filling workflow description

The first step of the workflow (**Figure 3.1**) is importing an annotated genome into a workspace in the KBase system. (KBase workspaces provide a way for users to store, share, and manage data objects that they have uploaded or generated by running KBase analyses.) The genes in the genome are then used to generate a draft model using the ModelSEED algorithm [46] and, for our likelihood-based approach, to compute annotation and reaction likelihoods. Next, gap filling is done on the model (either with or without likelihood weights, and with or without the iterative approach) to generate one or more solutions, which are integrated into the model to create a gap filled model. The initial gap filling solution allows growth on 'complete' media, which consists of all compounds for which the organism has transport reactions in the draft reconstruction. For iterative gap filling, the user has the option of performing a reaction sensitivity analysis to remove both poorly-supported gap filling solutions (those

with high cost) and those which have no effect on the model's solution space. Once the reaction sensitivity analysis is complete, the model is gap filled again to achieve growth on a minimal medium, which fills in more pathways and is necessary to permit simulations of Biolog data.

Generating a database of high-confidence gene annotations

In order to maximize the quality of computationally inferred functions of query genes, it was necessary to build a database of high-confidence gene annotations to compare against. We compiled a list of the protein sequences for all proteins whose function was either literature-supported or called as part of at least one SEED subsystem [54]. The functional annotations in the SEED subsystems are manually curated using multiple sources of information such as sequence similarity, phylogeny and gene context, and therefore represent a high-confidence reference set.

To minimize the amount of redundancy in the list of target proteins, they were binned into organism taxonomic units (OTUs) with roughly 97% 16S rRNA similarity [158]. The final target database included at most one protein from each OTU for each functional role. When possible, the representative protein was chosen from the representative organism of the OTU, which tends to be a better-understood organism with higher-quality annotations such as *Escherichia coli* K-12. If the representative organism for an OTU did not have a protein with that role in a subsystem or with a literature backing, a representative protein was chosen at random from another member of the OTU.

Calculating annotation likelihoods

The computation of annotation likelihood scores was designed based on the principle that genes with more similar sequences are more likely to share the same function, but recognizing that these relationships are far from perfectly predictive [159]. The computation thus attempts to quantify the uncertainty in relation to the available database of high-confidence annotations. Annotation likelihoods were calculated by first running BLASTP [86, 160] with an E-value cutoff of 10^{-5} against all of the genes in the high-confidence gene annotation data set. A log-score for each (query, target) pair was computed as:

$$S_{ij} = -\log(E_{ij} + k)$$

E_{ij} is the E-value for the BLAST hit between genes *i* and *j* and S_{ij} is the log-score between them. The parameter $k = 10^{-200}$ was used to prevent the log E-value from being undefined due to a reported E-value of zero. After calculating log-scores for all (query, target) pairs, a likelihood score that each gene $i \in G_O$, where G_O is the set of genes in the organism, has a given functional annotation *a* was computed as follows:

$$p(i \in A_a) = \frac{\frac{\sum_{i \in G_O, j \in A_a} S_{ij}^2}{M}}{\frac{\sum_{i \in G_O} S_{ij}^2}{M} + PC}$$

A_a represents the set of genes with annotation *a*, $M \equiv \max_{i \in G_O} S_{ij}$ is the maximum score of BLAST hits from a gene in the query organism to a gene in the high-quality database, and $PC = 40$ is a pseudocount used to dilute the likelihoods of annotations for annotations with weak homology to the query. The pseudocount was chosen to set the likelihood of a gene having moderately high homology (E=1E-40) to a single protein in the database to 50% and has proven to yield a reasonable spread of likelihoods. According to this formulation, in order to have a high likelihood score for annotation *a*, the query protein must have strongly significant sequence similarity to proteins with that annotation and not possess similarly strong similarity to proteins with other annotations. Therefore, the metric takes into account two different sources of annotation ambiguity: divergence of sequence and disparity of annotations for similar proteins in the target database.

Calculating reaction likelihoods

Reaction likelihoods were computed from annotation likelihoods using the ModelSEED reaction database [46], which links annotations to functions, protein complexes, and finally to reactions. In the first step, gene annotation likelihoods were converted into gene-specific role likelihoods to account for the possibility that an annotation implies multiple functional roles. The likelihood that each gene $i \in G_O$ had role *r* was computed as the sum of the likelihood of all annotations that implied that role, according to the database mappings from annotations to R_r, the set of all genes with role *r*:

$$p(i \in R_r) = \sum_{A_a \to R_r} p(i \in A_a)$$

This definition ensures that if a protein could be multi or single-functional, the final reaction likelihoods reflect both of those possibilities.

In the second step, the overall likelihood that *at least one* gene in G_O had role *r* was computed as the maximum likelihood of the role across all its genes.

$$p(R_r \cap G_O \neq \emptyset) = \max_{i \in G_O} p(i \in R_r)$$

The genes most likely to fulfill role *r* (within 80% of the maximum) were retained and linked with an OR relationship to form a Boolean Gene-Function relationship.

In the third step, the ModelSEED reaction database was used to compute the likelihood of existence of protein complexes from the likelihood of existence of functional roles within the cell. A protein complex represents a set of functional roles that must all be present for a complex to exist. Hence, the likelihood of the existence of a complex *c* in the cell was computed as the minimum likelihood of the roles associated with it.

$$p(c) = \min_{R_r \to c} p(R_r)$$

The individual functions in the complex were linked with an AND relationship to form a Boolean Gene-Protein relationship.

In the fourth step, reaction likelihoods were computed from protein complex likelihoods using complex-reaction links in the ModelSEED. Since multiple complexes can independently catalyze a reaction, the likelihood of the existence of a reaction *x* in the cell was computed as the maximum likelihood of the possible complexes that could catalyze it.

$$p(x) = \max_{c \to x} p(x)$$

The complexes that could catalyze the same reaction were linked with an OR relationship to form a Boolean Gene-Protein-Reaction relationship (GPR) [161]. Only complexes with a likelihood within 80% of the maximum complex likelihood associated with a reaction were retained in the GPR for that reaction. The computed GPR was used in simulations of gene knockouts for gap filled reactions, and the reaction likelihoods were used as weights in the objective function for likelihood-based gap filling (see below)

Draft metabolic models and network-based gap filling

The ModelSEED methodology for building draft metabolic models from a gene annotation has been previously described [46, 145]. The network-based gap filling approach, used in the ModelSEED for auto-completing models [46], has also been described previously [77, 145]. Details are available in **Appendix A**.

Likelihood-based gap filling

The likelihood-based gap filling approach uses the same MILP formulation as network-based gap filling. However, likelihood-based gap filling uses reaction likelihoods to re-weigh the objective coefficients. To do this, the likelihoods of reactions *p(x)* are first converted into costs *C(x)* by inverting them:

$$C(x) = \max(1 - p(x), 0)$$

Then, modified gap filling objective coefficients $\lambda_{gapfill,x}$ are computed as follows:

$$\lambda_{gapfill,x} = C(x)\left[1 + P_{kegg} + P_{structure} + P_{knownΔG} + P_{Role} + P_{transporter}\right] + P_{unfavored}\left(12 + \frac{\Delta G^{0m}_{x,EST}}{10}\right)$$

where $\lambda_{gapfill,x}$ is the objective coefficient in the gap filling formulation for reaction x and the P-values represent the parameters used in the existing network-based approach that penalize different reactions in the database (see **Appendix A**). In our modified formulation, higher-likelihood reactions are given lower costs (though the thermodynamic penalties for adding a reaction in the wrong direction are not

changed) and are therefore favored in the optimization provided their benefit outweighs costs of other reactions in a pathway. The numeric parameters (12 and 10) in the equation make changing the reversibility of a reaction with low estimated Gibbs energy equivalent to adding (on average) one to two intracellular reactions in a favorable direction, while changing a reaction with reaction with an estimated Gibbs energy of 10 kCal/mol is equivalent to adding three average intracellular reactions in a favorable direction.

Iterative gap filling

In targeted gap filling, a single reaction (e.g., biomass production) is targeted to enable a non-zero reaction rate under a specified media condition. In iterative gap filling, all reactions in the model that are associated with one or more genes are targeted to enable flux. Iterative gap filling is similar to the previously gap find and gap fill algorithms [77], but operates on inactive reactions rather than dead-end or orphaned metabolites. This is accomplished by performing targeted gap filling on one reaction at a time until as many reactions as possible are functional. The results of iterative gap filling depend on the order in which the targets are processed. In our studies, the order was selected based on the region of metabolism in which the reaction occurs. Central carbon reactions were gap filled first to ensure that core metabolism was functional. These were followed by reactions involved in biosynthesis of essential metabolites (amino acids, nucleotides, and cofactors), finally culminating in reactions involved in peripheral utilization and degradation pathways.

After ordering reactions according to this priority, flux variability analysis [93] was used to determine if each reaction had a non-zero maximum flux. If the maximum flux was zero, gap filling (likelihood or non-likelihood-based) was run to attempt to activate the reactions with pathways from the ModelSEED reaction database. If a gap filling solution was found, it was integrated into the model before moving onto the next reaction in the model. The final result was a set of pathways that activated a maximum number of reactions in the model.

Reaction sensitivity analysis

Since iterative gap filling attempts to fill the maximum number of gaps in a model, solutions that fill different gaps in the model are often redundant or very poorly supported. To solve this problem, we

have implemented a reaction sensitivity analysis that identifies for each gap filled reaction: a) whether each gap filled reaction causes other reactions in the model to become inactive when it is removed and b) whether the gap filled reaction is predicted to be essential for growth. Gap filled reactions which were non-essential and which did not activate any other reactions in the network were removed. For network-based iterative gap filling, reaction sensitivity was done on all reactions in the reverse order in which they were added, so that lower-priority gap filling solutions would be tested for removal first. For likelihood-based iterative gap filling, reaction sensitivity analysis was done in order from lowest to highest likelihood so that gap filled reactions that were unsupported by genetic evidence would be tested for removal first.

Phenotype simulations

The ModelSEED algorithm [46] was used to build a draft model for each of 22 organisms for which either gene knockout lethality data (8 organisms), Biolog data (9 organisms), or both (5 organisms) was available [90, 162-173]. All four gap filling workflows (targeted network-based, targeted likelihood-based, iterative network-based, and iterative likelihood-based) were independently applied to the draft model to build working models of each of these organisms (**Figure 3.1**). The gap filled models were verified to predict positive biomass production on Carbon-D-Glucose media using flux balance analysis [37] before performing further simulations.

To simulate gene knockout lethality phenotypes, the models growing on Carbon-D-Glucose media were first further gap filled (if necessary) to achieve nonzero biomass production on the media in which knockout experiments had been performed (this was only necessary for *Mycobacterium tuberculosis*). Subsequently, the knockouts were simulated by evaluating the Boolean GPR rules for each reaction and setting the maximum rate of each reaction whose GPR evaluated to FALSE to 0. Flux balance analysis was then used to maximize the biomass equation. The knockout was considered lethal if the predicted biomass production rate was less than $10^{-9} hr^{-1}$.

To simulate biolog data, the models growing on Carbon-D-Glucose media were modified to possess transporters for every compound in every media in the biolog array. After this modification, growth on each medium was tested by setting exchange reactions for each compound not in the media to zero and

using flux balance analysis to predict the biomass production rate. The model was considered non-growing if the predicted biomass production rate was less than $10^{-9} hr^{-1}$.

Workflow implementation details

All gap filling for this manuscript was performed outside of KBase using CPLEX under an academic license (IBM Corporation, version 12.5) [174]. Due to licensing restrictions, gap filling performed on KBase servers is done using SCIP 3.0.2 [175]. Phenotype simulations and sensitivity analysis were performed using GLPK version 4.43. The gap filling and likelihood computations are implemented in the KBase framework with web service APIs and a web interface (http://iris.kbase.us). Detailed descriptions of all steps in the workflow are available in **Appendices B and C**.

Acknowledgements

MNB and NDP gratefully acknowledge support from the Department of Energy awards #DE-FG02-10ER64999 and ER65103 and the Camille Dreyfus Teacher-Scholar Award. MM and NC gratefully acknowledge support from the Center for Individualized Medicine at the Mayo Clinic, the Minnesota Biotechnology Partnership, and from the Mayo Clinic Research National Institutes of Health (NIH) Relief Grant Program. CSH acknowledges support from the Office of Science, Office of Biological and Environmental Research, of the US Department of Energy under contract number DE-ACO2-06CH11357, as part of the DOE Systems Biology Knowledgebase.

Supplemental material

Supplemental text and figures for this chapter are provided as **Appendices A, B, and C** of the thesis.

Figures and Tables

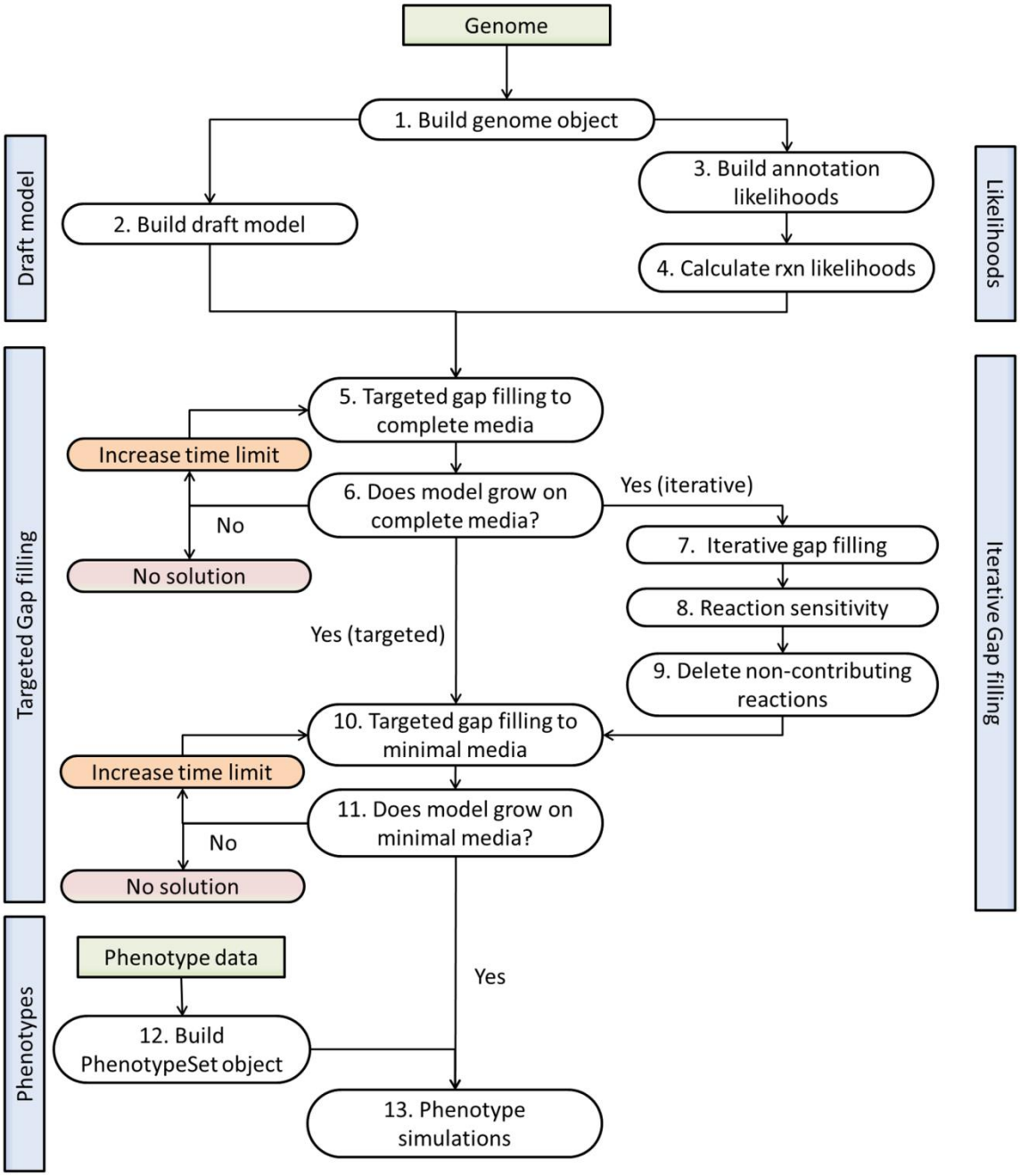

Figure 3.1. Gap filling workflows. We have developed four gap filling workflows and used them to generate the results in this paper: targeted network-based gap filling, targeted likelihood-based gap filling, iterative network-based gap filling, and iterative likelihood-based gap filling. The individual steps are described in detail in the methods, and the technical details of running them using the web interface are described in the supplementary material. Green boxes represent inputs to the workflows.

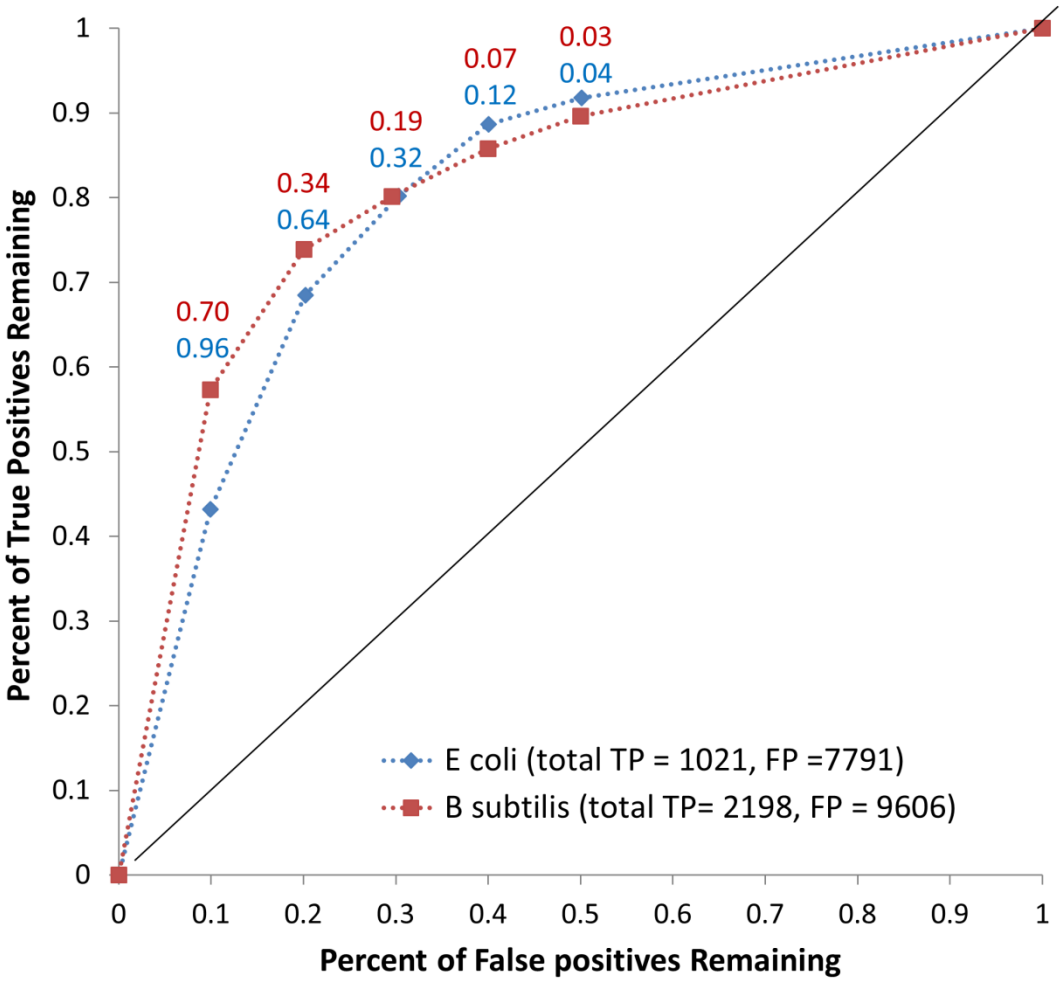

Figure 3.2. ROC curve for annotations. We computed the likelihood of all possible gene-reaction pairings from the ModelSEED database and compared the likelihoods of those pairings present in the iJR904 *E. coli* and iBSU1103 *B. subtilis* models ('true positives') to those which were not ('false positives'). Each point in the curve represents the percentage of true and false positive linkages remaining at different likelihood cutoffs (labeled on each point). We found that there was a significant enrichment of true positives at high likelihood levels and false positives at low likelihood levels compared to random assignment (solid line).

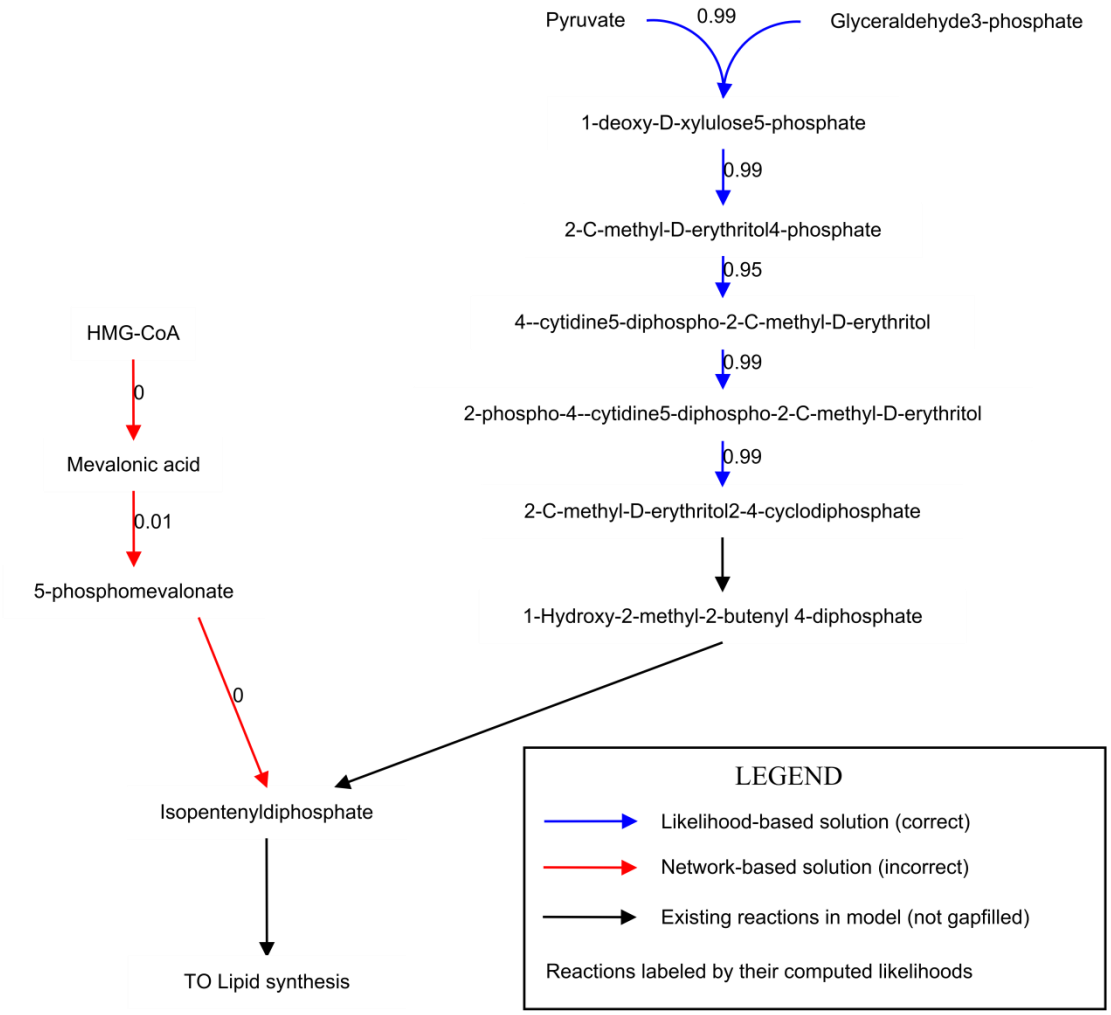

Figure 3.3. Proof of principle: Gap filling highly-likely reactions in *B. subtilis*. *B. subtilis* synthesizes lipids via the non-mevalonate pathway (blue) [155]. We removed this pathway from the *B. subtilis* genome-scale model and then tried to fill the gap using both the likelihood and network-based approaches. The network-based gap filling approach instead filled the gap with the mevalonate pathway (red), which is shorter but not supported by genetic evidence. The likelihood-based approach filled the gap with the correct pathway. Black indicates reactions that were not knocked out (there was no explicit link to literature evidence in the *B. subtilis* model). The numeric labels are the computed likelihoods of gap filling reactions.

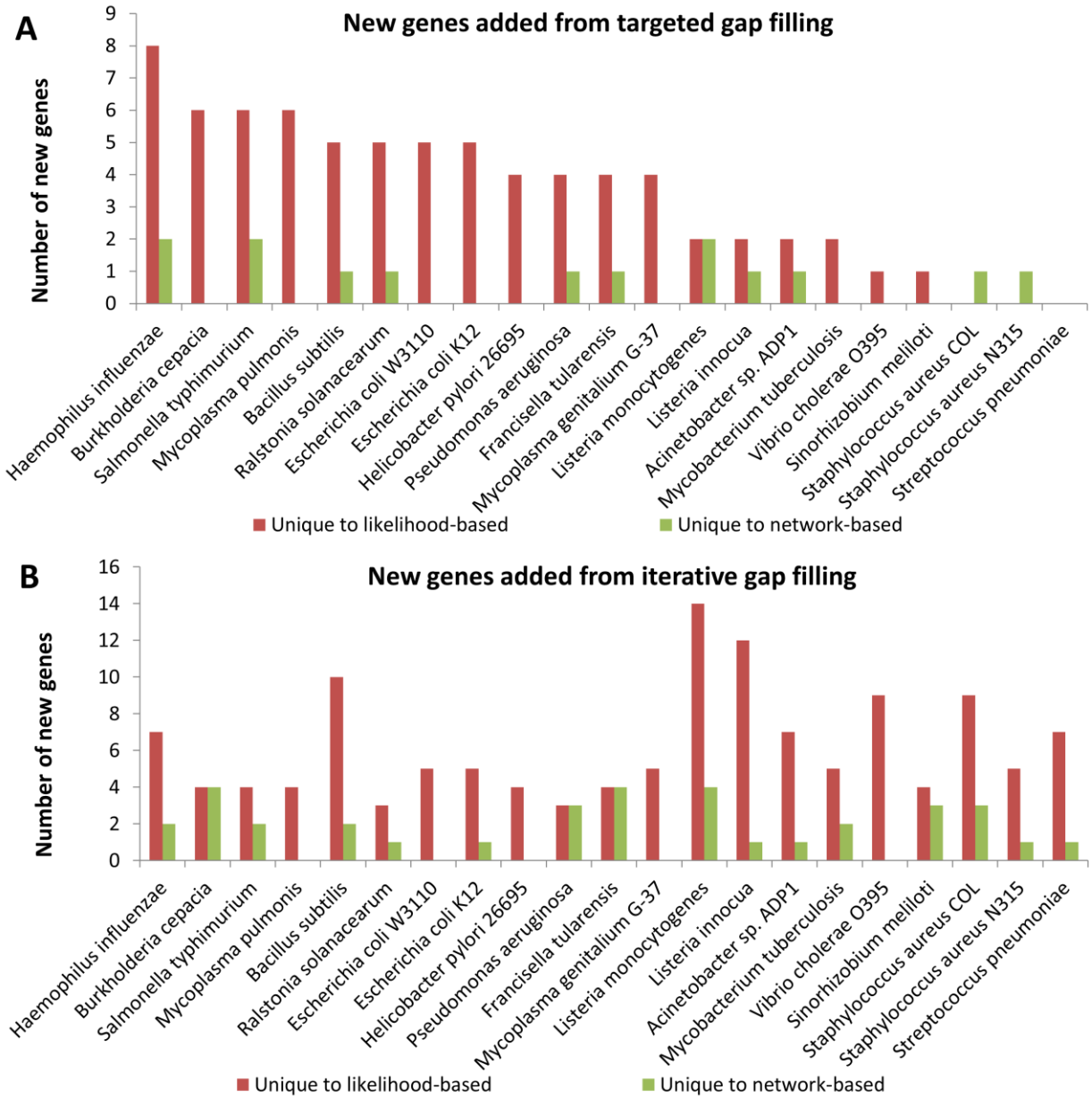

Figure 3.4. Genes added to the model using likelihood-based and network-based gap filling. Likelihood-based gap filling produced more new gene annotations than post-processing gap filled reactions generated using the network-based approach. The plot shows the number of uniquely-added genes by likelihood-based and network-based gap filling approaches (genes in common with both approaches are omitted for clarity but tended to be more than those unique to either approach). A) Number of genes added after targeted gap filling to activate biomass production. B) Number of genes added after iterative gap filling.

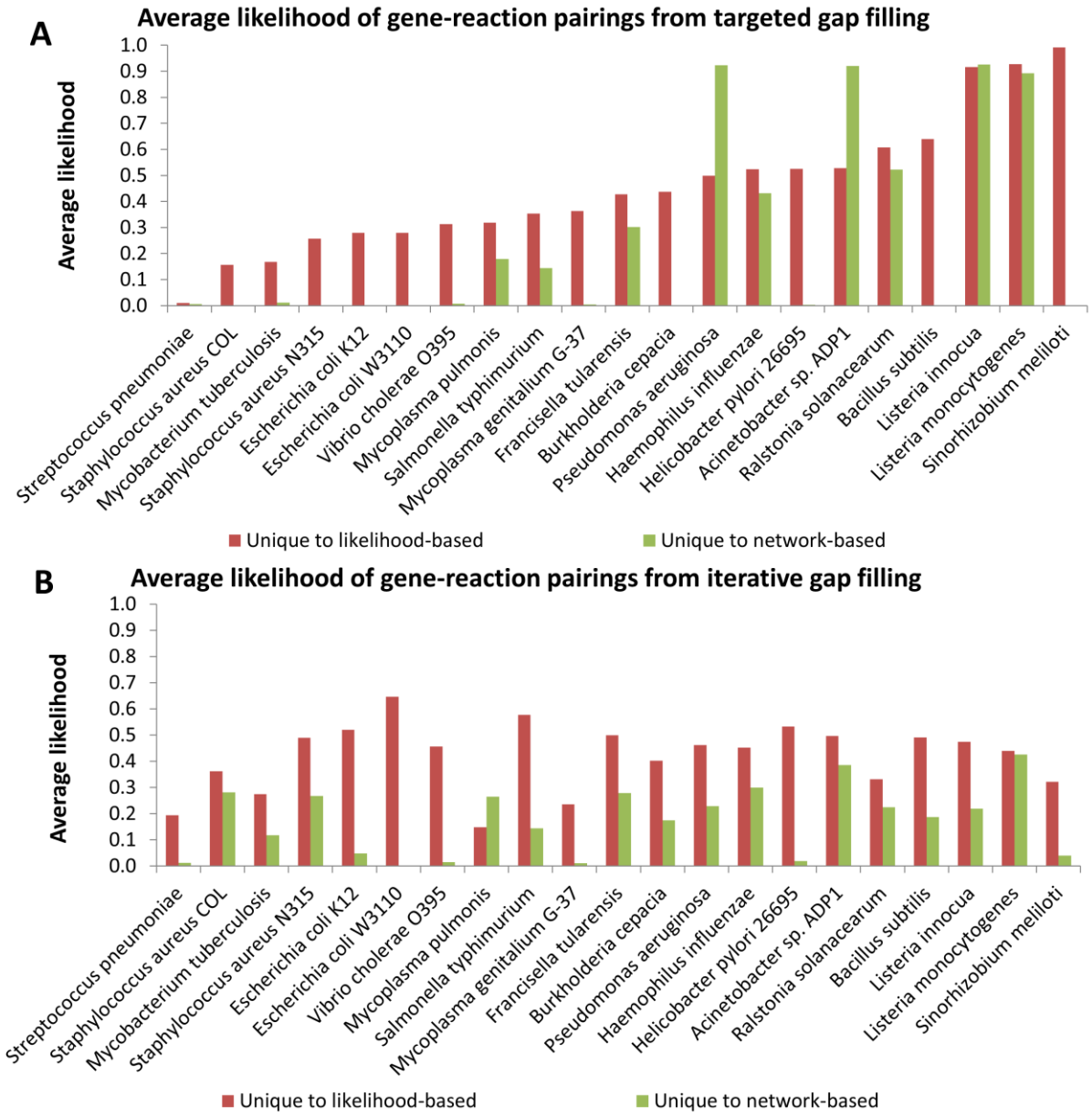

Figure 3.5. Likelihoods of gene-reaction associations added using likelihood-based and network-based gap filling. The average likelihood of links between genes and reactions that were added using likelihood-based gap filling tended to be greater than the average likelihood of links resulting from post-processing the network-based gap fillingresult. Note that it was not greater for all models (e.g., *Pseudomonas aeruginosa*) because the likelihood-based gap filling approach maximizes likelihood of reactions, not annotations, and as a result picks fewer reactions with 0 likelihood (no predicted gene associations). A) Targeted gap filling result. B) Iterative gap filling result.

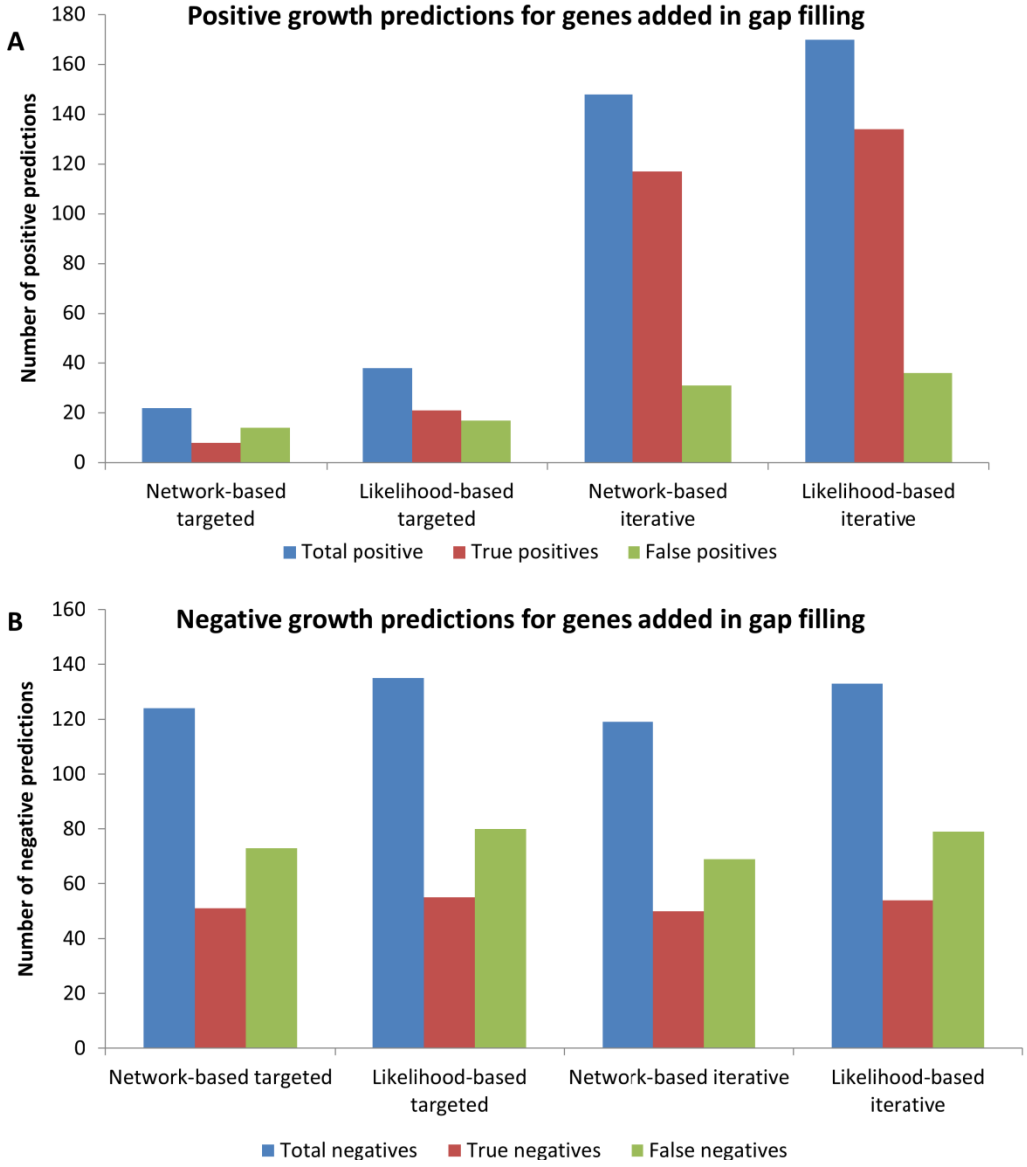

Figure 3.6. Knockout lethality accuracy for genes added in gap filling. Gene knockout simulations were performed for models gap filled with each of the four workflows to assess the consistency between lethality prediction and knockout lethality data for genes added in gap filling. Likelihood-based gap filling was able to produce the most candidate gene associations, with high specificity and low sensitivity in lethality predictions. The difference in accuracy between likelihood-based and network-based gap filling was not statistically significant. A) Number of positive growth predictions, B) Number of negative growth predictions.

Table 3.1. Average phenotype consistency across all test organisms for models gap filled using the four evaluated algorithms. Iterative gap filling greatly increased the sensitivity (more correct positive growth conditions) and reduced the specificity (more incorrect positive growth conditions) of Biolog simulations. The use of likelihoods did not have a significant effect on the specificity or sensitivity of Biolog simulations. The overall model accuracy for essentiality data was similar for all four algorithms because genes added due to likelihood-based gap filling represented only at most about 7% of the genes in the model. See **Figure 3.6** for the results of knockout simulations using only genes added to gap filling solutions.

	Biolog data		**Essentiality data**	
	Sensitivity	**Specificity**	**Sensitivity**	**Specificity**
Targeted network-based	56%	70%	86%	66%
Targeted likelihood-based	56%	70%	84%	67%
Iterative network-based	67%	57%	86%	64%
Iterative likelihood-based	67%	55%	85%	65%

Chapter 4: ITEP: An integrated toolkit for exploration of microbial pan-genomes.[4]

Abstract

Background

Comparative genomics is a powerful approach for studying variation in physiological traits as well as the evolution and ecology of microorganisms. Recent technological advances have enabled sequencing large numbers of related genomes in a single project, requiring computational tools for their integrated analysis. In particular, accurate annotations and identification of gene presence and absence are critical for understanding and modeling the cellular physiology of newly sequenced genomes. Although many tools are available to compare the gene contents of related genomes, new tools are necessary to enable close examination and curation of protein families from large numbers of closely related organisms, to integrate curation with the analysis of gain and loss, and to generate metabolic networks linking the annotations to observed phenotypes.

Results

We have developed ITEP, an Integrated Toolkit for Exploration of microbial Pan-genomes, to curate protein families, compute similarities to externally-defined domains, analyze gene gain and loss, and generate draft metabolic networks from one or more curated reference network reconstructions in groups of related microbial species among which the combination of core and variable genes constitute the their "pan-genomes". The ITEP toolkit consists of: (1) a series of modular command-line scripts for identification, comparison, curation, and analysis of protein families and their distribution across many genomes; (2) a set of Python libraries for programmatic access to the same data; and (3) pre-packaged

[4] This chapter uses previously published, open-access material and is reprinted with the permission of the publisher. The citation is as follows:

Benedict MN, Henriksen JR, Metcalf WW, Whitaker RJ, Price ND: **ITEP: An integrated toolkit for exploration of microbial pan-genomes.** *BMC Genomics* 2014, **15**:8.

scripts to perform common analysis workflows on a collection of genomes. ITEP's capabilities include *de novo* protein family prediction, ortholog detection, analysis of functional domains, identification of core and variable genes and gene regions, sequence alignments and tree generation, annotation curation, and the integration of cross-genome analysis and metabolic networks for study of metabolic network evolution.

Conclusions

ITEP is a powerful, flexible toolkit for generation and curation of protein families. ITEP's modular design allows for straightforward extension as analysis methods and tools evolve. By integrating comparative genomics with the development of draft metabolic networks, ITEP harnesses the power of comparative genomics to build confidence in links between genotype and phenotype and helps disambiguate gene annotations when they are evaluated in both evolutionary and metabolic network contexts.

Introduction

Technological advances in DNA sequencing have led to rapid increases in sequencing throughput and a decrease in sequencing cost [176]. These advances have enabled comparative studies of the whole genomes of many related species [177]. Such genome analyses have provided valuable insights into evolutionary mechanisms, diversity, and adaptability of life to environmental variation [72, 178, 179] as well as key trait variations among industrially or medically important strains [51, 53, 180, 181].

Identifying orthologs and orthologous protein families is an important step towards understanding and interpreting genome variation [182]. However, there is no single method that correctly predicts orthology in all cases, leading to the development of many different methods targeting different applications [183]. Due to the use of different algorithms and parameters used to perform clustering, automatically computed databases of orthologs often predict different protein families for the same proteins [66, 184]. Since orthologs are often taken to have the same function, these differences lead to differences and thus to uncertainty in the predicted functions of the genes [183].

Further confounding the ability to automatically infer protein function, clustering efficacy depends on the evolution rate of those families, which can vary widely [185]. The need to carefully curate protein functions and gene calls is also compounded by a rapid increase in the number of incomplete genomes [186], including the approximations to single-species genomes that arise from metagenomic assemblies [187]. Careful examination of gene calls and functional annotations is particularly important for accurately assessing the gain and loss of function in these incomplete genomes because genes are often left uncalled or incorrectly annotated due gene fragmentation or sequencing errors (leading to erroneous frame shifts or nonsense mutations).

A number of software packages have been developed to integrate orthologous group identification, visualization tools, and common comparative analyses based on protein content [59, 60, 62-64, 188-190]. However, due to the challenges cited above, many of these analyses require manual curation, which is difficult to scale to hundreds of genomes. Additional tools are necessary to help researchers curate annotations and evaluate the integrity of protein families across related genomes.

We present ITEP, a modular bioinformatics toolkit for the generation, curation, and analysis of protein families across closely-related microbial genomes in which the combination of core and variable genes constitute their "pan-genomes". The toolkit provides a consistent command-line interface between a user's genomic data and existing tools for protein family prediction by clustering, ortholog detection, analysis of functional domains, identification of core and variable genes and gene regions, alignments and trees, cluster curation, and the integration of cross-genome analysis and the generation of draft metabolic networks for study of metabolic network evolution. The toolkit makes it easier to identify and fix problems such as inaccurate annotations and missing (un-called) genes and to study the evolutionary history and physiological implications of the curated families. ITEP's architecture enables researchers to rapidly develop their own customized comparative analysis workflows, which are easily automated, allowing users to focus their curation effort, rapidly generate and test hypotheses, and build accurate metabolic networks.

Methods

The ITEP toolkit is a collection of Python and BASH scripts that interface with an SQLite database backend (**Additional file 1**) and a large number of existing tools to organize and analyze genomic content across related genomes (see **Figure 4.1** for overview). The toolkit runs on Linux natively; a virtual machine is also provided that includes a complete ITEP installation, which can be run on any operating system (linked to from the project homepage at https://price.systemsbiology.net/itep). The toolkit includes: (1) convenient functions for genome importing and formatting, (2) modular analysis scripts that can be linked by piping to quickly and flexibly create workflows, (3) several convenient wrapper scripts that link other functions together to perform common analysis and visualization, and (4) a set of underlying Python libraries for programmatic data access. Interfaces are available for processing genomic data from the GenBank database [191], RAST [192], or the DOE KnowledgeBase [193]. Standard GenBank files (.gbk) from any other source may also be imported into ITEP by running them through a provided pre-processing script.

ITEP's SQLite database stores information on gene locations, annotations and sequences, sequence homology data, *de novo*-computed protein families, protein similarities to externally defined orthologous groups (such as COGs), and the DNA sequence of each contig for every imported genome. Protein families are generated by creating a graph of similarities between proteins and running a clustering program (the most strongly supported clustering program is MCL [194], but a user can use any other clustering program as long as outputs are provided in the correct format). Setup scripts are provided to readily import these data into the SQLite database.

After the database is built, the user can use provided command-line scripts to access subsets of the data within it and perform the supported analyses (**Figure 4.1**). Most of the command-line access scripts are pipe commands, in which the output from one command is used as an input to another using pipes (|). This architecture allows users to rapidly prototype analyses and subsequently automate them in a Bash script. Many of the database access scripts generate tab-delimited outputs that are convenient for further command-line processing or import into spreadsheets. ITEP also contains commands to visualize phylogenies and gene context for genes in the database using freely available Python packages [195, 196] or export data to standard formats such as FASTA alignments and Newick files which are widely

supported in other visualization and bioinformatics software. Many of the same analyses implemented in the command-line scripts are also accessible programmatically via a set of Python libraries to aid developers who wish to build their own tools upon ITEP's data structures. Finally, pre-packaged workflow scripts are provided for common analysis tasks such as the generation of concatenated core gene trees. These can be used to quickly obtain a result or as a working starting point from which to develop new analysis pipelines.

De novo clustering for computation of protein families

Running the BLASTP program [86] all vs. all provides a graph of similarities between pairs of proteins, in which the genes are nodes and each significant pairing is an edge weighted by some similarity metric. The ITEP toolkit's setup scripts directly support the generation of protein families *de novo* by clustering these graphs using the Markov Cluster (MCL) algorithm [197]. The toolkit allows many different definitions of the homology graph: it can be generated from arbitrary subsets of organisms in the database with arbitrary cutoffs and inflation parameters (clustering sensitivity), and three scoring metrics that emphasize different aspects of the protein pair homology (**Additional file 2**) [197-199].

A user can also import results from any other orthologous family prediction method, allowing flexibility that is necessary due to differences in the strengths and weaknesses of individual algorithms. All downstream analyses (e.g. phylogenetic analysis of gene gain and loss) can then be performed in the same manner as if the clusters were generated using MCL. For example, a wrapper function is provided to interface between the ITEP database and OrthoMCL, a program that applies a percent identity cutoff between pairs of homologous proteins, identifies likely orthologs by using a modified bidirectional-best-hits approach, and then runs MCL to cluster the smaller subset of nodes and edges into protein families [200]. It thus performs MCL only on filtered subsets of the homologous pairs of organisms rather than simply applying a simple cutoff for a homology score. The consistent storage of clustering results from multiple different clustering methods in a single database enables users to easily compare the effects of the choice of clustering algorithm and the choices of organisms to cluster on the predicted protein families.

Protein family curation and visualization tools

Several biological and non-biological variables can cause automatically computed protein families to be incorrect or incomplete, such as the presence of gene fusions or multiple-domain proteins, incomplete or inaccurate gene calling, sequence and/or functional divergence, and the lack of rate homogeneity in evolution rates. In light of these challenges and in order to increase confidence that conclusions about the evolution of protein families are correct, we have implemented tools to generate and visualize multiple alignments and trees for protein families, to study gene neighborhoods of genes in a family, to search for possibly missing genes, and to assess the function of proteins in the light of their conserved domain architecture.

Multiple alignments and phylogenetic trees are useful to analyze the phylogenetic history of particular protein families and to sort out the potential presence of paralogs [201]. The ITEP toolkit contains convenient interfaces for generating protein and nucleotide alignments [202, 203], curating alignments [204], and generating maximum-likelihood phylogenies [205, 206]. ITEP's tree visualization capabilities provide an interface between a user's genomic data and the ETE Python package for tree manipulation and rendering [195]. The ITEP scripts include the option of appending gene neighborhood information to a protein tree, which is useful for identifying the functions of novel genes [64, 207]. The user also has the option to attach numeric data (as a heatmap) or arbitrary text tables to any tree (see **Figures 4.2, 4.3**).

To help identify missing genes, we have implemented an interface that links genomic data in ITEP to tBLASTn, which is useful for finding genes that are fragmented, miscalled (e.g. with frameshifts or nonsense mutations resulting from sequencing errors), or that are not yet annotated [65]. The ITEP interface to tBLASTn identifies significant hits from a set of query genes to a particular genome (or set of genomes) in the database, and then automatically identifies whether the hit was to a called gene and whether the called gene was on the same strand as the hit. From this result, a researcher can examine and (if appropriate) add missing proteins to protein families. The gene neighborhood and tree generation and visualization scripts support the visualization of tBLASTn hits in their genetic context in the same manner as called genes (see **Figure 4.3**). We have also provided a tool that attempts to identify frame shifts, insertions, and nonsense mutation events from the tBLASTn results, which helps identify

specific mutations that could lead to loss of function or that could indicate errors in the genome sequence.

Finally, to assist the curation of annotations, we have implemented automatic generation and storage of RPSBLAST hits to the NCBI CDD database [208]. The interface allows a user to rapidly search for the IDs of conserved domains that correspond to certain keywords (such as “purine synthesis”) and to identify all proteins in a genome that have significant homology to a specific set of conserved domains. ITEP also includes tools for identifying and visualizing all conserved domains that are found in a specific query protein or set of proteins (**Figure 4.4**), providing insight into the functions of those proteins.

Analysis of core and variable gene content

Studying gene gain and loss and examining the core (conserved) and variable (non-conserved) genes in a collection of organisms can provide insights into the plasticity of cellular functions and can be used to identify genes that define a clade [209]. To assist such analyses, ITEP includes functions that identify interesting subsets of genes based on presence and absence patterns, such as genes that are present in *all* of a particular group of organisms (conserved genes), *any* members of a group (present genes), *only* members of that group relative to those all of the organisms to generate the protein families (unique genes), or *none* of the members of that group. The script can also optionally identify genes that are conserved in any given fraction of a group of organisms, allowing for some flexibility due to missed gene calls or divergent sequences. Finally, if an organism phylogeny is available (or built with other ITEP scripts), a tool is also available to identify presence and absence patterns based on each phylogenetic clade, allowing a researcher to, for example, identify all of the genes that are conserved in or unique to each individual species or all genomes in a clade.

Integration with metabolic networks

A key reason to identify protein families is to use the results to propagate annotations and subsequently identify the physiological capabilities of an organism based on those of its relatives. In the context of genome-scale metabolic modeling, the predicted presence or absence of particular protein families may be used as evidence for the presence or absence of reactions in a metabolic network. In a metabolic network reconstruction, the relationship between a gene and the reactions catalyzed by the encoded

enzyme is typically encoded in a Boolean gene-protein-reaction relationship (GPR), in which complexes and other sets of genes that must all be present for a reaction to occur are given an AND relationship, while isozymes or sets of genes with unknown relationships are given an OR relationship [43]. To assess whether a reaction is catalyzed or not within a cell, each associated gene is assigned a 1 (TRUE) if it is present and a 0 (FALSE) if it is absent, and then the GPR is logically evaluated. If the GPR evaluates to TRUE then the reaction is present and otherwise it is absent.

We have implemented a function in ITEP that directly evaluates Boolean gene-protein-reaction relationships associated with existing metabolic reconstructions of strains in the database based on the presence-absence calls of *de novo* clustering with arbitrary parameters. In this way, a researcher can rapidly generate draft metabolic network reconstructions based on genomic comparisons with one or more reference networks. Subsequently, these network reconstructions can be curated to generate high-quality models of each related organism.

Results

Test data set

We chose to use the Group 1 Clostridia as a test case to illustrate capabilities of the ITEP toolkit. This metabolically diverse phylogenetic clade includes industrially important organisms such as the solventogenic organisms *Clostridium acetobutylicum* and *C. beijerinckii*, as well as several medically important strains such as *C. perfringes* and *C. botulinum* [210]. *C. botulinum* and *C. perfringes* genomes have both been heavily sampled, therefore providing the opportunity to study genetic differences at both species and at the genus-scale. In addition, manually-curated metabolic models are available for *C. acetobutylicum* ATCC 824 [211, 212] and *C. beijerinckii* NCIMB 8052 [31], affording an opportunity to use ITEP to examine metabolic differences between these and the other *Clostridium* species in the clade.

The species belonging to the Group 1 Clostridia were determined based on the PATRIC database [213] and the ARB Living Tree 16S rRNA tree [214]. All complete and draft genomes from this group were downloaded from RefSeq in March 2013 (including plasmids) along with the genome of an outgroup organism, *Acetobacterium woodii*. Overall, 26 complete and 26 incomplete Clostridia genomes were

downloaded and analyzed (see **Additional file 2** for complete strain names and RefSeq accession numbers).

The test dataset was chosen to be relatively small for purposes of illustration. ITEP currently supports creation of databases containing up to about 200 genomes on a modern workstation with 1TB of hard drive space, 16 GB of RAM, and 12 processors (using which all vs. all BLAST, MCL, and RPSBlast would take about 6 days altogether). Disk space and time requirements grow as $O(N^2)$ where N is the number of genomes.

In this example, MCL was used to perform clustering and predict protein families. The relative strengths of this and other methods for predicting protein function have been reviewed at length [184, 215-217]. Importantly, if the user desires to use different algorithms for clustering, ITEP supports exporting subsets of BLAST data in formats convenient for import into clustering tools, importing the clustering results back into the SQLite database, and applying the same workflows as described here to interpret and curate them.

Complete tutorials for performing the analyses described in this section and many others are available in the package documentation (included as **Additional file 5**). A link to an up-to-date web version of this documentation is linked to from the project website (https://price.systemsbiology.net/itep).

Analysis of gene gain and loss patterns across phylogeny

As a starting point for the analysis of the Group 1 *Clostridia* pan-genome, we used ITEP to compute the number of conserved gene families (one member or more in every organism) in each clade in the Group 1 *Clostridia* and in *A. woodii* (**Figure 4.2**). The results indicate that a large number of genes are conserved between closely related strains (such as *C. sporogenes* and *C. botulinum* A, B and F subtypes) but the number of conserved genes drops off rapidly as more diverse strains are added. The identities of the conserved genes can easily be extracted from ITEP and used to examine physiological differences between the clades of organisms and at what point a particular function was lost. In the same manner, ITEP can be used to identify gene families unique to each clade or those that are found in exactly one copy in each member. Importantly, the curation tools in ITEP can be used to verify conclusions drawn from analyzing these gain and loss patterns (see later sections for some examples).

Comparison of draft and complete genomes and curation of protein families

Draft genomes are prevalent in many environmental studies, but because they are incomplete, presence and especially absence calls are inherently less certain for them than they are for complete genomes. The grouping capabilities of ITEP are useful for evaluating the quality of draft genomes by comparing their gene content with closely related closed genomes. To illustrate this, we have generated MCL clusters including two different groups of organisms with identical clustering parameters: one group contained only the completely sequenced Group 1 Clostridia species (blue genomes in **Figure 4.3**), while the other contained both the completely-sequenced genomes and the draft genomes for strains in the same phylogenetic clades as the completely-sequenced species (green genomes in **Figure 4.3 -** only those genomes in the same clade were used to minimize differences due to species divergence). By comparing the protein content in these two groups, we found that 561 protein families were conserved in all of the completely sequenced genomes, but that 270 of them (48%) were missing in at least one of the draft genomes in the same clades (see **Additional file 2** for a complete list). The protein families that appeared to be missing in some of the draft Group 1 Clostridia genomes but not the complete ones covered many cellular subsystems, including 17 ribosomal protein families (**Figure 4.3**) and other widely conserved proteins such as the cell division protein FtsZ.

When a highly conserved gene appears to be absent in a particular genome but does not have a congruent loss pattern on the phylogenetic tree, these are candidates for missing or wrong annotations or gene calls. Importantly, ITEP includes ways to search for apparently missing genes in the incomplete genomes, making it possible to identify and correct certain types of gene calling and annotation errors. As an example, we have used the tBLASTn wrapper script in ITEP to search for copies of the L20 ribosomal protein in all of the Group 1 Clostridia and in *Acetobacterium woodii*. The search revealed a complete, uncalled copy of the L20 protein in *A. woodii* and an uncalled fragment (on the end of a contig) of a L20 protein in *C. perfringens* CPE F4969.

To find evidence that these were real L20 proteins, we used ITEP scripts to pull the homologous sequences suggested by tBLASTn out of the database, align them, and build a maximum-likelihood tree containing these proteins with neighborhoods mapped onto the tree. The multiple alignment confirmed that the newly identified L20 homologs are very similar to called ribosomal proteins in closely-related

complete genomes **(Figure 4.4 A)**, while mapping the neighborhoods of the uncalled genes revealed significant conservation of gene neighborhoods (**Figure 4.4 B)**, supporting the hypothesis that the identified proteins are really L20 ribosomal proteins and should be included in the gene annotation. The same methodology can also be applied to search for apparently missing metabolic or regulatory genes, which would help fill in gaps that appear when generating models of cellular physiology. In this way, the challenge of accurate gene annotation can be approached both from the bottom up (gene orthology) and top down (relationship to physiological functions), tying together microbial phylogeny and physiology.

Draft metabolic reconstruction and curation of metabolic protein families

The comparative analysis capabilities of ITEP can be used to generate draft metabolic networks as a starting point for generating high-quality metabolic models of organisms based on their similarity (or lack of similarity) to related genomes. To illustrate this capability, we have generated draft metabolic networks of each completely-sequenced Group 1 Clostridia strain using the published *C. beijerinckii* model [31] as a reference. This model was chosen as a reference because it is the most recent and most complete model of a member of the Group 1 *Clostridia* that has been published. We found that the presence and absence calls for metabolic functions in the other *Clostridia* were strongly dependent on the chosen homology cutoff: with a relatively stringent cutoff of 0.5, some organisms (such as *C. tetani*) appeared to be missing more than half of the 874 gene-associated metabolic reactions in the *C. beijerinckii* metabolic reconstruction, and even with a very lenient cutoff of 0.1, at least 100 of them were missing in each other organism (see **Additional file 2**). These missing reactions create gaps in the metabolic network that represent either real differences in physiology or incorrect absence calls due to methodological issues such as incorrect clustering, mis-annotation, or missing gene calls.

The presence of gaps in reconstructed networks makes it difficult to turn them into functional metabolic models [25]. The comparative genomics capabilities of ITEP can be used to help identify genes that fix gaps in metabolic pathways (either those generated by using ITEP's clustering capabilities or those built using other tools). For example, the draft metabolic reconstructions for *Clostridium botulinum* BKT105925 and *C. novyi* NT based on MCL clustering were predicted to lack the *purD* enzyme necessary for purine synthesis (down to a homology cutoff of 0.1 maxbit score). No genes were annotated to perform this function in the source GenBank files for these genomes. In an attempt to fill this gap, we

used ITEP to perform a tBLASTn search against these two organisms using the copy of *purD* from *C. beijerinckii* (Cbei_1060) as a reference. Interestingly, we found a very strong homology between the *C. beijerinckii purD* and the N-terminal end of much larger proteins in *C. botulinum* BKT105925 and *C. novyi* NT (CbC4_1757 and NT01CX_2418, respectively). Searching these genes against the RPSBLAST results that were stored in the ITEP database revealed that the large proteins from *C. botulinum* BKT105925 and *C. novyi* NT are in fact fusions of *purD* and *purL* (**Figure 4.5**), in agreement with the assignments based on MetaCyc [80], RAST [192], and the SEED [54]. Therefore, the gap in the metabolic network can be fixed by assigning the same function to both of these genes, making simulations performed using other tools [46, 91, 141] more accurate.

Conclusions

The ITEP toolkit integrates a large number of existing bioinformatics tools into a single cohesive, flexible framework for comparative analysis of physiological variation in microbial pan-genomes. The modular design of the toolkit makes it straightforward to add additional functionality to the toolkit, as illustrated by our implementation of novel tools for generation of draft metabolic reconstructions from a curated reference network. It also makes the analysis very flexible, empowering researchers to quickly develop analysis workflows while also providing a wide array of tools for curation of annotations and gene calls. The ability to rapidly curate protein families and propagate metabolic networks from reference organisms to related strains will streamline the process of generating high-quality physiological and evolutionary hypotheses and ultimately lead to an improvement in the inter-genome consistency of metabolic models of microbes.

Supplemental Material

Supplemental material related to this chapter is located online at **http://www.biomedcentral.com/1471-2164/15/8/abstract**

List of Abbreviations

AIR: Aminoimidazole ribotide; BLAST: Basic Local Alignment Search Tool; FGAM: 5'-Phosphoribosylformylglycinamidine; FGAR: N-Formylglycinamide ribonucleotide; GAR: Glycinamide ribonucleotide; GPR: Gene-Protein-Reaction relationship; ITEP: Integrated Toolkit for the Exploration of Pan-genomes; MCL: Markov Cluster (clustering algorithm); PRPP: 5-Phosphoribosyl 1-pyrophosphate; RAST: Rapid Annotation using Subsystem Technology, tBLASTn: Translated BLAST against nucleotides.

Figures and Tables

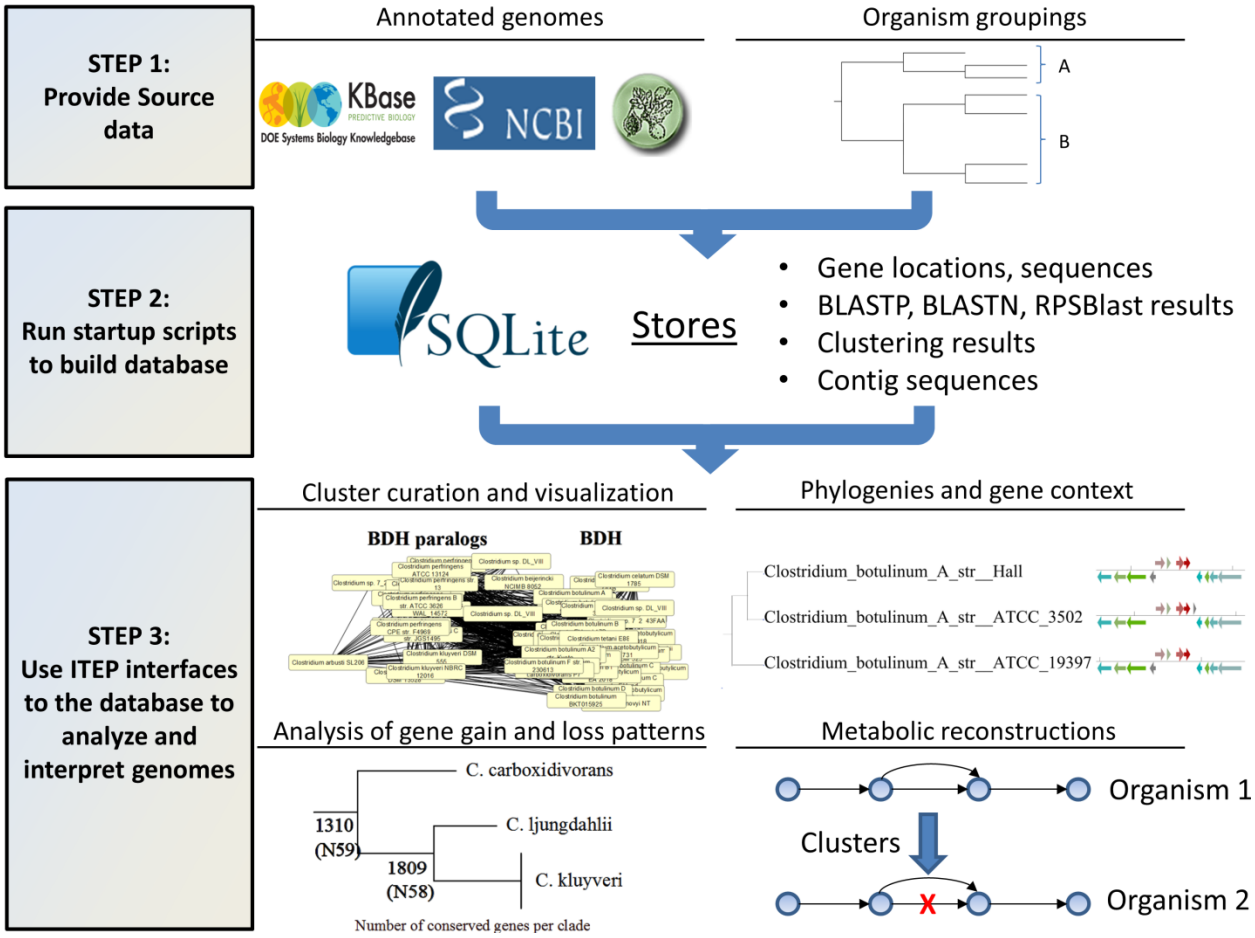

Figure 4.1. **Overview of the ITEP toolkit**. The ITEP toolkit is organized so that analyses can be performed in a three-step process. Step 1:. The ITEP toolkit takes three inputs: Genbank files of genomes; user-defined groupings of input organisms in which to identify protein families; and clustering parameters that define the details of the clustering method used to identify the families. Step 2. The user calls provided setup scripts to build a SQLite database containing pre-computed data such as homology and clustering results. Step 3:. After building the database, a user can use the provided interfaces to the database to identify core and variable genes, build protein and organism phylogenies, curate amd visualize protein families, or build draft metabolic reconstructions from a reference network. To accomplish ITEP interfaces with the SQLite database and many previously existing bioinformatics and programming packages [86, 195-197, 200, 202-206].

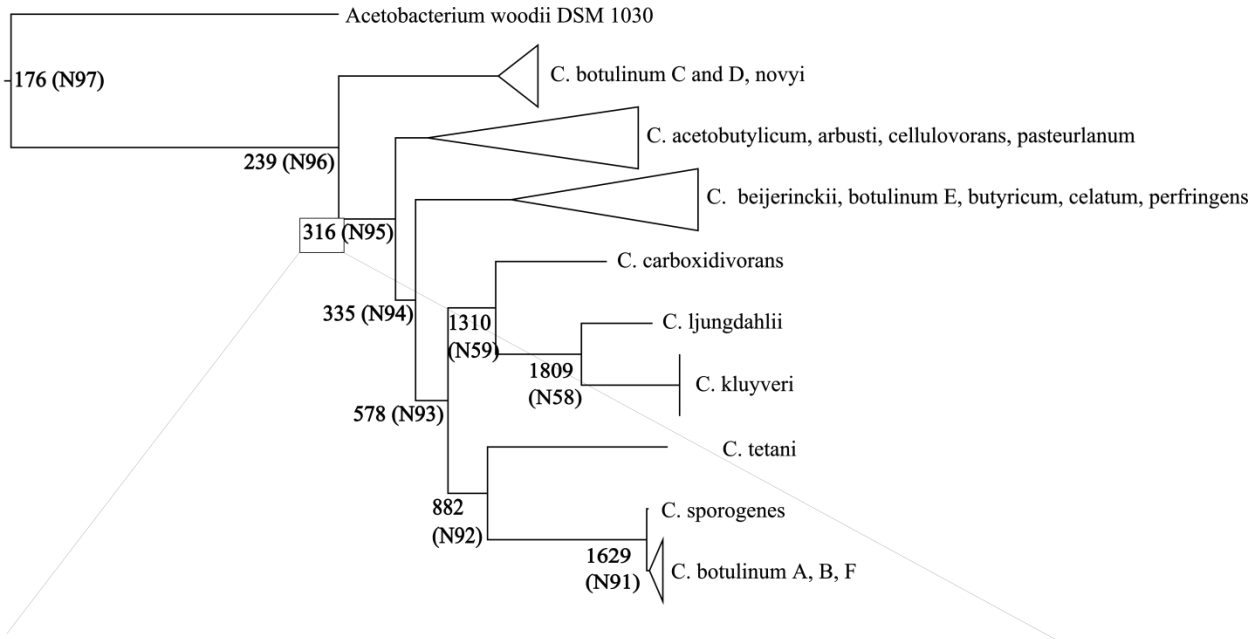

Run ID	Cluster	Functional annotation
all_l_2.0_c_0.3_m_maxbit	1	transcriptional regulator
all_l_2.0_c_0.3_m_maxbit	10	spermidine/putrescine abc transporter atp-binding protein_yp_001780207.1_cld_0189
all_l_2.0_c_0.3_m_maxbit	102	sporulation initiation inhibitor protein soj_zp_02865591.1_cpc_a0348
...		

Figure 4.2. **Illustration of ITEP's capabilities for studying gene gain and loss patterns across a phylogeny.** The node labels are the number of gene families (as computed by an MCL clustering of BLASTP results for both complete and draft genomes) that have at least one representative in each child of that node. Labels also contain a node identifier (N95) that can be used to look up the identities of all of the conserved families in tables outputted by the program. Examples of conserved families at node N95 are shown beneath the tree. The tree was generated from a concatenated alignment of ribosomal proteins uniquely identified in all of the genomes (17 families) with ITEP's scripts, using FastTree [205] and a WAG model of evolution. Clusters were generated with the parameters: MCL clustering, inflation parameter of 2.0 (default for MCL), maxbit score, cutoff of 0.3. The tree was drawn with FigTree [218].

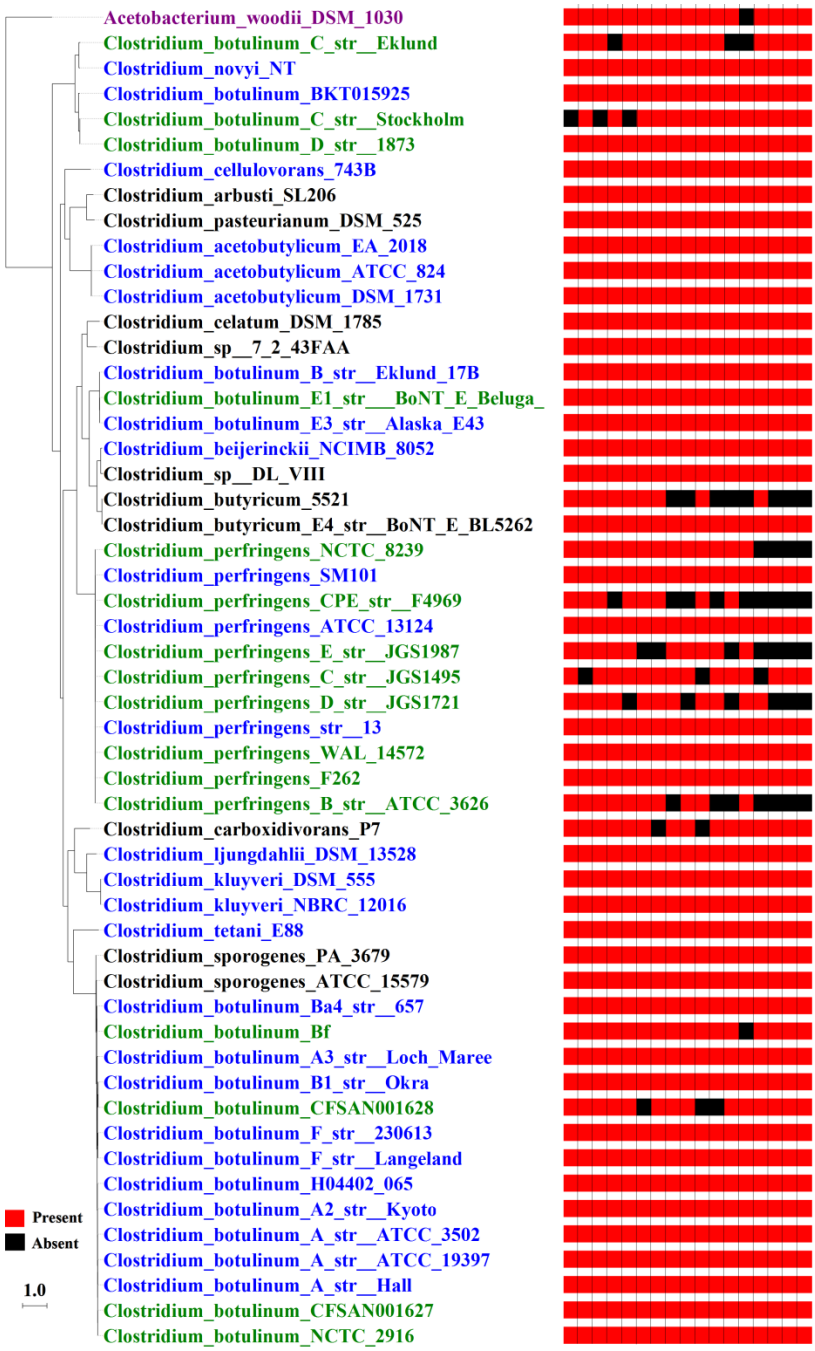

Figure 4.3. Ribosomal proteins apparently missing in draft genomes and present in all complete genomes. The heat map shows the presence (red) and absence (black) of the 17 ribosomal proteins that, according to RefSeq gene calls and the MCL clustering approach, were present in all complete Group 1 *Clostridia* genomes but missing in at least one draft genome within the same phylogenetic clades as the completely sequenced genomes. Blue strains: Completely sequenced genomes; green strains: draft genomes in the same clade as completely sequenced genomes; black strains: draft genomes in different clades from completely sequenced genomes. The tree is the same as that generated in **Figure 4.2** and was visualized with ITEP scripts with some formatting changes (genome colors and column labels).

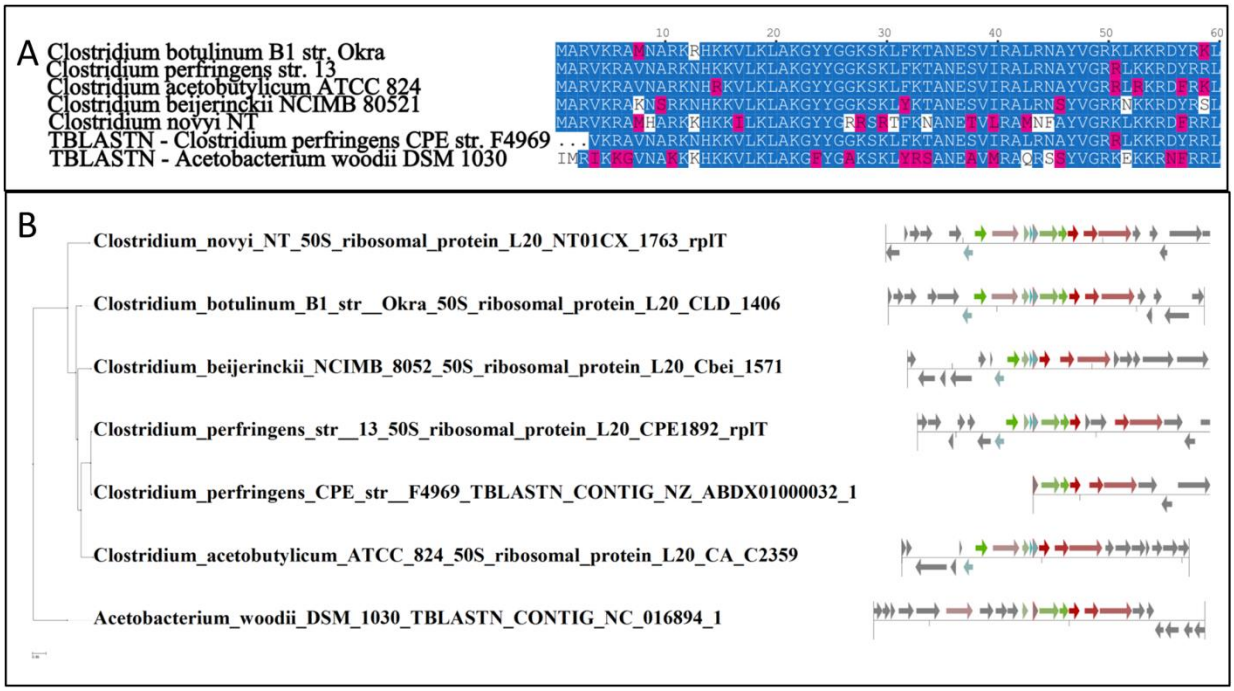

Figure 4.4. Protein family curation with ITEP. (A) A portion of the multiple alignment for the uncalled ribosomal protein L20 homologs in *Acetobacterium woodii* and *C. perfringens* str. CPE F4969, along with selected representatives of this protein from other *Clostridia*. Blue amino acids were conserved in more than 50% of the aligned proteins and pink amino acids are similar to the conserved acids. The figure in part (A) was generated by importing a multiple alignment generated by an ITEP script into the STRAP aligner [219]. (B) Gene neighborhoods for the proteins from part (A) attached to the maximum-likelihood phylogeny of the same proteins. Same-colored arrows indicate that the genes belonged to the same family according to MCL with the same parameters used to construct **Figure 4.2.** The visualization was done with an ITEP script.

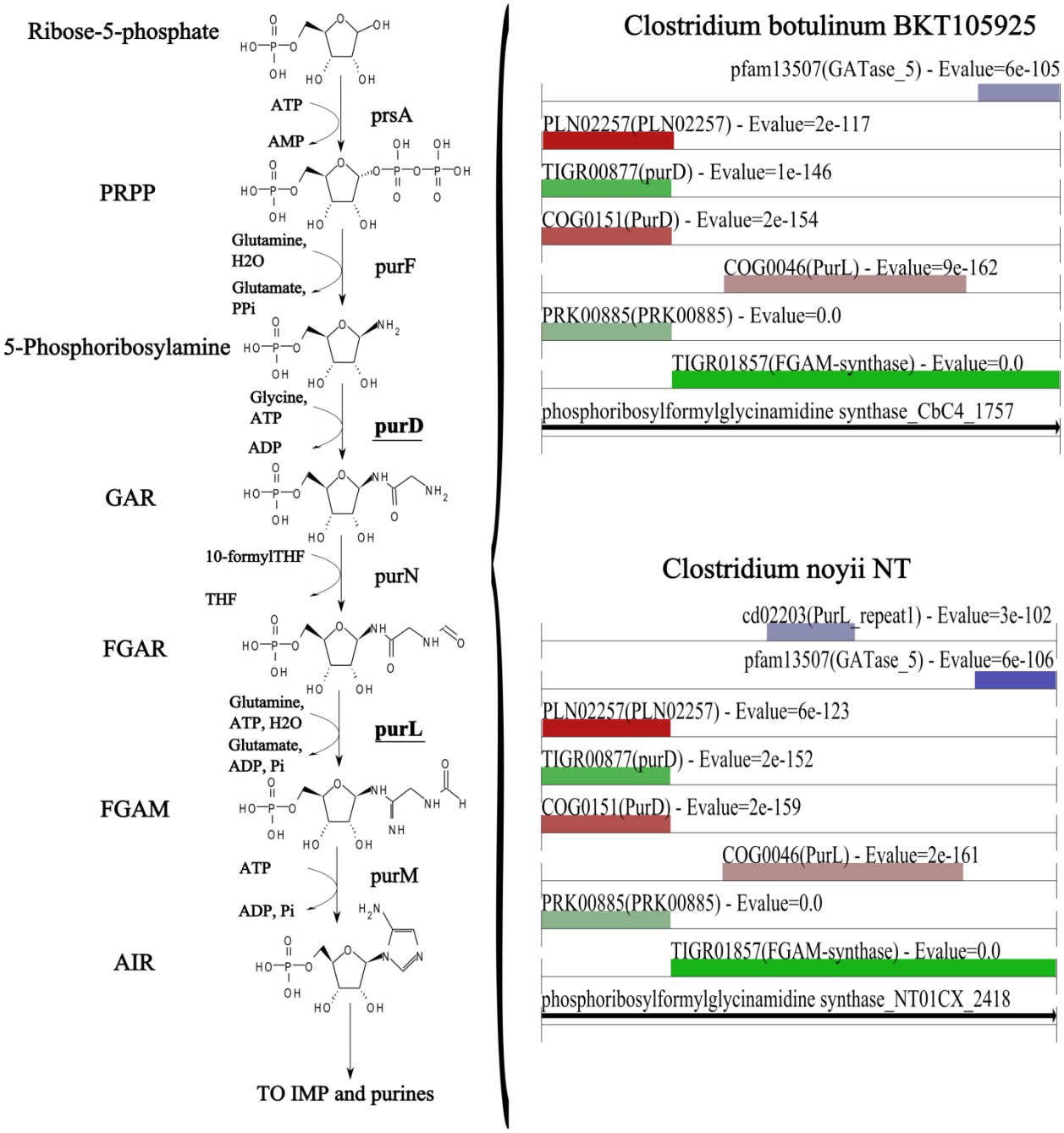

Figure 4.5. Curation of a metabolic protein family by comparison with conserved domains. Left side: a portion of the purine synthesis pathway in the group 1 Clostridia. Right side: conserved domain architecture of two *purD-purL* fusions in the group 1 Clostridia as computed and displayed by ITEP tools (with minor formatting changes). The comparison makes it clear that these two proteins are fusions of *purD* and *purL*. See list of abbreviations for full compound names. Only hits to conserved domains with E-values better than 1E-100 are shown.

Chapter 5: Curation of genome-scale metabolic networks using comparative genomics[5]

Abstract

Genome-scale metabolic modeling is a powerful way to turn genomic information into phenotype predictions. The most common approach to building the networks on which these models are based is to perform detailed reconstructions on a species-by-species basis. In this chapter, I argue that the accuracy of metabolic networks can be greatly enhanced by harnessing genomic information across multiple related species. Using the previously published ITEP tool and the genome-scale models for *Methanosarcina acetivorans* and *M.* barkeri, I show that genes that are predicted to be essential for growth are significantly more conserved than those that are not. However, many of these essential genes are not conserved in other *Methanosarcina* strains and species. Upon closer examination, I identify cases in which the gene calls or annotations in the other *Methanosarcina* genomes were clearly incorrect. I also discuss specific fixes that were made to the models based on biochemical knowledge, and remaining differences that may represent interesting physiological adaptations. The results of this chapter can be applied to any lesser-characterized genus to increase the quality of genome-scale metabolic networks.

Introduction

Genome-scale metabolic modeling is a powerful way to both consolidate large amounts of biological information and to synthesize this information to make novel predictions on the effects of perturbations on cellular function [42]. Metabolic modeling has applications ranging from biotechnology to medicine [28, 30, 45] and the range of applications has been growing every year [128, 161]. One important application of genome-scale metabolic models is the comparative analysis of metabolism for groups of related organisms. Although many metabolic enzymes are conserved across large swaths of the tree of life, there is a large amount of variability in metabolic *pathways* [220], which can be understood by building and comparing metabolic networks for related organisms. For example, in a recent study, genome-scale metabolic networks were built for 55 completely-sequenced strains of *E. coli* and used to

[5] This chapter uses unpublished genomic data used with permission from William Metcalf's lab at the University of Illinois at Urbana-Champaign. A manuscript describing the genomes is in preparation.

predict differences in substrate utilization and vitamin auxotrophies [221]. Auxotrophy predictions from 12 of the strains were experimentally tested, resulting in a 80% prediction accuracy [221].

In many comparative genomics applications, genome sequences being compared will vary in quality, particularly if they were sequenced as part of different projects or by different groups. Differences in quality can occur due to limited experimental resources, technical limitations such as short read length, or software issues such as differences in assemblies obtained using different pipelines [222]. In addition, problems with gene calling and annotation cause incorrect prediction of the functions present and absent in a cell [143]. As part of the curation process for metabolic networks, it is necessary to distinguish between these types of problems and real differences that lead to phenotypic insight. Given that the process of curating a metabolic network can take months to years to complete [43], it is imperative that tools and methods be developed to help make such distinctions.

In this chapter, I demonstrate how comparative genomics can identify problems both in genome annotation and in genome-scale models, therefore leading to increased confidence in both. I have utilized the ITEP tool [223] to compare the predicted metabolic capabilities of 30 strains of *Methanosarcina* compared to two previously-published manually curated genome-scale metabolic models of *Methanosarcina* species [40, 41]. I then identify discrepancies between expected and observed patterns in gene gain and loss and use tools such as tBLASTn [224] to search for and identify solutions to some of these discrepancies. The methods I have developed can be used for any clade for which a sufficient number of related genomes and one or more metabolic network reconstructions are available.

Methods

Genomic data

The genomes for *Methanosarcina acetivorans* str. C2A, *M. barkeri* str. Fusaro and *M. mazei* Gö1 have been previously sequenced and published [70-72]. The latest versions of these genomes (as of January 2014) were downloaded from GenBank [191]. An additional 27 *Methanosarcina* genomes included in this analysis have been sequenced by the Metcalf lab **(Table 5.1;** manuscript in preparation). Out of all of the genomes sequenced in the Metcalf lab, 20 were closed, 2 had only one sequencing gap, and 5

were not closed. The RAST server [192] was used to call genes and perform functional annotations for all *Methanosarcina* genomes sequenced by the Metcalf lab. The RAST gene calls were post-processed to remove very short genes and to fix pyrrolysine-containing genes before performing any bioinformatic analysis.

Metabolic network prediction using orthologous group prediction

The BLASTP algorithm was used to quantify the pairwise similarity between each pair of proteins encoded in the *Methanosarcina* genomes [86, 160]. OrthoMCL, a method which identifies bidirectional best hits and closely-related paralogs and then clusters them using a Markov chain-based clustering algorithm, was used to predict orthologous protein families [200]. The ITEP toolkit (**Chapter 4,** [223]) and various scripts within were used to store, manage and interpret the clustering results.

Curated lists of metabolic genes in the *Methanosarcina* were taken from two previously-published genome-scale metabolic models of organisms in this genus: the iMB745 model of *M. acetivorans* (**Chapter 2**, [40]**)** and the iMG746 model of *M. barkeri* [41]. The other organisms possessing an ortholog for each metabolic gene were identified based on the OrthoMCL result. Organisms lacking an ortholog to a metabolic gene were presumed not to possess the encoded function (this result was checked as described below for selected families).

Curation of orthology predictions

Orthology predictions for selected metabolic genes were verified by examining the phylogeny of the broader protein families and correcting the predictions if needed. Phylogenetic trees for the protein families to which these genes belong were computed using MAFFT to align the amino acid sequences [202]**,** Gblocks to trim the alignments (not allowing gaps) [204] and RAxML to compute a maximum-likelihood tree from the concatenated alignment using the WAG model of protein evolution [206].

After curating orthology predictions, each putatively absent metabolic gene was verified to be absent from the assembly using tBLASTn [224]. If significant, uncalled portions of these genes were identified in the assembly, we attempted to identify whether there was a likely insertion, frameshift, inversion, or mutation event that could cause loss of function by looking at the patterns of consecutive tBLASTn hits,

and also identified whether or not the gene in question fell on the end of a contig (such cases often indicate assembly issues). If no reasonable cause could be assigned to the putative absence of the gene, it was flagged as a likely gene-calling error.

Building a *Methanosarcina* species tree

A concatenated ribosomal protein tree was built and used to represent the organism phylogeny, as is common in the field (e.g. [225]). To build this tree, ITEP tools were used to extract a list of all conserved protein families and extracted from this a list of ribosomal protein families. Alignments for each ribosomal protein were built using MAFFT [202] and concatenated. The ribosomal protein tree was built using RaxML [206] with the WAG model of protein evolution. The tree was rooted with ribosomal proteins from *Methanococcoides burtonii*.

Phenotype simulations

Phenotype simulations used to obtain lists of essential genes were performed using Flux Balance Analysis [37] as implemented in the COBRA tookbox [91]. Knockout lethality predictions were computed based on models as they were published without further modification. Methanol was used as a growth substrate, since all the sequenced *Methanosarcina* strains are known to be able to grow on this substrate**.** The minimal media composition was as described by Sowers *et al.* [92], excluding non-essential growth factors.

Results

Consistency of nonessential and essential metabolic genes in *M. acetivorans* and *M. barkeri* models

I first examined the consistency of metabolic gene calls in the *M. acetivorans* and *M. barkeri* metabolic models, as a basis for comparison with other *Methanosarcina* strains. Taken together, the previously-published *M. acetivorans* and *M. barkeri* genome-scale metabolic networks contain a total of 1479 metabolic genes. OrthoMCL predicted that these fell into 804 distinct orthologous protein families. Of these, 698 had at least one representative in each organism, 62 were only found in *M. acetivorans*, and 44 were only found in *M. barkeri* (**Figure 5.1**). The genes predicted to be unique to *M. acetivorans*

included those in the *mrp* and *rnf* operons, which are well known to be absent from *M. barkeri* [104]. Those predicted to be unique to *M. barkeri* included the *ech* operon, which serves a similar role in *M. barkeri* and *M. mazei* to *rnf* in *M. acetivorans* [112, 114]. Other genes predicted to be unique to one of the two organisms included several families of transporters and enzymes involved in divergent carbohydrate metabolism.

Out of all of the metabolic genes from the two models, 385 were predicted to be essential for growth on methanol: 211 in *M. acetivorans* and 174 in *M. barkeri*. Almost all of the essential genes (382 out of 385) were predicted to be conserved in both *M. acetivorans* and *M. barkeri* (**Figure 5.1**), confirming the that although differences could occur (e.g. due to *bona fide* differences in growth requirements), most essential genes tend to be conserved across related organisms, at least in this genus.

Presence and absence patterns of essential genes in related *Methanosarcina*

After establishing that essential genes are well conserved between *M. acetivorans* and *M. barkeri*, I used the same methodology to test this pattern in the other 28 sequenced *Methanosarcina* strains. The presence and absence patterns for every essential metabolic gene cluster in the *Methanosarcina* strains is mapped onto the organism phylogeny (concatenated ribosomal protein tree) in **Figure 5.2**. Most essential metabolic genes (90%) were conserved across the *Methanosarcina* species. Each other group was missing in at least one strain. Perhaps unsurprisingly, the most divergent organisms in the clade - *M. baltica, M. calensis*, and *Methanosarcina* sp. MTP4 - were predicted to have the most essential genes missing. The two most divergent of these organisms (*M. baltica* and *M. calensis*) did not have closed genomes (**Table 5.2**), so it is possible that some of the metabolic genes were simply missing from the assembly. However, the genes that appeared to only be missing in these genomes could not be detected in tBLASTn searches, so if they are present, either too little of the gene was present in the assembly to be detected or the genes diverged beyond the sensitivity of the tBLASTn algorithm.

Identification of specific model issues and potential fixes

Some of the losses of essential genes appear to be phylogenetically coherent. Phylogenetically coheremt gene losses are arguably more likely to represent real, interesting differences in physiology. One of the observed differences, in cysteine synthesis, has been established previously. All *Methanosarcina* possess

a tRNA-dependent pathway for cysteine synthesis, the SepRS pathway, wherein a cys-tRNA is created for use in protein synthesis [226]. Some *Methanosarcina,* but not all of them, also possess a copy of the tRNA-independent cysteine pathway that was horizontally transferred from the bacteria. Interestingly, the models predicted that cysteine synthesis was essential for growth (the bacterial pathway is found in both *M. barkeri* Fusaro and *M. acetivorans*). Cysteine synthase was predicted to be essential because the model lacked a mechanism by which free cysteine could be generated from cys-tRNA **(Figure 5.3)**. Free cysteine is required for synthesis of several cofactors, including Coenzyme M [227], but to the author's knowledge no mechanism has been described for generating it via the SepRS pathway. This therefore could be an interesting avenue for further investigation.

The comparative genomics approach can also expose gene associations or biochemistry that are suspect in a model. For example, one gene, Mbar_A1762 (annotated as a formylmethanofuran dehydrogenase subunit "Formylmethanofuran dehydrogenase [molybdenum] subunit C"), was predicted to be essential in the *M. barkeri* model. However, orthologs were only identified in one other *Methanosarcina* strain. Upon closer examination, I found that this gene and the next (Mbar_A1763) are short fragments with high homology to the real subunit C, Mbar_A1290, and therefore should not be considered essential for this reaction to occur. Therefore, the network's accuracy would be improved by removing these two genes from the gene-protein-reaction relationship for this reaction.

Identification of specific genome issues and potential fixes

Genes are often incorrectly predicted to be absent from an organism because of problems with gene calling. Mistakes in gene calls often occur when a gene falls on the end of a contig or when one gene overlaps with another gene by a small number of base pairs. Incorrect calls of gene overlaps are often caused by an incorrect translation start site prediction for the downstream gene. Although long overlaps between genes are uncommon except in viruses, there are documented cases of short overlaps in the coding regions of neighboring genes in the Bacteria [228].

The tBLASTn wrapper tool in ITEP [224] can readily be used to search for genes in a genome independently of gene calls, and therefore is useful for identifying potential gene calling errors. For example, in the *Methanosracina* genomes, the gene Glucose-1-phosphate thymidylyltransferase, which is essential for synthesis of carbohydrates, was predicted to be present in all the Methanosarcina strains

except *M. mazei* SarPi. However, upon running tBLASTn to verify the absence, I found that the genome sequence for that organism possesses the code for an almost identical protein (97% similarity) with extremely high consistency in genome context **(Figure 5.4)**. The high consistency of gene context and sequence suggests that the gene calling software made an error and this gene should be considered present in *M. mazei* SarPi.

Discussion

As the price of sequencing continues to fall, datasets with dozens (or even hundreds) of related genomes are becoming increasingly common [177]. New ways to take advantage of this genomic data to make stronger biological insights are sorely needed. In this chapter, I have demonstrated how comparative genomics allows a user to take advantage of evolutionary theories such as conservation of gene context [229] and the relatively slow rate of gain and loss of metabolic enzymes [220] to both propagate and check the accuracy of metabolic networks and models. I have demonstrated that this can be done by identifying phyologenetically consistent gene losses, which often indicate interesting physiological divergence between clades, and by using of gene context and nucleotide sequence searches (tBLASTn) to check and fix incorrect gene calls highlighted by comparing to a reference network. The approaches are useful for improving the accuracy of both annotations and networks across a set of related organisms.

Importantly, the approaches I have developed sidestep many issues with comparing metabolic models, and particularly the effects of nomenclature conflicts. This is important because although great care was taken to make sure nomenclature in the *Methanosarcina* models is consistent, nomenclature conflicts between different models are a very common problem. In order to get around this, the described methods do not check whether the genes are attached to the same reactions, but rather check if a metabolic gene in one model has closely related genes in the other. Using my approach, it would be possible to compare models with different biochemical frameworks and conventions (e.g. one built using the SEED [46] and one using KEGG [230]) as long as gene IDs can be converted to a common standard.

One important finding from this study is that, consistent with the previous study of *E. coli* metabolic networks, there is significant variation in metabolic capabilities, even among closely-related clades.

Although almost all genes that were predicted to be essential for growth were conserved between *M. acetivorans* and *M. barkeri*, many of them were missing in other strains. As a result, if direct propagation was to be used to build models of the other *Methanosarcina* strains, most of them would be unable to predict growth on the same minimal media used to simulate *M. acetivorans* and *M. barkeri*. This complicates the process of building *models* for a clade, particularly when genomes are incomplete, since one of the steps for converting a reconstruction to a model is to fill gaps to enforce growth on a defined media (**Chapter 3**). Data on specific growth requirements of each clade member may be necessary to distinguish gene calling, annotation and assembly errors (fixed by gap filling) from real differences in metabolic capabilities.

Figures and Tables

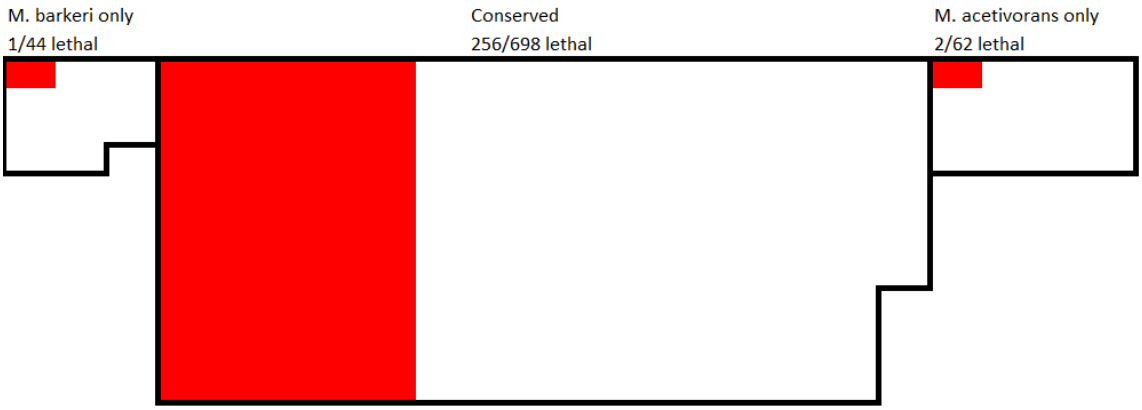

Figure 5.1. Presence and absence of predicted-lethal genes in the two modeled organisms *M. acetivorans* and *M. barkeri*. In this diagram, each box represents four metabolic gene families as predicted by OrthoMCL (rounded up) and each shaded box represents four genes with predicted lethal knockouts. Almost all genes that were predicted to be lethal in either model were conserved between the two models.

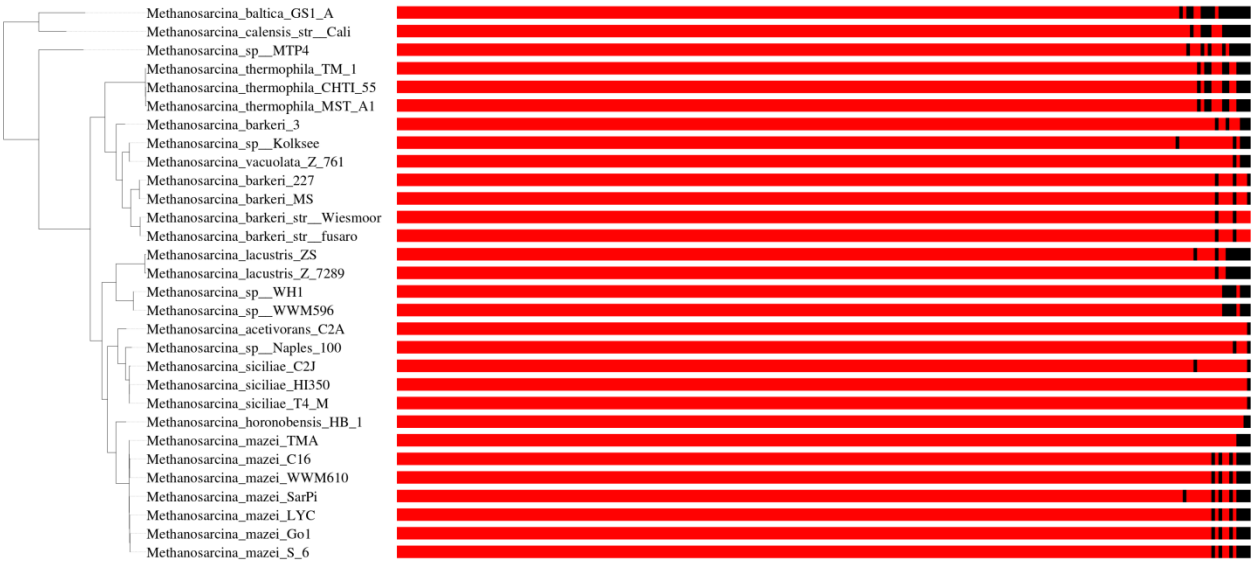

Figure 5.2. Presence and absence of predicted-lethal genes in all sequenced *Methanosarcina*. In the figure, each black box represents an absent gene and each red box a present one. Most essential genes were conserved across all the *Methanosarcina* but there were also an appreciable number that, though present in both *M. acetivorans* and *M. barkeri*, were predicted to be absent in at least one other *Methanosarcina* strain.

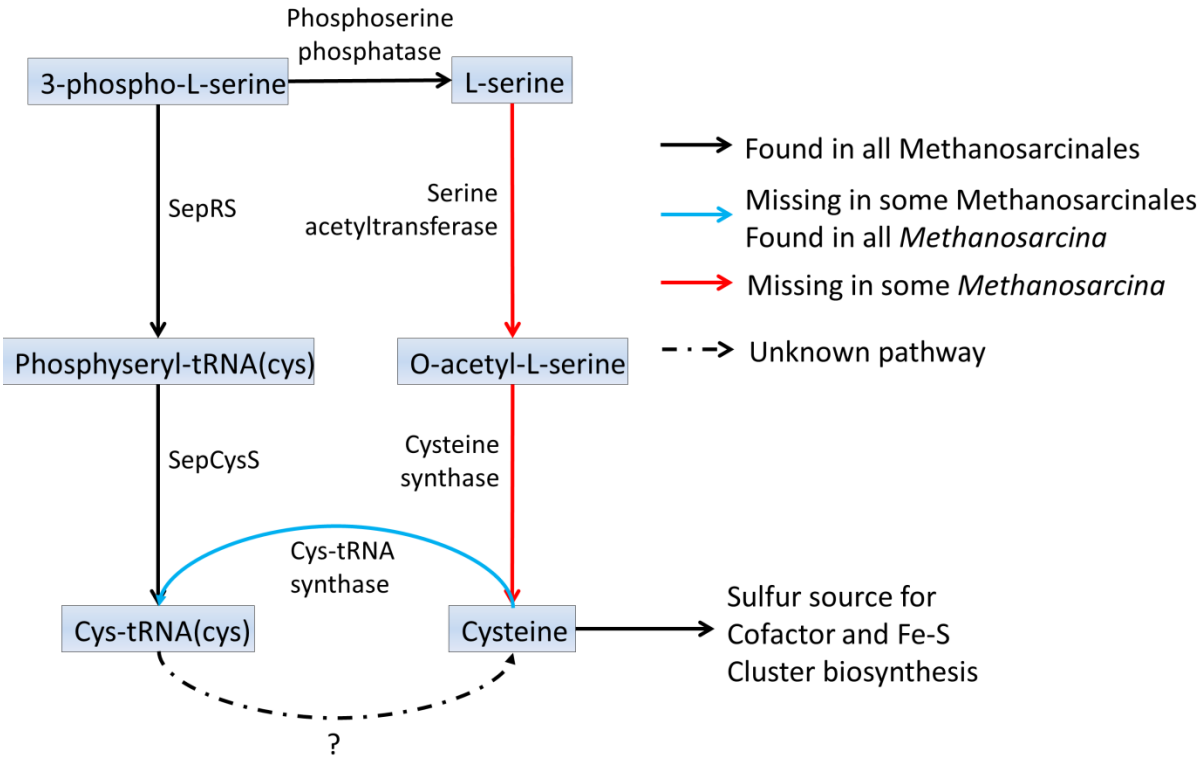

Figure 5.3. Cysteine synthesis pathways in the *Methanosarcina*. Some *Methanosarcina* possess two pathways for synthesizing cysteine (the bacterial pathway and the SepRS pathway), while some only possess the SepRS pathway. However, the models predicted that the bacterial pathway was essential despite not being conserved. The predicted essentiality was due to a gap in our understanding of how the SepRS pathway generates free cysteine, which is necessary for cofactor synthesis.

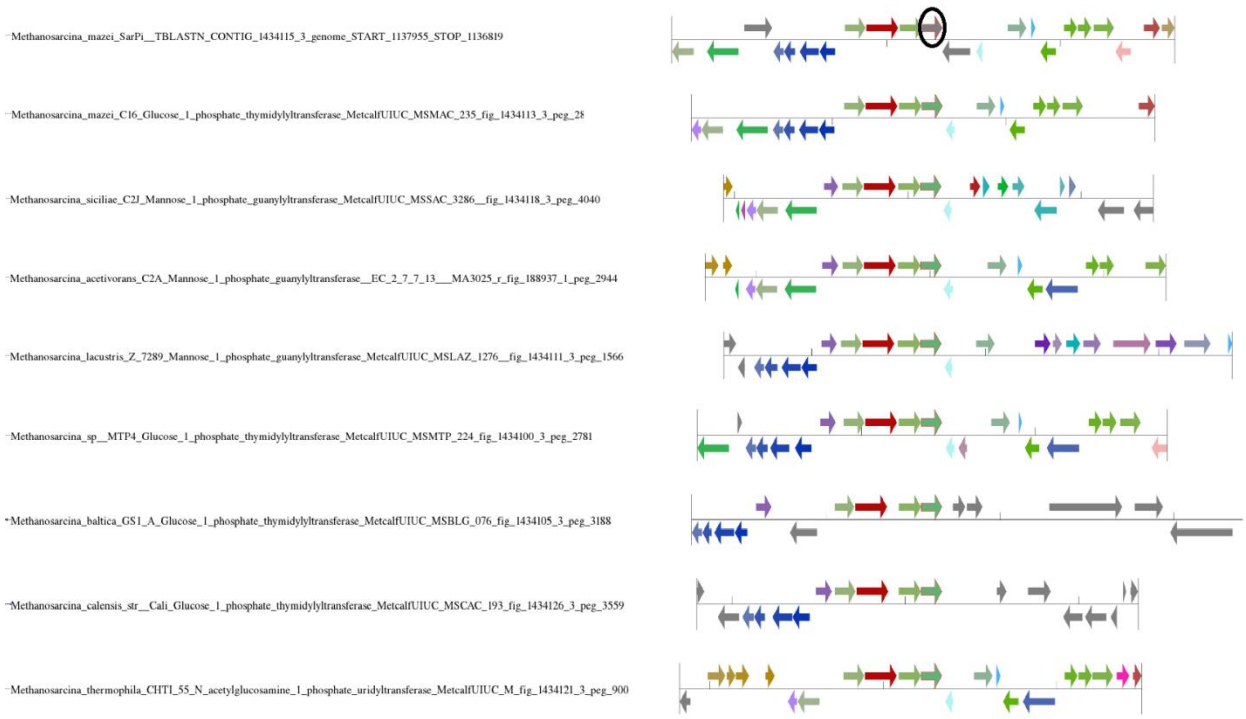

Figure 5.4. Phylogeny and gene context for Glucose-1-phosphate thymidylyltransferase in the *Methanosarcina*. Shown here is a protein phylogeny for the Glucose-1-phosphate thymidylyltransferase family (some annotated as mannose-1-phosophate guanydylyltransferase) in representative strains of *Methanosarcina*. The missing protein identified via tBLASTn is circled. Identical colors indicate proteins found in the same OrthoMCL clusters, indicating they likely share a function.

Table 5.1. *Methanosarcina* strains studied

Organism	Genome reference	Genome Status
Methanosarcina acetivorans C2A	[71]	Closed
Methanosarcina barkeri Fusaro	[72]	Closed
Methanosarcina mazei Gö1	[70]	Closed
Methanosarcina baltica GS1_A	Unpublished	Not closed (33 contigs)
Methanosarcina barkeri 227	Unpublished	Closed
Methanosarcina barkeri 3	Unpublished	Closed
Methanosarcina barkeri MS	Unpublished	Closed
Methanosarcina barkeri Wiesmoor	Unpublished	Closed
Methanosarcina calensis Cali	Unpublished	Not closed (9 contigs)
Methanosarcina horonobensis HB_1	Unpublished	Closed
Methanosarcina lacustris Z_7289	Unpublished	Closed
Methanosarcina lacustris ZS	Unpublished	Closed
Methanosarcina mazei C16	Unpublished	Closed
Methanosarcina mazei LYC	Unpublished	Closed
Methanosarcina mazei S_6	Unpublished	Closed
Methanosarcina mazei SarPi	Unpublished	Closed
Methanosarcina mazei TMA	Unpublished	Not closed (65 contigs)
Methanosarcina mazei WWM610	Unpublished	Closed
Methanosarcina siciliae C2J	Unpublished	Closed
Methanosarcina siciliae HI350	Unpublished	Closed
Methanosarcina siciliae T4/M	Unpublished	Closed
Methanosarcina sp. Kolksee	Unpublished	Closed
Methanosarcina sp. MTP4	Unpublished	Closed
Methanosarcina sp. Naples 100	Unpublished	Not closed (5 contigs)
Methanosarcina sp. WH1	Unpublished	Closed
Methanosarcina sp. WWM596	Unpublished	Closed
Methanosarcina thermophila CHTI_55	Unpublished	Nearly closed (1 contig)
Methanosarcina thermophila MST_A1	Unpublished	Not closed
Methanosarcina thermophila TM_1	Unpublished	Nearly closed (1 contig)
Methanosarcina vacuolata Z_761	Unpublished	Closed

Chapter 6: Conclusions and future work

The work I have described in this thesis centers on the generation of high-quality genome-scale metabolic networks. High-quality metabolic networks are essential for building accurate models of metabolism, which have applications in medicine and in biotechnology. My experience in building genome-scale metabolic networks began with generating one for a methanogen, *Methanosarcina acetivorans* (**Chapter 2**), using a careful, manual curation approach. From this work, I identified bottlenecks in the curation process, including database and algorithmic problems, that must be addressed to make an accurate network. For the remainder of this thesis (**Chapters 3-5**), I focused on approaches that I implemented and applied to address one of these bottlenecks: inaccuracies in functional annotations for genes. The tools I have built will help those building metabolic models in the future ensure the quality of their models and tie together more tightly the processes of correcting annotations and building metabolic networks.

In this chapter, I discuss the genome-scale reconstruction process with a particular focus on the bottlenecks in analysis and how my tools and other tools that have been developed in the field have addressed them. I then discuss what I believe to be key future challenges in the genome-scale modeling field.

Bottlenecks in the genome-scale metabolic reconstruction process

I began my Ph.D. work by manually building a genome-scale metabolic model of *Methanosarcina acetivorans* (**Chapter 2**). During the course of this work, I carefully curated the metabolic network and linked a maximum number of reactions to literature evidence [40]. Like many other manually curated genome-scale models, it took a long time to build this model to sufficient accuracy that it could be used to make reasonable predictions and gain biological insights. I experienced first-hand what the bottlenecks are for building and curating metabolic networks - an experience which heavily influenced the focus of the remainder of my Ph.D. In my opinion, the majority of the effort involved in building the network was involved in identifying and fixing problems in one of the following four categories:

1. Inconsistencies between databases of biochemical information
2. Incomplete, incorrect, or ambiguous biochemistry
3. Incorrect or ambiguous gene annotations

4. Incorrect or missing links between gene annotations and biochemistry

This thesis has focused primarily on methods to identify and fix incorrect or ambiguous gene annotations (problem 3), but much progress has been made in the field to address the others. The following paragraphs describe how each of these problems affects genome-scale metabolic models and progress that has been made in the field to mitigate them.

Inconsistencies between databases of biochemical information

There is no one standard source of data from which to build a genome-scale metabolic network. Different curated networks are built based on an agglomeration of biochemical knowledge from an array of sources, including KEGG [79], MetaCYC [80], existing genome-scale metabolic reconstructions of other organisms [84], and biochemical literature. Although incorporation of biochemical knowledge from different sources can increase the breadth of the metabolic network [31], it also makes it necessary to perform extensive cross-comparison of the databases to prevent redundancy and reduce effects of database-specific annotation errors.

One of the inconsistencies between biochemical information databases is the use of different representations of identical chemical transformations. One source of this inconsistency is the relatively poor set of links between identifiers for identical compounds and reactions. There has been a push for the use of database-independent identifiers in metabolic models [43], but unfortunately, links from databases of biochemistry to these identifiers are incomplete, and different databases refer to different sets of universal identifiers, making it difficult to compare them. In addition, slightly different versions of a compound could be used in an otherwise-identical reaction in two different databases. For example, in the KEGG database [79], certain methanogenesis reactions use the cofactor "F_{420}" (C00876) as an electron carrier. On the other hand, the manually-curated metabolic networks of *Methanosarcina barkeri* and *M. acetivorans* use a version of F_{420} ("f420-2") that is modified by covalent attachment of two glutamates [41, 83]. This version of the cofactor is not found in KEGG but is technically the most common form found in this organism [231]. The choice of which version to use in the model does not affect the simulation results. Instead, it is a tradeoff between technical correctness of one model and consistency across many. Manually-curated models tend to favor the former at the expense of the latter, making comparisons between them notoriously difficult.

Incomplete, incorrect, or ambiguous biochemistry

Metabolic models have strict requirements for biochemical reactions that are not required for other applications such as pathway visualization. All reactions in a metabolic model must be mass and charge balanced (at the same pH) and should not contain ambiguous compounds. Ubiquitous compounds such as water are often omitted from reactions cited in biochemical literature and therefore the reactions taken from these sources must be carefully checked before adding to a metabolic network. The quality of compiled biochemical databases varies: while some databases strive to use consistent mass and charge balancing at a standard pH [80], some do not explicitly specify these standards or use different methods of calculating charge that can yield different results for the same compounds. Similarly, levels of evidence necessary for inclusion of a particular reaction in the database differ from source to source.

Fortunately, in the time since I began the *M. acetivorans* reconstruction, databases have been built that are designed to synthesize biochemical information across different sources and present it in formats suitable for modeling. In particular, the ModelSEED project [46] has made a great deal of progress on this by providing a standard nomenclature for reactions and compounds that is linked to many other biochemical databases, all of which are mass and charge balanced at a standard pH. The existence of this database makes it much easier to focus curation efforts on organism-specific problems. Other databases such as MetRxn [232] have also been developed to synthesize different sources of biochemical information.

Incorrect or ambiguous gene annotations

The first step in building a genome-scale metabolic model is to use the predicted functions of each of the genes in a genome to automatically build a draft metabolic network. However, the draft metabolic network is always incorrect because of two separate but equally important problems: incorrect functional annotations for genes, and insufficient links between annotations and metabolic activity. One major focus of my thesis has been the development of tools to assist users in curating functional annotations for genes and the resultant metabolic networks.

In one particular study of the quality of annotations in commonly-used databases (such as Refseq), up to 40% of annotations were found to be incorrect [143]. The prevalence of incorrect gene annotations varied depending on the source database [143] and was shown to have become worse over time as the available genomic data has expanded. Incorrect gene annotations cause problems in metabolic modeling because they link to incorrect biochemistry and therefore result in false positives in the network. Unfortunately, most gene annotations available online do not have quality metrics or evidence attached to them, making it difficult to identify these problems except by essentially re-annotating the genome as part of the model-building process. Methods to quantify gene annotation support have been implemented [47]**,** but they tend not to be linked to existing biochemical and annotation databases. In addition, because annotations are different across different databases and the annotation processes involved are somewhat opaque, it can be difficult to compare and evaluate them.

Incorrect or missing links between gene annotations and biochemistry

Functional annotations must be linked to the correct reactions in order to use them to reconstruct the metabolic capabilities of an organism. Arguably the best way to create and maintain these links is to create and maintain a controlled vocabulary for annotations, in which all genes with the same function are given the same name. The SEED's focus on maintaining uniform, consistent functional roles across the tree of life [54] is largely responsible for the success of the ModelSEED. In databases which do not enforce such a controlled vocabulary , annotations for genes with identical function can vary wildly. For example, as of January 2014 the KEGG annotation for *E. coli* K12 MG1655 phosphofructokinase is "6-phosphofructokinase I (EC:2.7.1.11)" while the annotation for the *E. coli* O55:H7 CB9615 ortholog is "6-phosphofructokinase isozyme 1". While it is obvious to a human observer that these two genes are intended to have identical function, it is far from obvious to a computational algorithm trying to link these annotations to the appropriate biochemistry.

Many genome databases attempt to get around the inconsistency in annotations across genomes by clustering genes based on sequence data and assigning the same function to each member of a cluster (e.g. [79, 200]). However, despite the usefulness of clustering for identifying similar groups of proteins, different clustering methods will produce different groupings and are appropriate under different circumstances. As a result, it is necessary to carefully examine the clusters, assumptions, and methods

behind them. With existing tools, such details are often not transparent or difficult to adjust for individual datasets.

How my work addresses problems in metabolic reconstruction and modeling

In this thesis, I have described two distinct approaches for dealing with inaccuracies in gene functional annotations during the metabolic reconstruction process. My approaches have focused on the rapid identification of potential problems in annotations and their effects on metabolic networks. Importantly, my tools can also often be used to pinpoint potential solutions to these problems, helping expert modelers of the future ensure the quality of their models and tie together more tightly the processes of correcting annotations and building metabolic networks.

In my first approach, I have designed and implemented an algorithm that uses estimates for the uncertainty of functional annotations to find maximally-consistent ways to fill gaps in metabolic networks (**Chapter 3**). Importantly, the method I have implemented directly ties together likelihood computations with an existing annotation database (the SEED subsystems [54]) and biochemical database (the ModelSEED [46]), making it possible for modeling experts to directly evaluate evidence for inclusion of reactions against these databases. The quantification of reaction and annotation likelihoods included as part of the algorithm helps define targets for further experimentation, while their use in the gap filling algorithm ensures the identification of the most strongly-supported pathways. As part of that work, I found that the use of likelihoods in gap filling did not have a significant effect on the models' consistency with phenotype data. This finding suggests that the often-used approach of modifying the network to reconciling model predictions with phenotype data [76, 78, 145] would not necessarily improve the accuracy of the network's representation of cellular biochemistry.

My second approach to dealing with annotation inaccuracy has been the development of ITEP, a tool that allows users to flexibly generate, compare, and assess the quality of gene clusters for their own genomes (**Chapter 4)**. I have demonstrated the use of ITEP tools to readily identify and suggest solutions for inconsistencies between the curated metabolic networks of *Methanosarcina acetivorans* and *M. barkeri* and networks implied by other strains in that genus (**Chapter 5)**. The comparative analysis approach implemented in ITEP has been fruitful in expediting the discovery of key metabolic

within the *Methanosarcina* and *Clostridia* and is general enough to apply to any closely-related microbial clade.

Future directions for the project

Due to the increasing prevalence of multiple-genome sequencing projects, there is an increasing opportunity to use comparative genomics to assess the consistency of predicted gene functions in models across a species or a genus. One key direction in which this project will be taken is the integration of the likelihood-based gapfill approach with the comparative genomics approaches I have outlined in this thesis. By combining these approaches, high-quality metabolic network models can be constructed not only for individual strains but also for all members of a clade [221]. Studying a clade as a whole can lead to phenotypic insights that have medical or biotechnological applications, such as the identification of potential differences in sensitivity to a particular drug in different strains of a pathogen. In addition, by building models of clade members, it will be possible to find patterns in commonly lost pathways and correlations with the environment in which they are found, leading to insight into the nature of metabolic network evolution.

I show in **Chapter 3** how the use of likelihoods to inform the model building process can lead to improved metabolic networks, but the likelihood-based gapfill approach that I outlined uses only very simplistic computations of likelihood based on sequence similarity. The likelihood approach itself is very general, and as a result could be used to incorporate many other forms of evidence that are not completely certain but that can push a network in a particular direction. For example, conservation of gene context [47, 229] can often be used to predict gene functions that are difficult to identify by sequence alone, but these predictions also come with their own level of uncertainty. Another possibility is to use quantified likelihood of existence of particular compounds from metabolomics experiments to influence the choice of pathways in a model. By combining multiple levels of evidence, pathways can be built that maximize utilization of available data. As likelihood scores become more robust, it is likely that they will be used not only for gap filling but during the entire network-building process.

The future of genomics and of modeling lies not in the analysis of individual organisms but in communities. There is an increasing volume of metagenomic data arising from a wide range of ecosystems such as the human gut [233], aquatic ecosystems [234], deep subsurface [235], and the air

of a typical urban environment [236]. Modeling will play a key role in turning these data into testable hypothesis and phenotypic insight, but due to the volume of genomes and scarcity of experimental data on many of the members of the ecosystem, the automated generation of high-quality draft networks will become more and more important. Both the likelihood-based gap filling approach and comparative genomics-based genome curation using ITEP have important roles to play in the process of building community models. Likelihood-based gap filling helps build a draft networks that are as accurate as possible given limitations in reference data, while the ITEP tools help solve problems common to incomplete genome sequences that characterize metagenomic assemblies. While it is likely that ITEP and likelihood-based reconstruction techniques will need to be adapted to unique challenges facing the analysis of metagenomes, it is my hope that they will provide a solid foundation.

Bibliography

1. Tyler SC: **The global methane budget**. In: *Microbial production and consumption of greenhouse gases: methane, nitrogen oxides, and halomethanes.* Edited by Rodgers JE, Whitman WB. Washington, D.C: American Society for Microbiology; 1991.
2. Thauer RK, Kaster AK, Seedorf H, Buckel W, Hedderich R: **Methanogenic archaea: ecologically relevant differences in energy conservation**. *Nat Rev Microbiol* 2008, **6**(8):579-591.
3. Solomon S, Intergovernmental Panel on Climate Change., Intergovernmental Panel on Climate Change. Working Group I.: **Climate change 2007 : the physical science basis : contribution of Working Group I to the Fourth Assessment Report of the Intergovernmental Panel on Climate Change**. Cambridge ; New York: Cambridge University Press; 2007.
4. Dlugokencky EJ, Nisbet EG, Fisher R, Lowry D: **Global atmospheric methane: budget, changes and dangers**. *Philos Trans A Math Phys Eng Sci* 2011, **369**(1943):2058-2072.
5. Anderson B, Bartlett K, Frolking S, Hayhoe K, Jenkins J, Salas W, Report ER: **Methane and Nitrous Oxide Emissions from Natural Sources**. In.: Environmental Protection Agency; 2010.
6. Garcia JL, Patel BK, Ollivier B: **Taxonomic, phylogenetic, and ecological diversity of methanogenic Archaea**. *Anaerobe* 2000, **6**(4):205-226.
7. Oremland RS, Polcin S: **Methanogenesis and sulfate reduction: competitive and noncompetitive substrates in estuarine sediments**. *Appl Environ Microbiol* 1982, **44**(6):1270-1276.
8. Raskin L, Rittmann BE, Stahl DA: **Competition and coexistence of sulfate-reducing and methanogenic populations in anaerobic biofilms**. *Appl Environ Microbiol* 1996, **62**(10):3847-3857.
9. Achtnich C, Bak F, Conrad R: **Competition for Electron-Donors among Nitrate Reducers, Ferric Iron Reducers, Sulfate Reducers, and Methanogens in Anoxic Paddy Soil**. *Biology and Fertility of Soils* 1995, **19**(1):65-72.
10. Deppenmeier U: **The unique biochemistry of methanogenesis**. *Prog Nucleic Acid Res Mol Biol* 2002, **71**:223-283.
11. Anderson I, Ulrich LE, Lupa B, Susanti D, Porat I, Hooper SD, Lykidis A, Sieprawska-Lupa M, Dharmarajan L, Goltsman E *et al*: **Genomic characterization of methanomicrobiales reveals three classes of methanogens**. *PLoS One* 2009, **4**(6):e5797.
12. Leigh JA, Albers SV, Atomi H, Allers T: **Model organisms for genetics in the domain Archaea: methanogens, halophiles, Thermococcales and Sulfolobales**. *FEMS Microbiol Rev* 2011, **35**(4):577-608.
13. Jones WJ, Paynter MJB, Gupta R: **Characterization of Methanococcus-Maripaludis Sp-Nov, a New Methanogen Isolated from Salt-Marsh Sediment**. *Archives of Microbiology* 1983, **135**(2):91-97.
14. Miller TL, Wolin MJ: **Methanosphaera stadtmaniae gen. nov., sp. nov.: a species that forms methane by reducing methanol with hydrogen**. *Arch Microbiol* 1985, **141**(2):116-122.
15. Imachi H, Sakai S, Nagai H, Yamaguchi T, Takai K: **Methanofollis ethanolicus sp. nov., an ethanol-utilizing methanogen isolated from a lotus field**. *Int J Syst Evol Microbiol* 2009, **59**(Pt 4):800-805.
16. Widdel F: **Growth of methanogenic bacteria in pure culture with 2-propanol and other alcohols as hydrogen donors**. *Appl Environ Microbiol* 1986, **51**(5):1056-1062.

17. Sowers KR, Baron SF, Ferry JG: **Methanosarcina acetivorans sp. nov., an Acetotrophic Methane-Producing Bacterium Isolated from Marine Sediments**. *Appl Environ Microbiol* 1984, **47**(5):971-978.
18. Guss AM, Kulkarni G, Metcalf WW: **Differences in hydrogenase gene expression between Methanosarcina acetivorans and Methanosarcina barkeri**. *J Bacteriol* 2009, **191**(8):2826-2833.
19. Zhang JK, White AK, Kuettner HC, Boccazzi P, Metcalf WW: **Directed mutagenesis and plasmid-based complementation in the methanogenic archaeon Methanosarcina acetivorans C2A demonstrated by genetic analysis of proline biosynthesis**. *J Bacteriol* 2002, **184**(5):1449-1454.
20. Zhang JK, Pritchett MA, Lampe DJ, Robertson HM, Metcalf WW: **In vivo transposon mutagenesis of the methanogenic archaeon Methanosarcina acetivorans C2A using a modified version of the insect mariner-family transposable element Himar1**. *Proc Natl Acad Sci U S A* 2000, **97**(17):9665-9670.
21. Kohler PR, Metcalf WW: **Genetic manipulation of Methanosarcina spp**. *Front Microbiol* 2012, **3**:259.
22. Boccazzi P, Zhang JK, Metcalf WW: **Generation of dominant selectable markers for resistance to pseudomonic acid by cloning and mutagenesis of the ileS gene from the archaeon Methanosarcina barkeri fusaro**. *J Bacteriol* 2000, **182**(9):2611-2618.
23. Gardner WL, Whitman WB: **Expression vectors for Methanococcus maripaludis: overexpression of acetohydroxyacid synthase and beta-galactosidase**. *Genetics* 1999, **152**(4):1439-1447.
24. Lessner DJ, Lhu L, Wahal CS, Ferry JG: **An engineered methanogenic pathway derived from the domains bacteria and archaea**. *MBio* 2010, **1**(5).
25. Durot M, Bourguignon PY, Schachter V: **Genome-scale models of bacterial metabolism: reconstruction and applications**. *FEMS Microbiol Rev* 2009, **33**(1):164-190.
26. Barabasi AL, Gulbahce N, Loscalzo J: **Network medicine: a network-based approach to human disease**. *Nat Rev Genet* 2011, **12**(1):56-68.
27. Colijn C, Brandes A, Zucker J, Lun DS, Weiner B, Farhat MR, Cheng TY, Moody DB, Murray M, Galagan JE: **Interpreting expression data with metabolic flux models: predicting Mycobacterium tuberculosis mycolic acid production**. *PLoS Comput Biol* 2009, **5**(8):e1000489.
28. Folger O, Jerby L, Frezza C, Gottlieb E, Ruppin E, Shlomi T: **Predicting selective drug targets in cancer through metabolic networks**. *Mol Syst Biol* 2011, **7**:501.
29. Sigurdsson G, Fleming RM, Heinken A, Thiele I: **A systems biology approach to drug targets in Pseudomonas aeruginosa biofilm**. *PLoS One* 2012, **7**(4):e34337.
30. Milne CB, Kim PJ, Eddy JA, Price ND: **Accomplishments in genome-scale in silico modeling for industrial and medical biotechnology**. *Biotechnol J* 2009, **4**(12):1653-1670.
31. Milne CB, Eddy JA, Raju R, Ardekani S, Kim PJ, Senger RS, Jin YS, Blaschek HP, Price ND: **Metabolic network reconstruction and genome-scale model of butanol-producing strain Clostridium beijerinckii NCIMB 8052**. *BMC Syst Biol* 2011, **5**:130.
32. Price ND, Reed JL, Palsson BO: **Genome-scale models of microbial cells: evaluating the consequences of constraints**. *Nat Rev Microbiol* 2004, **2**(11):886-897.
33. Shlomi T, Cabili MN, Herrgard MJ, Palsson BO, Ruppin E: **Network-based prediction of human tissue-specific metabolism**. *Nat Biotechnol* 2008, **26**(9):1003-1010.
34. Chandrasekaran S, Price ND: **Probabilistic integrative modeling of genome-scale metabolic and regulatory networks in Escherichia coli and Mycobacterium tuberculosis**. *Proc Natl Acad Sci U S A* 2010, **107**(41):17845-17850.
35. Labhsetwar P, Cole JA, Roberts E, Price ND, Luthey-Schulten ZA: **Heterogeneity in protein expression induces metabolic variability in a modeled Escherichia coli population**. *Proc Natl Acad Sci U S A* 2013, **110**(34):14006-14011.

36. Hoppe A, Hoffmann S, Holzhutter HG: **Including metabolite concentrations into flux balance analysis: thermodynamic realizability as a constraint on flux distributions in metabolic networks**. *BMC Syst Biol* 2007, **1**:23.
37. Orth JD, Thiele I, Palsson BØ: **What is flux balance analysis?** *Nat Biotechnol* 2010, **28**(3):245-248.
38. Schuetz R, Kuepfer L, Sauer U: **Systematic evaluation of objective functions for predicting intracellular fluxes in Escherichia coli**. *Mol Syst Biol* 2007, **3**:119.
39. Feist AM, Palsson BO: **The biomass objective function**. *Curr Opin Microbiol* 2010, **13**(3):344-349.
40. Benedict MN, Gonnerman MC, Metcalf WW, Price ND: **Genome-Scale Metabolic Reconstruction and Hypothesis Testing in the Methanogenic Archaeon Methanosarcina acetivorans C2A**. *J Bacteriol* 2012, **194**(4):855-865.
41. Gonnerman MC, Benedict MN, Feist AM, Metcalf WW, Price ND: **Genomically and biochemically accurate metabolic reconstruction of Methanosarcina barkeri Fusaro, iMG746**. *Biotechnol J* 2013, **8**(9):1070-1079.
42. Oberhardt MA, Palsson BO, Papin JA: **Applications of genome-scale metabolic reconstructions**. *Mol Syst Biol* 2009, **5**:320.
43. Thiele I, Palsson BØ: **A protocol for generating a high-quality genome-scale metabolic reconstruction**. *Nat Protoc* 2010, **5**(1):93-121.
44. Galperin MY, Fernandez-Suarez XM: **The 2012 Nucleic Acids Research Database Issue and the online Molecular Biology Database Collection**. *Nucleic Acids Res* 2012, **40**(Database issue):D1-8.
45. Kim TY, Sohn SB, Kim YB, Kim WJ, Lee SY: **Recent advances in reconstruction and applications of genome-scale metabolic models**. *Curr Opin Biotechnol* 2012, **23**(4):617-623.
46. Henry CS, DeJongh M, Best AA, Frybarger PM, Linsay B, Stevens RL: **High-throughput generation, optimization and analysis of genome-scale metabolic models**. *Nat Biotechnol* 2010, **28**(9):977-982.
47. von Mering C, Huynen M, Jaeggi D, Schmidt S, Bork P, Snel B: **STRING: a database of predicted functional associations between proteins**. *Nucleic Acids Res* 2003, **31**(1):258-261.
48. Hayden EC: **Nanopore genome sequencer makes its debut**. In: *Nature News.* 2012.
49. Medini D, Donati C, Tettelin H, Masignani V, Rappuoli R: **The microbial pan-genome**. *Curr Opin Genet Dev* 2005, **15**(6):589-594.
50. Rasko DA, Rosovitz MJ, Myers GS, Mongodin EF, Fricke WF, Gajer P, Crabtree J, Sebaihia M, Thomson NR, Chaudhuri R *et al*: **The pangenome structure of Escherichia coli: comparative genomic analysis of E. coli commensal and pathogenic isolates**. *J Bacteriol* 2008, **190**(20):6881-6893.
51. Jacobsen A, Hendriksen RS, Aaresturp FM, Ussery DW, Friis C: **The Salmonella enterica pan-genome**. *Microb Ecol* 2011, **62**(3):487-504.
52. Chen PE, Cook C, Stewart AC, Nagarajan N, Sommer DD, Pop M, Thomason B, Thomason MP, Lentz S, Nolan N *et al*: **Genomic characterization of the Yersinia genus**. *Genome Biol* 2010, **11**(1):R1.
53. Hao P, Zheng H, Yu Y, Ding G, Gu W, Chen S, Yu Z, Ren S, Oda M, Konno T *et al*: **Complete sequencing and pan-genomic analysis of Lactobacillus delbrueckii subsp. bulgaricus reveal its genetic basis for industrial yogurt production**. *PLoS One* 2011, **6**(1):e15964.
54. Overbeek R, Begley T, Butler RM, Choudhuri JV, Chuang HY, Cohoon M, de Crecy-Lagard V, Diaz N, Disz T, Edwards R *et al*: **The subsystems approach to genome annotation and its use in the project to annotate 1000 genomes**. *Nucleic Acids Res* 2005, **33**(17):5691-5702.
55. Dehal PS, Joachimiak MP, Price MN, Bates JT, Baumohl JK, Chivian D, Friedland GD, Huang KH, Keller K, Novichkov PS *et al*: **MicrobesOnline: an integrated portal for comparative and functional genomics**. *Nucleic Acids Res* 2010, **38**(Database issue):D396-400.

56. Wang T, Liu J, Shen L, Tonti-Filippini J, Zhu Y, Jia H, Lister R, Whitaker JW, Ecker JR, Millar AH *et al*: **STAR: an integrated solution to management and visualization of sequencing data**. *Bioinformatics* 2013, **29**(24):3204-3210.
57. Delcher AL, Salzberg SL, Phillippy AM: **Using MUMmer to identify similar regions in large sequence sets**. *Curr Protoc Bioinformatics* 2003, **Chapter 10**:Unit 10 13.
58. Darling AC, Mau B, Blattner FR, Perna NT: **Mauve: multiple alignment of conserved genomic sequence with rearrangements**. *Genome Res* 2004, **14**(7):1394-1403.
59. Tamura K, Peterson D, Peterson N, Stecher G, Nei M, Kumar S: **MEGA5: molecular evolutionary genetics analysis using maximum likelihood, evolutionary distance, and maximum parsimony methods**. *Mol Biol Evol* 2011, **28**(10):2731-2739.
60. Zhao Y, Wu J, Yang J, Sun S, Xiao J, Yu J: **PGAP: pan-genomes analysis pipeline**. *Bioinformatics* 2012, **28**(3):416-418.
61. Fouts DE, Brinkac L, Beck E, Inman J, Sutton G: **PanOCT: automated clustering of orthologs using conserved gene neighborhood for pan-genomic analysis of bacterial strains and closely related species**. *Nucleic Acids Res* 2012, **40**(22):e172.
62. Linard B, Thompson JD, Poch O, Lecompte O: **OrthoInspector: comprehensive orthology analysis and visual exploration**. *BMC Bioinformatics* 2011, **12**:11.
63. Laing C, Buchanan C, Taboada EN, Zhang Y, Kropinski A, Villegas A, Thomas JE, Gannon VP: **Pan-genome sequence analysis using Panseq: an online tool for the rapid analysis of core and accessory genomic regions**. *BMC Bioinformatics* 2010, **11**:461.
64. Seitzer P, Huynh TA, Facciotti MT: **JContextExplorer: a tree-based approach to facilitate cross-species genomic context comparison**. *BMC Bioinformatics* 2013, **14**:18.
65. Pati A, Ivanova NN, Mikhailova N, Ovchinnikova G, Hooper SD, Lykidis A, Kyrpides NC: **GenePRIMP: a gene prediction improvement pipeline for prokaryotic genomes**. *Nat Methods* 2010, **7**(6):455-457.
66. Filippova D, Gadani A, Kingsford C: **Coral: an integrated suite of visualizations for comparing clusterings**. *BMC Bioinformatics* 2012, **13**:276.
67. Capone DG, Kiene RP: **Comparison of Microbial Dynamics in Marine and Freshwater Sediments: Contrasts in Anaerobic Carbon Catabolism**. *Limnol Oceanogr* 1988, **33**:725-749.
68. Milich L: **The role of methane in global warming: where might mitigation strategies be focused?** *Global Environmental Change* 1999, **9**:179-201.
69. Welander PV, Metcalf WW: **Loss of the mtr operon in Methanosarcina blocks growth on methanol, but not methanogenesis, and reveals an unknown methanogenic pathway**. *Proc Natl Acad Sci U S A* 2005, **102**(30):10664-10669.
70. Deppenmeier U, Johann A, Hartsch T, Merkl R, Schmitz RA, Martinez-Arias R, Henne A, Wiezer A, Bäumer S, Jacobi C *et al*: **The genome of Methanosarcina mazei: evidence for lateral gene transfer between bacteria and archaea**. *J Mol Microbiol Biotechnol* 2002, **4**(4):453-461.
71. Galagan JE, Nusbaum C, Roy A, Endrizzi MG, Macdonald P, FitzHugh W, Calvo S, Engels R, Smirnov S, Atnoor D *et al*: **The genome of M. acetivorans reveals extensive metabolic and physiological diversity**. *Genome Res* 2002, **12**(4):532-542.
72. Maeder DL, Anderson I, Brettin TS, Bruce DC, Gilna P, Han CS, Lapidus A, Metcalf WW, Saunders E, Tapia R *et al*: **The Methanosarcina barkeri genome: comparative analysis with Methanosarcina acetivorans and Methanosarcina mazei reveals extensive rearrangement within methanosarcinal genomes**. *J Bacteriol* 2006, **188**(22):7922-7931.
73. Apolinario EE, Jackson KM, Sowers KR: **Development of a plasmid-mediated reporter system for in vivo monitoring of gene expression in the archaeon Methanosarcina acetivorans**. *Appl Environ Microbiol* 2005, **71**(8):4914-4918.

74. Xu H, Aurora R, Rose GD, White RH: **Identifying two ancient enzymes in Archaea using predicted secondary structure alignment**. *Nat Struct Biol* 1999, **6**(8):750-754.
75. Oberhardt MA, Palsson BØ, Papin JA: **Applications of genome-scale metabolic reconstructions**. *Mol Syst Biol* 2009, **5**:320.
76. Kumar VS, Ferry J, Maranas C: **Metabolic reconstruction of the archaeon methanogen Methanosarcina Acetivorans**. *BMC Systems Biology* 2011, **5**(1):28.
77. Kumar VS, Dasika MS, Maranas CD: **Optimization based automated curation of metabolic reconstructions**. *BMC Bioinformatics* 2007, **8**:212.
78. Kumar VS, Maranas CD: **GrowMatch: an automated method for reconciling in silico/in vivo growth predictions**. *PLoS Comput Biol* 2009, **5**(3):e1000308.
79. Kanehisa M, Goto S, Furumichi M, Tanabe M, Hirakawa M: **KEGG for representation and analysis of molecular networks involving diseases and drugs**. *Nucleic Acids Res* 2010, **38**(Database issue):D355-360.
80. Caspi R, Altman T, Dale JM, Dreher K, Fulcher CA, Gilham F, Kaipa P, Karthikeyan AS, Kothari A, Krummenacker M *et al*: **The MetaCyc database of metabolic pathways and enzymes and the BioCyc collection of pathway/genome databases**. *Nucleic Acids Res* 2010, **38**(Database issue):D473-479.
81. Ren Q, Chen K, Paulsen IT: **TransportDB: a comprehensive database resource for cytoplasmic membrane transport systems and outer membrane channels**. *Nucleic Acids Res* 2007, **35**(Database issue):D274-279.
82. The Uniprot C: **The Universal Protein Resource (UniProt) in 2010**. *Nucleic Acids Res* 2010, **38**(Database issue):D142-148.
83. Feist AM, Scholten JCM, Palsson BØ, Brockman FJ, Ideker T: **Modeling methanogenesis with a genome-scale metabolic reconstruction of Methanosarcina barkeri**. *Mol Syst Biol* 2006, **2**:2006.0004.
84. Schellenberger J, Park JO, Conrad TM, Palsson BO: **BiGG: a Biochemical Genetic and Genomic knowledgebase of large scale metabolic reconstructions**. *BMC Bioinformatics* 2010, **11**:213.
85. Arakaki AK, Huang Y, Skolnick J: **EFICAz2: enzyme function inference by a combined approach enhanced by machine learning**. *BMC Bioinformatics* 2009, **10**:107.
86. Camacho C, Coulouris G, Avagyan V, Ma N, Papadopoulos J, Bealer K, Madden TL: **BLAST+: architecture and applications**. *BMC Bioinformatics* 2009, **10**:421.
87. Kandler O, Hippe H: **Lack of peptidoglycan in the cell walls of Methanosarcina barkeri**. *Arch Microbiol* 1977, **113**(1-2):57-60.
88. Mahlmann A, Deppenmeier U, Gottschalk G: **Methanofuran-B Is Required for Co2 Formation from Formaldehyde by Methanosarcina-Barkeri**. *Fems Microbiology Letters* 1989, **61**(1-2):115-120.
89. Sprott GD, Dicaire CJ, Choquet CG, Patel GB, Ekiel I: **Hydroxydiether Lipid Structures in Methanosarcina spp. and Methanococcus voltae**. *Appl Environ Microbiol* 1993, **59**(3):912-914.
90. Feist AM, Henry CS, Reed JL, Krummenacker M, Joyce AR, Karp PD, Broadbelt LJ, Hatzimanikatis V, Palsson BØ: **A genome-scale metabolic reconstruction for Escherichia coli K-12 MG1655 that accounts for 1260 ORFs and thermodynamic information**. *Mol Syst Biol* 2007, **3**:121.
91. Becker SA, Feist AM, Mo ML, Hannum G, Palsson BØ, Herrgard MJ: **Quantitative prediction of cellular metabolism with constraint-based models: the COBRA Toolbox**. *Nat Protoc* 2007, **2**(3):727-738.
92. Sowers KR, Boone JE, Gunsalus RP: **Disaggregation of Methanosarcina spp. and Growth as Single Cells at Elevated Osmolarity**. *Appl Environ Microbiol* 1993, **59**(11):3832-3839.
93. Mahadevan R, Schilling CH: **The effects of alternate optimal solutions in constraint-based genome-scale metabolic models**. *Metab Eng* 2003, **5**(4):264-276.

94. Summer H: **Improved approach for transferring and cultivating Methanosarcina acetivorans C2A (DSM 2834)**. *Lett Appl Microbiol* 2009, **48**(6):786-789.
95. Thauer RK, Jungermann K, Decker K: **Energy conservation in chemotrophic anaerobic bacteria**. *Bacteriol Rev* 1977, **41**(1):100-180.
96. Alberty RA: **Thermodynamics of biochemical reactions**. Cambridge, MA: Massachusetts Institute of Technology; 2003.
97. Jankowski MD, Henry CS, Broadbelt LJ, Hatzimanikatis V: **Group contribution method for thermodynamic analysis of complex metabolic networks**. *Biophys J* 2008, **95**(3):1487-1499.
98. Feist AM, Herrgard MJ, Thiele I, Reed JL, Palsson BO: **Reconstruction of biochemical networks in microorganisms**. *Nat Rev Microbiol* 2009, **7**(2):129-143.
99. Grochowski LL, Xu H, White RH: **Ribose-5-phosphate biosynthesis in Methanocaldococcus jannaschii occurs in the absence of a pentose-phosphate pathway**. *J Bacteriol* 2005, **187**(21):7382-7389.
100. Buan NR, Metcalf WW: **Methanogenesis by Methanosarcina acetivorans involves two structurally and functionally distinct classes of heterodisulfide reductase**. *Mol Microbiol* 2010, **75**(4):843-853.
101. Oelgeschläger E, Rother M: **Influence of carbon monoxide on metabolite formation in Methanosarcina acetivorans**. *FEMS Microbiol Lett* 2009, **292**(2):254-260.
102. Rother M, Metcalf WW: **Anaerobic growth of Methanosarcina acetivorans C2A on carbon monoxide: an unusual way of life for a methanogenic archaeon**. *Proc Natl Acad Sci U S A* 2004, **101**(48):16929-16934.
103. Tallant TC, Krzycki JA: **Methylthiol:coenzyme M methyltransferase from Methanosarcina barkeri, an enzyme of methanogenesis from dimethylsulfide and methylmercaptopropionate**. *J Bacteriol* 1997, **179**(22):6902-6911.
104. Rohlin L, Gunsalus RP: **Carbon-dependent control of electron transfer and central carbon pathway genes for methane biosynthesis in the Archaean, Methanosarcina acetivorans strain C2A**. *BMC Microbiol* 2010, **10**:62.
105. Li Q, Li L, Rejtar T, Lessner DJ, Karger BL, Ferry JG: **Electron transport in the pathway of acetate conversion to methane in the marine archaeon Methanosarcina acetivorans**. *J Bacteriol* 2006, **188**(2):702-710.
106. Taglicht D, Padan E, Schuldiner S: **Overproduction and purification of a functional Na+/H+ antiporter coded by nhaA (ant) from Escherichia coli**. *J Biol Chem* 1991, **266**(17):11289-11294.
107. Pinner E, Padan E, Schuldiner S: **Kinetic properties of NhaB, a Na+/H+ antiporter from Escherichia coli**. *J Biol Chem* 1994, **269**(42):26274-26279.
108. Aronson PS: **Kinetic properties of the plasma membrane Na+-H+ exchanger**. *Annu Rev Physiol* 1985, **47**:545-560.
109. Baumer S, Ide T, Jacobi C, Johann A, Gottschalk G, Deppenmeier U: **The F420H2 dehydrogenase from Methanosarcina mazei is a Redox-driven proton pump closely related to NADH dehydrogenases**. *J Biol Chem* 2000, **275**(24):17968-17973.
110. Ferry JG: **CO in methanogenesis**. *Ann Microbiol* 2008, **190**:257-269.
111. O'Brien JM, Wolkin RH, Moench TT, Morgan JB, Zeikus JG: **Association of hydrogen metabolism with unitrophic or mixotrophic growth of Methanosarcina barkeri on carbon monoxide**. *J Bacteriol* 1984, **158**(1):373-375.
112. Meuer J, Kuettner HC, Zhang JK, Hedderich R, Metcalf WW: **Genetic analysis of the archaeon Methanosarcina barkeri Fusaro reveals a central role for Ech hydrogenase and ferredoxin in methanogenesis and carbon fixation**. *Proc Natl Acad Sci U S A* 2002, **99**(8):5632-5637.

113. Lessner DJ, Li L, Li Q, Rejtar T, Andreev VP, Reichlen M, Hill K, Moran JJ, Karger BL, Ferry JG: **An unconventional pathway for reduction of CO2 to methane in CO-grown Methanosarcina acetivorans revealed by proteomics**. *Proc Natl Acad Sci U S A* 2006, **103**(47):17921-17926.
114. Welte C, Krätzer C, Deppenmeier U: **Involvement of Ech hydrogenase in energy conservation of Methanosarcina mazei**. *FEBS J* 2010, **277**(16):3396-3403.
115. Guss AM, Mukhopadhyay B, Zhang JK, Metcalf WW: **Genetic analysis of mch mutants in two Methanosarcina species demonstrates multiple roles for the methanopterin-dependent C-1 oxidation/reduction pathway and differences in H(2) metabolism between closely related species**. *Mol Microbiol* 2005, **55**(6):1671-1680.
116. Raemakers-Franken PC, Brand RJ, Kortstee AJ, Van der Drift C, Vogels GD: **Ammonia assimilation and glutamate incorporation in coenzyme F420 derivatives of Methanosarcina barkeri**. *Antonie Van Leeuwenhoek* 1991, **59**(4):243-248.
117. Bose A, Kulkarni G, Metcalf WW: **Regulation of putative methyl-sulphide methyltransferases in Methanosarcina acetivorans C2A**. *Mol Microbiol* 2009, **74**(1):227-238.
118. Musfeldt M, Schönheit P: **Novel type of ADP-forming acetyl coenzyme A synthetase in hyperthermophilic archaea: heterologous expression and characterization of isoenzymes from the sulfate reducer Archaeoglobus fulgidus and the methanogen Methanococcus jannaschii**. *J Bacteriol* 2002, **184**(3):636-644.
119. Sowers KR, Nelson MJ, Ferry JG: **Growth of acetotrophic, methane-producing bacteria in a pH auxostat**. *Curr Microbiol* 1984, **11**:227-229.
120. Blaut M, Muller V, Fiebig K, Gottschalk G: **Sodium ions and an energized membrane required by Methanosarcina barkeri for the oxidation of methanol to the level of formaldehyde**. *J Bacteriol* 1985, **164**(1):95-101.
121. Rother M, Oelgeschläger E, Metcalf WM: **Genetic and proteomic analyses of CO utilization by Methanosarcina acetivorans**. *Arch Microbiol* 2007, **188**(5):463-472.
122. Heo J, Skjeldal L, Staples CR, Ludden PW: **Carbon monoxide dehydrogenase from Rhodospirillum rubrum produces formate**. *J Biol Inorg Chem* 2002, **7**(7-8):810-814.
123. Oelgeschlager E, Rother M: **In vivo role of three fused corrinoid/methyl transfer proteins in Methanosarcina acetivorans**. *Mol Microbiol* 2009, **72**(5):1260-1272.
124. Ferguson T, Soares JA, Lienard T, Gottschalk G, Krzycki JA: **RamA, a protein required for reductive activation of corrinoid-dependent methylamine methyltransferase reactions in methanogenic archaea**. *J Biol Chem* 2009, **284**(4):2285-2295.
125. Stojanowic A, Mander GJ, Duin EC, Hedderich R: **Physiological role of the F420-non-reducing hydrogenase (Mvh) from Methanothermobacter marburgensis**. *Arch Microbiol* 2003, **180**(3):194-203.
126. Li Q, Li L, Rejtar T, Karger BL, Ferry JG: **Proteome of Methanosarcina acetivorans Part II: comparison of protein levels in acetate- and methanol-grown cells**. *J Proteome Res* 2005, **4**(1):129-135.
127. Tsoka S, Simon D, Ouzounis CA: **Automated metabolic reconstruction for Methanococcus jannaschii**. *Archaea* 2004, **1**(4):223-229.
128. Feist AM, Palsson BO: **The growing scope of applications of genome-scale metabolic reconstructions using Escherichia coli**. *Nat Biotechnol* 2008, **26**(6):659-667.
129. Edwards J, Palsson B: **The Escherichia coli MG1655 in silico metabolic genotype: its definition, characteristics, and capabilities**. *Proceedings of the National Academy of Sciences* 2000, **97**(10):5528-5533.
130. Reed JL, Vo TD, Schilling CH, Palsson BO, others: **An expanded genome-scale model of Escherichia coli K-12 (iJR904 GSM/GPR)**. *Genome Biol* 2003, **4**(9):R54.

131. Duarte NC, Herrgäard MJ, Palsson BØ: **Reconstruction and validation of Saccharomyces cerevisiae iND750, a fully compartmentalized genome-scale metabolic model**. *Genome research* 2004, **14**(7):1298-1309.
132. Woese CR, Fox GE: **Phylogenetic structure of the prokaryotic domain: the primary kingdoms**. *Proceedings of the National Academy of Sciences* 1977, **74**(11):5088-5090.
133. Ibarra RU, Edwards JS, Palsson BO: **Escherichia coli K-12 undergoes adaptive evolution to achieve in silico predicted optimal growth**. *Nature* 2002, **420**(6912):186-189.
134. Ma H, Zeng A-P: **Reconstruction of metabolic networks from genome data and analysis of their global structure for various organisms**. *Bioinformatics* 2003, **19**(2):270-277.
135. Pál C, Papp B, Lercher MJ: **Adaptive evolution of bacterial metabolic networks by horizontal gene transfer**. *Nature Genetics* 2005, **37**(12):1372-1375.
136. Lee JY, Jang Y-S, Lee J, Papoutsakis ET, Lee SY: **Metabolic engineering of Clostridium acetobutylicum M5 for highly selective butanol production**. *Biotechnology journal* 2009, **4**(10):1432-1440.
137. Lee D-S, Burd H, Liu J, Almaas E, Wiest O, Barabási A-L, Oltvai ZN, Kapatral V: **Comparative genome-scale metabolic reconstruction and flux balance analysis of multiple Staphylococcus aureus genomes identify novel antimicrobial drug targets**. *Journal of bacteriology* 2009, **191**(12):4015-4024.
138. Nelson KE, Weinstock GM, Highlander SK, Worley KC, Creasy HH, Wortman JR, Rusch DB, Mitreva M, Sodergren E, Chinwalla AT *et al*: **A catalog of reference genomes from the human microbiome.** *Science (New York, NY)* 2010, **328**(5981):994-999.
139. Kanehisa M, Goto S, Sato Y, Furumichi M, Tanabe M: **KEGG for integration and interpretation of large-scale molecular data sets**. *Nucleic acids research* 2012, **40**(D1):D109-D114.
140. DeJongh M, Formsma K, Boillot P, Gould J, Rycenga M, Best A: **Toward the automated generation of genome-scale metabolic networks in the SEED**. *BMC Bioinformatics* 2007, **8**(1):139.
141. Agren R, Liu L, Shoaie S, Vongsangnak W, Nookaew I, Nielsen J: **The RAVEN toolbox and its use for generating a genome-scale metabolic model for Penicillium chrysogenum**. *PLoS Comput Biol* 2013, **9**(3):e1002980.
142. Schellenberger J, Que R, Fleming RM, Thiele I, Orth JD, Feist AM, Zielinski DC, Bordbar A, Lewis NE, Rahmanian S *et al*: **Quantitative prediction of cellular metabolism with constraint-based models: the COBRA Toolbox v2. 0**. *Nature Protocols* 2011, **6**(9):1290-1307.
143. Schnoes AM, Brown SD, Dodevski I, Babbitt PC: **Annotation error in public databases: misannotation of molecular function in enzyme superfamilies**. *PLoS Comput Biol* 2009, **5**(12):e1000605.
144. Orth JD, Palsson BØ: **Systematizing the generation of missing metabolic knowledge**. *Biotechnology and bioengineering* 2010, **107**(3):403-412.
145. Henry CS, Zinner JF, Cohoon MP, Stevens RL: **iBsu1103: a new genome-scale metabolic model of Bacillus subtilis based on SEED annotations**. *Genome Biol* 2009, **10**(6):R69.
146. Karp PD, Paley S, Romero P: **The pathway tools software**. *Bioinformatics* 2002, **18**(suppl 1):S225-S232.
147. Herrgäard MJ, Fong SS, Palsson BØ: **Identification of genome-scale metabolic network models using experimentally measured flux profiles**. *PLoS computational biology* 2006, **2**(7):e72.
148. Vitkin E, Shlomi T: **MIRAGE: a functional genomics-based approach for metabolic network model reconstruction and its application to cyanobacteria networks**. *Genome biology* 2012, **13**(11):R111.

149. Heavner BD, Smallbone K, Price ND, Walker LP: **Version 6 of the consensus yeast metabolic network refines biochemical coverage and improves model performance**. *Database: the journal of biological databases and curation* 2013, **2013**.
150. Blais EM, Chavali AK, Papin JA: **Linking Genome-Scale Metabolic Modeling and Genome Annotation**. In: *Systems Metabolic Engineering.* Springer; 2013: 61-83.
151. Lewis NE, Nagarajan H, Palsson BO: **Constraining the metabolic genotype-phenotype relationship using a phylogeny of in silico methods**. *Nature Reviews Microbiology* 2012, **10**(4):291-305.
152. Oh YK, Palsson BØ, Schilling CH, R M: **Genome-scale reconstruction of metabolic network in Bacillus subtilis based on high-throughput phenotyping and gene essentiality data**. *Journal of Biological Chemistry* 2007, **282**:28791-28799.
153. Kuzuyama T: **Mevalonate and nonmevalonate pathways for the biosynthesis of isoprene units**. *Bioscience, biotechnology, and biochemistry* 2002, **66**(8):1619-1627.
154. Rohdich F, Kis K, Bacher A, Eisenreich W: **The non-mevalonate pathway of isoprenoids: genes, enzymes and intermediates**. *Current opinion in chemical biology* 2001, **5**(5):535-540.
155. Eisenreich W, Bacher A, Arigoni D, Rohdich F: **Biosynthesis of isoprenoids via the non-mevalonate pathway**. *Cellular and Molecular Life Sciences CMLS* 2004, **61**(12):1401-1426.
156. Taffs R, Aston J, Brileya K, Jay Z, Klatt C, McGlynn S, Mallette N, Montross S, Gerlach R, Inskeep W *et al*: **In silico approaches to study mass and energy flows in microbial consortia: a syntrophic case study**. *BMC systems biology* 2009, **3**(1):114.
157. Plata G, Fuhrer T, Hsiao T-L, Sauer U, Vitkup D: **Global probabilistic annotation of metabolic networks enables enzyme discovery**. *Nature Chemical Biology* 2012, **8**(10):848-854.
158. Davis JJ, Olsen GJ, Overbeek R, Vonstein V, Xia F: **In search of genome annotation consistency: solid gene clusters and how to use them**. *3 Biotech* 2013:1-5.
159. Eisen JA: **Phylogenomics: improving functional predictions for uncharacterized genes by evolutionary analysis**. *Genome research* 1998, **8**(3):163-167.
160. Altschul SF, Gish W, Miller W, Myers EW, Lipman DJ: **Basic local alignment search tool**. *J Mol Biol* 1990, **215**(3):403-410.
161. Reed JL, Palsson BØ: **Thirteen years of building constraint-based in silico models of Escherichia coli**. *Journal of Bacteriology* 2003, **185**(9):2692-2699.
162. Forsyth RA, Haselback RJ, Ohlsen KL, Yamamoto RT, Xu H, al. e: **A genome-wide strategy for the identification of essential genes in Staphylococcus aureus**. *Molecular Microbiology* 2002, **43**(6):1387-1400.
163. Salama N, Shepherd B, Falkow S: **Global transposon mutagenesis and essential gene analysis of Helicobacter pylori**. *Journal of Bacteriology* 2004, **186**(23):7926-7935.
164. Sassetti C, Boyd D, Rubin E: **Genes required for mycobacterial growth defined by high density mutagenesis**. *Molecular Microbiology* 2003, **48**(1):77-84.
165. Akerley B, Rubin E, Novick V, Amaya K, Judson N, Mekalanos J: **A genome-scale analysis for identification of genes required for growth or survival of Haemophilus influenzae**. *Proceedings of the National Academy of Sciences* 2002, **99**(2):966-977.
166. Durot M, Le Fèvre F, de Berardinis V, Kreimeyer A, Vallenet D, Combe C, Smidtas S, Salanoubat M, Weissenbach J, V S: **Iterative reconstruction of a global metabolic model of Acinetobacter baylyi ADP1 using high-throughput growth phenotype and gene essentiality data**. *BMC Systems Biology* 2008, **2**(85).
167. Gallagher L, Ramage E, Jacobs M, Kaul R, Brittnacher M, Manoil C: **A comprehensive transposon mutant library of Francisella novicida, a bioweapon surrogate**. *Proceedings of the National Academy of Sciences* 2007, **104**(3):1009-1014.

168. French C, Lao P, Loraine A, BT M, Yu H, K D: **Large-scale transposon mutagenesis of Mycoplasma pulmonis**. *Molecular Microbiology* 2008, **69**(1):67-76.
169. Glass J, Assad-Garcia N, Alperovich N, Yooseph S, Lewis M, Maruf M, Hutchison Cr, Smith H, Venter J: **Essential genes of a minimal bacterium**. *Proceedings of the National Academy of Sciences* 2006, **103**(2):425-430.
170. Kobayashi K, al. e: **Essential Bacillus subtilis genes**. *Proceedings of the National Academy of Sciences* 2003, **100**(8):4678-4683.
171. Jacobs M, Alwood A, Thaipisuttikul I, Spencer D, Haugen E, Ernst S, Will O, Kaul R, Raymond C, Levy R *et al*: **Comprehensive transposon mutant library of Pseudomonas aeruginosa**. *Proceedings of the National Academy of Sciences* 2003, **100**(24):14339-14344.
172. Thanassi JA, Hartman-Neumann SL, Dougherty TJ, Dougherty BA, Pucci MJ: **Identification of 113 conserved essential genes using a high-througput gene disruption system in Streptococcus pneumoniae**. *Nucleic Acids Research* 2002, **30**(14):3152-3162.
173. Ji Y, Zhang B, Van SF, Horn PW, Woodnutt G, Burnham MKR, Rosenberg M: **Identification of Critical Staphylococcal Genes Using Conditional Phenotypes Generated by Anitsense RNA**. *Science (New York, NY)* 2001, **293**(5538):2266-2269.
174. **High-performance software for mathematical programming and optimization**
175. Achterberg T: **SCIP: solving constraint integer programs**. *Mathematical Programming Computation* 2009, **1**(1):1-41.
176. Mardis ER: **A decade's perspective on DNA sequencing technology**. *Nature* 2011, **470**(7333):198-203.
177. Mira A, Martin-Cuadrado AB, D'Auria G, Rodriguez-Valera F: **The bacterial pan-genome:a new paradigm in microbiology**. *Int Microbiol* 2010, **13**(2):45-57.
178. Reno ML, Held NL, Fields CJ, Burke PV, Whitaker RJ: **Biogeography of the Sulfolobus islandicus pan-genome**. *Proc Natl Acad Sci U S A* 2009, **106**(21):8605-8610.
179. Huynen MA, Bork P: **Measuring genome evolution**. *Proc Natl Acad Sci U S A* 1998, **95**(11):5849-5856.
180. Borneman AR, McCarthy JM, Chambers PJ, Bartowsky EJ: **Comparative analysis of the Oenococcus oeni pan genome reveals genetic diversity in industrially-relevant pathways**. *BMC Genomics* 2012, **13**:373.
181. Conlan S, Mijares LA, Becker J, Blakesley RW, Bouffard GG, Brooks S, Coleman H, Gupta J, Gurson N, Park M *et al*: **Staphylococcus epidermidis pan-genome sequence analysis reveals diversity of skin commensal and hospital infection-associated isolates**. *Genome Biol* 2012, **13**(7):R64.
182. Koonin EV: **Orthologs, paralogs, and evolutionary genomics**. *Annu Rev Genet* 2005, **39**:309-338.
183. Dessimoz C, Gabaldon T, Roos DS, Sonnhammer EL, Herrero J: **Toward community standards in the quest for orthologs**. *Bioinformatics* 2012, **28**(6):900-904.
184. Altenhoff AM, Dessimoz C: **Phylogenetic and functional assessment of orthologs inference projects and methods**. *PLoS Comput Biol* 2009, **5**(1):e1000262.
185. Luz H, Vingron M: **Family specific rates of protein evolution**. *Bioinformatics* 2006, **22**(10):1166-1171.
186. Chain PS, Grafham DV, Fulton RS, Fitzgerald MG, Hostetler J, Muzny D, Ali J, Birren B, Bruce DC, Buhay C *et al*: **Genomics. Genome project standards in a new era of sequencing**. *Science* 2009, **326**(5950):236-237.
187. Teeling H, Glockner FO: **Current opportunities and challenges in microbial metagenome analysis--a bioinformatic perspective**. *Brief Bioinform* 2012, **13**(6):728-742.

188. Caporaso JG, Kuczynski J, Stombaugh J, Bittinger K, Bushman FD, Costello EK, Fierer N, Pena AG, Goodrich JK, Gordon JI *et al*: **QIIME allows analysis of high-throughput community sequencing data**. *Nat Methods* 2010, **7**(5):335-336.
189. Novichkov PS, Ratnere I, Wolf YI, Koonin EV, Dubchak I: **ATGC: a database of orthologous genes from closely related prokaryotic genomes and a research platform for microevolution of prokaryotes**. *Nucleic Acids Res* 2009, **37**(Database issue):D448-454.
190. Richter M, Lombardot T, Kostadinov I, Kottmann R, Duhaime MB, Peplies J, Glockner FO: **JCoast - a biologist-centric software tool for data mining and comparison of prokaryotic (meta)genomes**. *BMC Bioinformatics* 2008, **9**:177.
191. Benson DA, Karsch-Mizrachi I, Clark K, Lipman DJ, Ostell J, Sayers EW: **GenBank**. *Nucleic Acids Res* 2012, **40**(Database issue):D48-53.
192. Aziz RK, Bartels D, Best AA, DeJongh M, Disz T, Edwards RA, Formsma K, Gerdes S, Glass EM, Kubal M *et al*: **The RAST Server: rapid annotations using subsystems technology**. *BMC Genomics* 2008, **9**:75.
193. **DOE Systems Biology KnowledgeBase** [http://kbase.science.energy.gov]
194. van Dongen S, Abreu-Goodger C: **Using MCL to Extract Clusters from Networks**. *Bacterial Molecular Networks: Methods and Protocols* 2012, **804**:281-295.
195. Huerta-Cepas J, Dopazo J, Gabaldon T: **ETE: a python Environment for Tree Exploration**. *BMC Bioinformatics* 2010, **11**:24.
196. Cock PJ, Antao T, Chang JT, Chapman BA, Cox CJ, Dalke A, Friedberg I, Hamelryck T, Kauff F, Wilczynski B *et al*: **Biopython: freely available Python tools for computational molecular biology and bioinformatics**. *Bioinformatics* 2009, **25**(11):1422-1423.
197. Enright AJ, Van Dongen S, Ouzounis CA: **An efficient algorithm for large-scale detection of protein families**. *Nucleic Acids Res* 2002, **30**(7):1575-1584.
198. Van Dongen S: **Graph Clustering by Flow Simulation**. Amsterdam, Netherlands: University of Utrecht; 2000.
199. Chan CX, Mahbob M, Ragan MA: **Clustering evolving proteins into homologous families**. *BMC Bioinformatics* 2013, **14**(1):120.
200. Li L, Stoeckert CJ, Jr., Roos DS: **OrthoMCL: identification of ortholog groups for eukaryotic genomes**. *Genome Res* 2003, **13**(9):2178-2189.
201. Dufayard JF, Duret L, Penel S, Gouy M, Rechenmann F, Perriere G: **Tree pattern matching in phylogenetic trees: automatic search for orthologs or paralogs in homologous gene sequence databases**. *Bioinformatics* 2005, **21**(11):2596-2603.
202. Katoh K, Standley DM: **MAFFT Multiple Sequence Alignment Software Version 7: Improvements in Performance and Usability**. *Mol Biol Evol* 2013, **30**(4):772-780.
203. Suyama M, Torrents D, Bork P: **PAL2NAL: robust conversion of protein sequence alignments into the corresponding codon alignments**. *Nucleic Acids Res* 2006, **34**(Web Server issue):W609-612.
204. Talavera G, Castresana J: **Improvement of phylogenies after removing divergent and ambiguously aligned blocks from protein sequence alignments**. *Syst Biol* 2007, **56**(4):564-577.
205. Price MN, Dehal PS, Arkin AP: **FastTree 2--approximately maximum-likelihood trees for large alignments**. *PLoS One* 2010, **5**(3):e9490.
206. Stamatakis A: **RAxML-VI-HPC: maximum likelihood-based phylogenetic analyses with thousands of taxa and mixed models**. *Bioinformatics* 2006, **22**(21):2688-2690.
207. Overbeek R, Fonstein M, D'Souza M, Pusch GD, Maltsev N: **The use of gene clusters to infer functional coupling**. *Proc Natl Acad Sci U S A* 1999, **96**(6):2896-2901.

208. Marchler-Bauer A, Zheng C, Chitsaz F, Derbyshire MK, Geer LY, Geer RC, Gonzales NR, Gwadz M, Hurwitz DI, Lanczycki CJ *et al*: **CDD: conserved domains and protein three-dimensional structure**. *Nucleic Acids Res* 2013, **41**(Database issue):D348-352.
209. Ochman H, Lerat E, Daubin V: **Examining bacterial species under the specter of gene transfer and exchange**. *Proc Natl Acad Sci U S A* 2005, **102 Suppl 1**:6595-6599.
210. Collins MD, Lawson PA, Willems A, Cordoba JJ, Fernandez-Garayzabal J, Garcia P, Cai J, Hippe H, Farrow JA: **The phylogeny of the genus Clostridium: proposal of five new genera and eleven new species combinations**. *Int J Syst Bacteriol* 1994, **44**(4):812-826.
211. Lee J, Yun H, Feist AM, Palsson BO, Lee SY: **Genome-scale reconstruction and in silico analysis of the Clostridium acetobutylicum ATCC 824 metabolic network**. *Appl Microbiol Biotechnol* 2008, **80**(5):849-862.
212. Senger RS, Papoutsakis ET: **Genome-scale model for Clostridium acetobutylicum: Part I. Metabolic network resolution and analysis**. *Biotechnol Bioeng* 2008, **101**(5):1036-1052.
213. Gillespie JJ, Wattam AR, Cammer SA, Gabbard JL, Shukla MP, Dalay O, Driscoll T, Hix D, Mane SP, Mao C *et al*: **PATRIC: the comprehensive bacterial bioinformatics resource with a focus on human pathogenic species**. *Infect Immun* 2011, **79**(11):4286-4298.
214. Yarza P, Ludwig W, Euzeby J, Amann R, Schleifer KH, Glockner FO, Rossello-Mora R: **Update of the All-Species Living Tree Project based on 16S and 23S rRNA sequence analyses**. *Syst Appl Microbiol* 2010, **33**(6):291-299.
215. Kuzniar A, van Ham RC, Pongor S, Leunissen JA: **The quest for orthologs: finding the corresponding gene across genomes**. *Trends Genet* 2008, **24**(11):539-551.
216. Kristensen DM, Wolf YI, Mushegian AR, Koonin EV: **Computational methods for Gene Orthology inference**. *Brief Bioinform* 2011, **12**(5):379-391.
217. Frech C, Chen N: **Genome-wide comparative gene family classification**. *PLoS One* 2010, **5**(10):e13409.
218. **FigTree** [http://tree.bio.ed.ac.uk/software/figtree/]
219. Gille C, Frommel C: **STRAP: editor for STRuctural Alignments of Proteins**. *Bioinformatics* 2001, **17**(4):377-378.
220. Peregrin-Alvarez JM, Tsoka S, Ouzounis CA: **The phylogenetic extent of metabolic enzymes and pathways**. *Genome Res* 2003, **13**(3):422-427.
221. Monk JM, Charusanti P, Aziz RK, Lerman JA, Premyodhin N, Orth JD, Feist AM, Palsson BO: **Genome-scale metabolic reconstructions of multiple Escherichia coli strains highlight strain-specific adaptations to nutritional environments**. *Proc Natl Acad Sci U S A* 2013, **110**(50):20338-20343.
222. Birney E: **Assemblies: the good, the bad, the ugly**. *Nat Methods* 2011, **8**(1):59-60.
223. Benedict MN, Henriksen JR, Metcalf WW, Whitaker RJ, Price ND: **ITEP: An integrated toolkit for exploration of microbial pan-genomes**. *BMC Genomics* 2014, **15**(1):8.
224. Gertz EM, Yu YK, Agarwala R, Schaffer AA, Altschul SF: **Composition-based statistics and translated nucleotide searches: improving the TBLASTN module of BLAST**. *BMC Biol* 2006, **4**:41.
225. Matte-Tailliez O, Brochier C, Forterre P, Philippe H: **Archaeal phylogeny based on ribosomal proteins**. *Mol Biol Evol* 2002, **19**(5):631-639.
226. Sauerwald A, Zhu W, Major TA, Roy H, Palioura S, Jahn D, Whitman WB, Yates JR, 3rd, Ibba M, Soll D: **RNA-dependent cysteine biosynthesis in archaea**. *Science* 2005, **307**(5717):1969-1972.
227. Graham DE, Taylor SM, Wolf RZ, Namboori SC: **Convergent evolution of coenzyme M biosynthesis in the Methanosarcinales: cysteate synthase evolved from an ancestral threonine synthase**. *Biochem J* 2009, **424**(3):467-478.
228. Scherbakov DV, Garber MB: **Overlapping genes in bacterial and phage genomes**. *Molecular Biology* 2000, **34**(4):485-495.

229. Osterman A, Overbeek R: **Missing genes in metabolic pathways: a comparative genomics approach**. *Curr Opin Chem Biol* 2003, **7**(2):238-251.
230. Ogata H, Goto S, Sato K, Fujibuchi W, Bono H, Kanehisa M: **KEGG: Kyoto encyclopedia of genes and genomes**. *Nucleic acids research* 1999, **27**(1):29-34.
231. Peck MW: **Changes in concentrations of coenzyme F420 analogs during batch growth of Methanosarcina barkeri and Methanosarcina mazei**. *Appl Environ Microbiol* 1989, **55**(4):940-945.
232. Kumar A, Suthers PF, Maranas CD: **MetRxn: a knowledgebase of metabolites and reactions spanning metabolic models and databases**. *BMC Bioinformatics* 2012, **13**:6.
233. Le Chatelier E, Nielsen T, Qin J, Prifti E, Hildebrand F, Falony G, Almeida M, Arumugam M, Batto JM, Kennedy S *et al*: **Richness of human gut microbiome correlates with metabolic markers**. *Nature* 2013, **500**(7464):541-546.
234. Debroas D, Humbert JF, Enault F, Bronner G, Faubladier M, Cornillot E: **Metagenomic approach studying the taxonomic and functional diversity of the bacterial community in a mesotrophic lake (Lac du Bourget--France)**. *Environ Microbiol* 2009, **11**(9):2412-2424.
235. Dong Y, Kumar CG, Chia N, Kim PJ, Miller PA, Price ND, Cann IK, Flynn TM, Sanford RA, Krapac IG *et al*: **Halomonas sulfidaeris-dominated microbial community inhabits a 1.8 km-deep subsurface Cambrian Sandstone reservoir**. *Environ Microbiol* 2013.
236. Tringe SG, Zhang T, Liu X, Yu Y, Lee WH, Yap J, Yao F, Suan ST, Ing SK, Haynes M *et al*: **The airborne metagenome in an indoor urban environment**. *PLoS One* 2008, **3**(4):e1862.

Appendix A: Supplemental methods for likelihood-based gap filling

Building draft metabolic models

Draft metabolic models were built using the procedure outlined in a previous manuscript [46]. Genomes were first annotated using vocabulary controlled in the SEED subsystems [54]. Then a biochemistry database maintained in the ModelSEED was used to translate these annotations into gene functions, protein complexes, and finally reactions predicted to be present in the reconstructed organism. The ModelSEED biochemistry database is based on KEGG and 13 previously-published, manually-curated genome-scale models (see manuscript [46] for details). Universal and spontaneous reactions such as diffusion of carbon dioxide were automatically added to the draft network. The reversibility of reactions in the draft networks were determined using thermodynamic predictions based on a group contribution method [97]. Thermodynamic estimates were performed on a 1mM basis at 25 ^{o}C, 1 atm and a pH of 7.

Network-based Gap Filling

The mixed-integer linear programming (MILP) formulation for network-based gap filling has been published previously [77, 145]:

$$
\begin{aligned}
&Minimize\ \sum \lambda_{gapfill,x} z_x \\
&Subject\ to \\
&\boldsymbol{N}v = 0 \\
&0 \le v_x \le v_{max,x} z_x \\
&v_{target} \ge \epsilon
\end{aligned}
$$

Here, $\varepsilon=10^{-3}$, **N** is the stoichiometric matrix for all reactions in the biochemistry database from which gap filled reactions are drawn, v is the reaction rate, $v_{max,x}$ is the maximum reaction rate for reaction x, and z_x is 1 if the reaction x is added to the model and 0 otherwise. v_{target} is the reaction rate of a target reaction which is to be activated by the gap fill algorithm. The objective coefficient $\lambda_{gapfill,x}$ is computed as [46]:

$$
\lambda_{gapfill,x} = 1 + P_{KEGG} + P_{STRUCTURE} + P_{TRANSPORT} + P_{ROLE} + P_{Known\,\Delta G} + P_{UNFAVORED} * (12 + \frac{\Delta G^{0m}_{x,EST}}{10})
$$

The first five P-values are penalties for adding reactions not in the KEGG database, unknown structures, transporters, missing roles, or for which the Gibbs free energy could not be estimated using a group contribution method. The final coefficient $P_{UNFAVORED}$ penalizes the addition of reactions in the predicted thermodynamically-unfavorable direction. $\Delta G^{0m}_{x,EST}$ is the estimated Gibbs free energy of reaction by the group contribution method [97].

The values of the penalties used in this manuscript were as follows (though they can be adjusted by the user).

- P_{KEGG}: 0 for reactions in KEGG and 1 for other reactions,
- $P_{STRUCTURE}$: 0 for reactions with only metabolites with known structure and 1 otherwise
- $P_{TRANSPORT}$: 25, which works out to about 3-4 internal reaction changes on average.
- $P_{Known\ delta\ G}$: 0 for reactions with estimated Gibbs energy and 1 otherwise
- $P_{UNFAVORED}$: 0 if the reaction is in the thermodynamically favorable direction (or if it is predicted to be reversible) and 1 otherwise. This makes changing a reaction with an estimated Gibbs energy of 10 kCal/mol equivalent to adding (on average) three intracellular reactions in a favorable direction.

The same values of the parameters were used for network-based and likelihood-based gap filling; thus the likelihood-based algorithm reduces to the network-based algorithm in the limit of 0 likelihood for every reaction.

Appendix B: Tutorial for building models and running likelihood-based gap filling in the DOE KnowledgeBase using the web-based CLI

Overview

This tutorial describes how to build metabolic models using the four workflows that we have described in the manuscript. There are actually two ways to run this workflow:

- Using the **Client API**, or
- Using the **Web-based command line interface**

This tutorial focuses on the second one. The web-based command line interface is available at:

http://iris.kbase.us

Users log in (signing up is easy and free), create a workspace, and run the commands sequentially in the provided window. The API is described in a separate tutorial.

This tutorial is divided into three parts: A quick command reference (commands are outlined with minimal explanation), a brief overview of the KBase infrastructure necessary to run the commands, and detailed information about each step we ran in the manuscript to come up with the reported results.

Depending on the type of gap filling you wish to run there are a total of up to 13 steps. See **Figure B.1** for detailed workflows for reproducing our results from the manuscript (or running your own) with network-based gap filling, iterative gap filling, likelihood-based gap filling, and likelihood-based iterative gap filling. Look up the appropriate section below for a detailed description of the commands for each step. Skip over anything in gray for a particular analysis.

Quick command reference

The following is a list of all the commands (in order) that you can run in IRIS to perform a complete analysis from loading a genome from the SEED to performing a likelihood-based gap filling and analyzing phenotype data (in the same manner as was done in the manuscript). The numbers here correspond to the numbers in the workflows above. Anything denoted as `$STUFF` should be replaced with the actual name of the desired inputs and outputs.

In order to run any of these commands you will need to first need a Globus Online account. If you dont have one, create one here:

https://gologin.kbase.us/SignUp

Go to IRIS (http://iris.kbase.us) and log in. You will then need a workspace in which to store your data. If you don't have one, create one using:

```
$ ws-createws $WORKSPACE_NAME
```

Then switch to that workspace using:

```
$ ws-workspace $WORKSPACE_NAME
```

1. Build a genome object (this example imports the genome from the PubSEED, other options are availbale)

```
$ fba-loadgenome --seed $SEED_ID
```

This will create a Genome object called `$SEED_ID` in your workspace (this is hereafter referred to as `$GENOME_OBJECT_NAME` since other sources are possible)

2. Build draft model

```
$ fba-buildfbamodel $GENOME_OBJECT_NAME --model $DRAFT_MODEL_NAME
```

This will create a Model object called `$DRAFT_MODEL_NAME` in your workspace.

3. Build annotation likelihoods

```
$ pa-annotate $GENOME_OBJECT_NAME $PROBANNO_OBJECT_NAME
```

This will create a ProbAnno object called `$PROBANNO_OBJECT_NAME` in your workspace. This is a long-running job (takes about 4-5 hours on average). You can check the status of your job using

```
$ pa-checkjob --job 52efbcb7e4b0ef8357332113
   Job '52efbcb7e4b0ef8357332113' (pa-annotate for genome 171101.1.genome to
   probanno 171101.1.probanno for user mmundy) has status 'running blast' and is
   working on task 3 of 5.  Check again later.
```

4. Calculate reaction likelihoods

```
$ pa-calculate $PROBANNO_OBJECT_NAME $RXNPROBS_OBJECT_NAME
```

This will create a RxnProbs object called `$RXNPROBS_OBJECT_NAME` in your workspace.

5. Fill gaps on complete media. How you do this depends on the type of gap filling you want to do. This is a long-running job (takes from 1 hour to 1 day depending on the number of gaps in the original network).

Network-based gap fill:

```
$ fba-gapfill $DRAFT_MODEL_NAME --modelout $GAPFILLED_MODEL_NAME \
   --transpen 25 --singletranspen 25 --biomasstranspen 25 --directionpen 12 \
   --intsol
```

Likelihood-based gap fill:

```
$ fba-gapfill $DRAFT_MODEL_NAME --modelout $GAPFILLED_MODEL_NAME \
   --transpen 25 --singletranspen 25 --biomasstranspen 25 --directionpen 12 \
```

```
    --intsol  --probrxn $RXNPROBS_OBJECT_NAME
```

6. Check growth on complete media

```
$ fba-runfba $GAPFILLED_MODEL_NAME --fbaid $FBA_OBJECT_NAME.
```

Should give you non-zero objective value. The results are stored in an FBA object named `$FBA_OBJECT_NAME` for future reference.

7. If you are doing iterative gap filling, run the following after doing all the above for targeted gap filling (this is a long-running job, it takes 2-3 days on average to run):

Iterative gap fill:

```
$ fba-gapfill $GAPFILLED_MODEL_NAME --modelout $ITER_GAPFILLED_MODEL_NAME \
   --transpen 25 --singletranspen 25 --biomasstranspen 25 --directionpen 12 \
   --intsol --iterativegf
```

Likelihood-based iterative gap fill:

```
$ fba-gapfill $GAPFILLED_MODEL_NAME --modelout $ITER_GAPFILLED_MODEL_NAME \
   --transpen 25 --singletranspen 25 --biomasstranspen 25 --directionpen 12 \
   --intsol  --iterativegf --probrxn $RXNPROBS_OBJECT_NAME
```

Note that this job can take up to a couple days for some problems. The final result will be a new Model object `$ITER_GAPFILLED_MODEL_NAME` in the workspace.

8. Reaction sensitivity analysis (iterative gap fill only)

To run a reaction sensitivity analysis you need a GapFill solution ID. Run this:

```
$ fba-getmodels --pretty $gapfilled_model_name $WORKSPACE_ID \
       > $gapfilled_model_filename
```

Then search for "integrated_gapfillings" in the output file .

```
 "integrated_gapfillings" : [
        [
           "kb|g.166872.fbamdl1.gf.3",
           "652/14/1",
           "Complete",
           "262/34/1",
           0,
           []
        ]
     ],
```

You want the first element of the array (`kb|g.166872.fbamdl1.gf.3` in this example). Add "gfsol.0" to that string to get the GapFill solution ID (note - the 0 means you want to integrate solution number 0, i.e. the first solution):

```
kb|g.166872.fbamdl1.gf.3.gfsol.0
```

For **iterative gap fill**:

```
$ fba-reactionsensitivity $ITER_GAPFILLED_MODEL_NAME \
      --rxnsensid $RXN_SENSITIVITY_NAME  \
      --gapfill $GAPFILL_SOLUTION_ID --deleterxns
```

For **likelihood-based iterative gap fill**:

```
$ fba-reactionsensitivity $ITER_GAPFILLED_MODEL_NAME \
      --rxnsensid $RXN_SENSITIVITY_NAME \
      --gapfill $GAPFILL_SOLUTION_ID --deleterxns --rxnprobs $RXNPROBS_OBJECT_NAME
```

The result will be a RxnSensitivity object `$RXN_SENSITIVITY_NAME` in your workspace.

9. Delete non-contributing reactions

```
$ fba-delete_noncontributing_reactions $RXN_SENSITIVITY_NAME \
  --newmodel $FILTERED_MODEL_NAME
```

It will make new Model object `$FILTERED_MODEL_NAME` in your workspace with flagged reactions deleted.

10. Gapfill to minimal media

We used Carbon-D-Glucose but other minimal media will work as well. For **network-based** (targeted or iterative) gap fill, use the following to fill gaps to Carbon-D-Glucose (do not use iterative gapfill again on minimal media even if you did it on complete media):

```
$ fba-gapfill $INPUT_MODEL_NAME --modelout $MINIMAL_GAPFILL_MODEL_NAME \
   --transpen 25 --singletranspen 25 --biomasstranspen 25 --directionpen 12 \
   --intsol  --media Carbon-D-Glucose --mediaws KBaseMedia
```

For **likelihood-based** or **likelihood-based iterative** use the following:

```
$ fba-gapfill $INPUT_MODEL_NAME --modelout $MINIMAL_GAPFILL_MODEL_NAME \
   --transpen 25 --singletranspen 25 --biomasstranspen 25 --directionpen 12 \
   --intsol  --probrxn $RXNPROBS_OBJECT_NAME --media Carbon-D-Glucose \
   --mediaws KbaseMedia
```

Depending on whether you have are doing targeted or iterative gap fill workflows, `$INPUT_MODEL_NAME` should be `$GAPFILLED_MODEL_NAME` or `$FILTERED_MODEL_NAME`, respectively.

11. Check for growth on minimal media

```
$ fba-runfba $MINIMAL_GAPFILL_MODEL_NAME --fbaid $MINIMAL_FBA_OBJECT_NAME \
      --media Carbon-D-Glucose --mediaws KBaseMedia
```

Like before, you should get a non-zero objective. If it fails try rerunning gap filling with higher time limits.

12. Import phenotype data

Note - we already loaded the phenotype data cited in the manuscript in the KBasePhenotypeDatasets directory so if you want to use that data you can skip this step.

Compile your phenotype data into a tab-delimted table (see detailed description below). Then run:

```
$ fba-importpheno $GENOME_ID $YOUR_PHENOTYPE_FILE \
      --phenoid $PHENOTYPE_SET_ID
```

The function will create a PhenotypeSet object `$PHENOTYPE_SET_ID` in your workspace.

13. Do phenotype simulations

For biolog data make sure you specify to add transporters for growth conditions. The input model `$MODEL_NAME` should be the model that has been gap filled to grow on minimal media.

```
$ fba-simpheno $MINIMAL_GAPFILL_MODEL_NAME $PHENOTYPE_SET_ID \
       --phenows KBasePhenotypeDatasets \
       --phenosimid $OUTPUT_SIMULTATIONS --alltransporters
```

For knockout data just make sure the model grows on the media in which knockouts were done (if not, do a gap filling to that media - step 9-10, but replace Carbon-D-Glucose with your media). Then run:

```
  $ fba-simpheno $MINIMAL_GAPFILL_MODEL_NAME $PHENOTYPE_SET_ID \
      --phenows KBasePhenotypeDatasets  \
        --phenosimid $OUTPUT_SIMULATIONS
```

These commands will create a PhenotypeSimulationSet object called `$OUTPUT_SIMULATIONS` in your workspace, storing all the simulation results.

A very brief introduction to the KBase

The DOE KnowledgeBase (KBase) is, to me, three things:

a. A database with consistent identifiers, cross-linked to show connections between genomes, genes, functions, and (perhaps most importantly) biochemistry. We won't talk about this much in the demo but it does make it much easier to import external data and have it generate the right links...

b. A set of tools (particularly, modeling tools) that can be used to analyze that data, along with a set of consistent APIs that can be used to develop your own tools and a web front-end that can run them from anywhere

c. A provider of computational resources such as processing and storage

In the KBase your data will be saved on KBase machines (which are backed up regularly) and processed on their servers. All of the below commands are run in a web environment hosted by the KBase team.

A. Sign up for a KBase account.

To use the KBase you will need to sign up for an account through Globus Online. Do so through their website:

https://gologin.kbase.us/SignUp

B. IRIS

IRIS is a web-based command line tool, located here:

http://iris.kbase.us

I'll show you some commands you can use to build models in IRIS - you just type them in and they run on some computer in KBase-land. No installation necessary.

To begin using IRIS, you need to log in using your Globus Online account.

After you log in, you can upload your data, run commands with it, and export the data back to your computer. If you log in on another computer, your data will still be there. A nice tutorial on the interface for IRIS is available here so I won't repeat the words from it. I recommend you read it to become familiar with how to upload and download files, run commands etc.

http://kbase.science.energy.gov/developer-zone/tutorials/iris/introduction-to-the-kbase-iris-interface/

C. Workspaces and objects (KBase data storage)

After you upload your data you will need to run a script to convert it into a KBase object. For example, there is a command to take a FASTA file and turn it into a **genome object**, to take a SBML file and turn it into a **model object**, etc. There are also interfaces to automatically download data from various databases (such as the SEED) and save them as KBase objects.

All KBase objects are given a specific type and saved in a **workspace** (think of it like a folder) on the KBase computers. Most KBase commands take an object of one type and convert them into another object of the same type or an object of a different type (for example, there is a command to convert a genome object into a model object).

In order to move forward you will need to create a workspace to store your files. Do that with the **ws-createws** command. Type the following into IRIS to create a workspace, replacing $WORKSPACE_NAME with the name of the workspace you want to create (which by default no one but you can read. You can always change permissions later):

```
$ ws-createws $WORKSPACE_NAME
```

Then change to that workspace using **ws-workspace**

```
$ ws-workspace $WORKSPACE_NAME
```

You are now in your workspace `$WORKSPACE_NAME`. You can list the objects in that workspace at any time by typing **ws-listobj**

```
$ ws-listobj
```

To list objects in a specific workspace (not the one you're currently in) use -w. For example use this command to list all the media in the KBaseMedia workspace.

```
$ ws-listobj --workspace KBaseMedia
```

The functions used in this workflow can take both an ID and a workspace for any of the objects that they require as inputs. They usually will use your current workspace by default if you don't specify it; this is omitted in the example commands below, in which we assume you are currently in the workspace that you wish to save objects into.

D. KBase services

A **service** is basically a collection of related commands (often operating on just a few different types of objects). There are lots of services in the KBase for genome annotation, clustering and orthology analysis, analysis of transcription data, etc. I haven't used most of them myself. To do likelihood-based gap filling, you will need to use commands in three of them:

- The **workspace service**, which is used to save, move, and retrieve data from workspaces (think of them as personal folders on KBase machines that store objects with specific formats). You'll need to use this with practically every other service.
- The **modeling service,** which has functions to import and annotate genomes, import existing models or generate new ones from an annotated genome, run gap filling, compare models, etc. It uses the ModelSEED as a back-end
- The **probabilistic annotation service**, which calculates annotation and reaction likelihoods for use in gap filling.

In IRIS you can see the list of services in the tab on the left (**Figure B.2**).

Detailed workflow tutorial

The following is a detailed description of the relevant commands to run our workflow in IRIS. Anytime you see `$STUFF`, replace it with the actual name of your input and outputs.

1. Build genome object

In order to work with your genome in the KBase you will need to import it into a workspace. Genomes, like everything else in workspaces, are saved as **typed objects** which have formats that all of the KBase functions understand and store all necessary information.

Fortunately, doing this conversion is rather simple, especially for genomes in the SEED, the KBase central store, or RAST. Note that for model building to work properly you will need to be using the same annotation conventions as are used in the SEED\RAST\KBase central store so it is highly recommended that you take your genomes from one of those sources. For example, pull a genome from the SEED by its SEED ID using:

```
$ fba-loadgenome --seed $SEED_ID
```

This will create a Genome object called `$SEED_ID` in your workspace (this is hereafter referred to as `$GENOME_OBJECT_NAME` since other sources are possible). Take a look at the other options for fba-loadgenome if your source is different.

2. Build draft model

After you load your genome into a workspace, you can use the ModelSEED algorithm (**Ref:** see Henry *et al.* 2010) to build a draft model using:

```
$ fba-buildfbamodel $GENOME_OBJECT_NAME --model $DRAFT_MODEL_NAME
```

This will create a Model object called `$DRAFT_MODEL_NAME` in your workspace based on the annotations in the genome object.

The draft model is *not yet gap filled* so it will not grow due to missing or incorrect annotations. However, a biomass equation will automatically be created and after gap filling is done (see later steps) it should be able to grow provided the solving did not fail.

3. Build annotation likelihoods

The **pa-annotate** command (in the Probabilistic Annotation service on IRIS) is responsible for computing the likelihoods of annotations for each gene in a genome as described in the manuscript. It takes a genome object as an input and produces a ProbAnno object:

```
$ pa-annotate $GENOME_OBJECT_NAME $PROBANNO_OBJECT_NAME
```

Running this command will result in queueing a probanno job on the KBase servers. The command takes about 4 hours to run on average, and therefore the job is placed in a queue and runs when the queue is cleared. You can always check on your job using ws-checkjob:

```
$ pa-checkjob $JOB_ID
```

When the job is complete, a ProbAnno object called `$PROBANNO_OBJECT_NAME` will be created in your workspace. This object will contain multiple possible annotations for each gene, each attached to a likelihood.

4. Building reaction likelihoods

The **pa-calculate** function takes a ProbAnno object as an input and calculates the likelihood of each reaction based on the procedure outlined in the manuscript. It is run as follows:

```
$ pa-calculate $PROBANNO_OBJECT_NAME $RXNPROBS_OBJECT_NAME
```

The result is a RxnProbs object called `$RXNPROBS_OBJECT_NAME`, which is saved in your workspace (unlike pa-annotate, pa-calculate runs quickly). The RxnProbs object stores computed reaction likelihoods along with the predicted gene-protein-reaction (GPR) relationships for each reaction and some data on the complexes used to build them.

You can use either a RxnProbs object or a ProbAnno object as an input to gap filling. These are the inputs to likelihood-based gap filling as described in the manuscript. However, we recommend using the RxnProbs object so that you can use it as input to other functions to help interpret gap filling results.

5. Running Gap filling to Complete Media

Draft models build using **fba-buildfbamodel** will not be able to simulate growth in general, due to the existence of annotation gaps. It is necessary to fill gaps in the model to achieve growth. Gap filling is done using the **fba-gapfill** command, which has many options (some of which were not used in this manuscript). The total commands used were as follows, which are described in detail below

Network-based gap fill:

```
$ fba-gapfill $DRAFT_MODEL_NAME --modelout $GAPFILLED_MODEL_NAME \
   --transpen 25 --singletranspen 25 --biomasstranspen 25 --directionpen 12 \
   --intsol
```

Likelihood-based gap fill:

```
$ fba-gapfill $DRAFT_MODEL_NAME --modelout $GAPFILLED_MODEL_NAME \
   --transpen 25 --singletranspen 25 --biomasstranspen 25 --directionpen 12 \
   --intsol  --probrxn $RXNPROBS_OBJECT_NAME
```

The following options to **fba-gapfill** were *always* used in simulations done in this manuscript:

```
--transpen 25 --singletranspen 25 --biomasstranspen 25 --directionpen 12 \
--intsol
```

--transpen, --singletranspen, --biomasstranspen, and **--directionpen** are penalties for adding transporters for various things instead of intracellular reactions (I like to set these to be quite high but you can feel free to play with them) and the base penalty for changing reversibility if a reaction is not thermodynamically favorable in the reverse direction.

--intsol means "integrate solution"; gap fill will NOT automatically integrate the solution into your model unless you select this option. If you want to look at the solution and decide whether you agree before adding the reactions to your model, you can do so by omitting this option. We do not talk in this tutorial about how to integrate solutions after-the-fact but you can look at the fba-integratesolution command for some details.

When you run **fba-gapfill,** it will do some pre-processing and then will queue the job and give you an ID. Gapfill takes quite a while to run so go do something else for a day, come back and it should be done (if you are doing iterative gapfill, give it two or three days). You can always check the status of your job by using **ws-checkjob**.

If the solver fails and gives you a nonsense solution (e.g. 3000 reactions), try increasing the time per solution and total time using **--timepersol** and **--timelimit** (the default time limit for solving is 3600 seconds per solution).

Likelihood-based gapfilling

To do likelihood-based gapfilling as described in the manuscript, you need to either provide a **probabilistic annotation** object or a **probabilistic reaction** object (which contains the reaction likelihoods calculated from the probabilistic annotation object), which are calculated as described in **steps 3-4** of this tutorial.

The ProbAnno object can be incorporated directly into gapfilling (without calculating reaction likelihoods) with the **--probanno** flag to **fba-gapfill.**

However, we recommend using the **pa-calculate** function to compute them yourself and get a RxnProbs object so that you can take a look at the reaction likelihoods that are generated. The RxnProbs object can be used as input to gapfilling by providing the **--probrxn** flag to **fba-gapfill**.

6. Checking growth on complete media

You can run FBA within the KBase tool (along with many other simple simulations such as FVA, doing simulation to try to figure out what biomass components can't be produced in a model, etc…) using the **fba-runfba** command. I recommend doing this to make sure the gapfilling was successful in producing a growing model. The **fba-runfba** command will create an FBA object which stores the FBA results including the fluxes of every reaction (and if you ask for it, FVA results, results of running knockouts, etc. - I won't cover all of that stuff but take a look at the help text for an idea of what it can do).

I suggest saving the FBA object to a place where you know where to find it \ how it was run using the **--fba** flag:

```
$ fba-runfba --fba $FBA_OBJECT_NAME $GAPFILLED_MODEL_NAME
```

The default is to run FBA on complete media so this is all you need to do to test if growth is possible. If the growth rate is 0, the gapfill failed. Depending on the reasons for failure you might be able to get a good solution by re-running gapfill with a higher time limit. Try increasing the time per solution and total time using **--timepersol** and **--timelimit** (the default time limit for solving is 3600 seconds per solution).

7. Iterative gapfilling

Iterative gapfilling, as described in the manuscript, is the gapfilling of ALL of the dead-ends in a model, not just those that have to be filled to achieve growth. It is called iterative because it fills them one a time according to a pre-defined priority until they are all filled (or as many as can be filled given what is in the database).

Here are some recommendations on how to use it for maximum effectiveness.

- You only need to ask for one solution (do not use **--**numsol. It will be ignored anyway)
- You should only do iterative gapfilling on **complete media** (which is the default - don't use the -m/--media or --mediaws flags).
- You should only do iterative gap fill **after** doing a normal gap filling (and integrating the solution and checking to make sure the model achieves growth on complete media). This greatly reduces the computation time necessary because gap filling to biomass makes many other gap fills unnecessary.
- Be aware that iterative gapfilling takes a long time because you're filling so many gaps. This is why we only use it when gapfilling to complete media and not when gapfilling to minimal media (**step 10**)
- Use **--intsol** - since you're only getting one solution you might as well just integrate it automatically. In fact, for iterative gapfill this is set whether you set it or not, but set it anyway so you don't forget.

To do an iterative gapfilling use the **--iterativegf** flag in the **fba-gapfill** function.

Likelihood-based iterative gap filling

Likelihood-based iterative gap filling can be done by providing both **--probrxn** (or --probanno) and **--iterativegf** to the **fba-gapfill** function. Otherwise, use the same guidelines as for network-based iterative gap filling.

The overall commands we used were as follows:

Iterative gap fill:

```
$ fba-gapfill $GAPFILLED_MODEL_NAME --modelout $ITER_GAPFILLED_MODEL_NAME \
   --transpen 25 --singletranspen 25 --biomasstranspen 25 --directionpen 12 \
   --intsol --iterativegf
```

Likelihood-based iterative gap fill:

```
$ fba-gapfill $GAPFILLED_MODEL_NAME --modelout $ITER_GAPFILLED_MODEL_NAME \
```

```
    --transpen 25 --singletranspen 25 --biomasstranspen 25 --directionpen 12 \
    --intsol  --iterativegf --probrxn $RXNPROBS_OBJECT_NAME
```

8. Reaction sensitivity analysis

Reaction sensitivity analysis as described in the manuscript is a way to prune unneeded gap filling solutions by testing the effects of removing each one on the activity of other reactions in the network and on the ability of the cell to predict nonzero biomass production rates. If deleting a gap filled reaction is nonlethal and does not inactivate any reactions in the model, it is flagged as unnecessary. Reaction sensitivity analysis is done using the **fba-reactionsensitivity** function in IRIS. This function can be run in two different ways (only one of which is covered above, because it's the one we used when doing our simulations):

1. The user can specify (in the order that he or she wants to test them) a list of reactions in the model for which the sensitivity should be tested. To do this use the **--rxnstotest** flag. For example, if rxn00001 and rxn00002 are in your model `$MODEL_ID`, you can test the effects of deleting them by running this command:

```
$ fba-reactionsensitivity $ITER_GAPFILLED_MODEL_NAME  --rxnstotest "rxn00001;rxn00002"
```

   You can also specify a direction (e.g. "+rxn00001") to test.

2. The user can specify a **GapFill solution ID**. If the user specifies this, then the following happens:
   1. A list is generated of all of the reaction changes (with the direction) added by that specific gap filling run.
   2. For **network-based gap fill** (no RxnProbs object specified), the order of reactions to test is the *reverse* of the order in which they were added by the algorithm, with the idea that later gapfills are to lower-priority parts of the network so we want to try to remove them first.
   3. For **likelihood-based gap fill**, specify a RxnProbs object with **--rxnprobs** . A further stable sort will be done based on the reaction likelihoods and the lowest-likelihood reactions will be tested for removal first. Ties are broken by using the same ordering as for non-likelihood-based gap filling.

The process of getting a GapFill solution ID is as follows. Given a model that has an integrated iterative gapfill (using --intsol), run:

```
  $ fba-getmodels –pretty $gapfilled_model_name $WORKSPACE_ID \
        > $gapfilled_model_filename
```

Then search for "integrated_gapfillings" in the output file .

```
 "integrated_gapfillings" : [
        [
           "kb|g.166872.fbamdl1.gf.3",
           "652/14/1",
           "Complete",
           "262/34/1",
           0,
           []
        ]
     ],
```

You want the first element of the array (`kb|g.166872.fbamdl1.gf.3` in this example). Add "gfsol.0" to that string to get the GapFill solution ID (note - the 0 means you want to integrate solution number 0, i.e. the first solution):

```
kb|g.166872.fbamdl1.gf.3.gfsol.0
```

Optionally, the reaction sensitivity analysis will delete each reaction that is unnecessary before proceeding to the next one (in this case, the reactions will be flagged for deletion in the Reaction Sensitivity object and the sensitivity results of every reaction after it will depend on the fact that that reaction was deleted). To get this behavior specify **--deleterxns** on the command line. We used this flag in the manuscript workflow.

Putting all of this together, the final commands we used as part of the manuscript workflow were:

Network-based gap fill

```
$ fba-reactionsensitivity $ITER_GAPFILLED_MODEL_NAME --rxnsensid $RXN_SENSITIVITY_NAME
      --gapfill $GAPFILL_SOLUTION_ID --deleterxns
```

For **likelihood-based gap fill**:

```
$ fba-reactionsensitivity $ITER_GAPFILLED_MODEL_NAME --rxnsensid $RXN_SENSITIVITY_NAME
       --gapfill $GAPFILL_SOLUTION_ID --deleterxns --rxnprobs $RXNPROBS_OBJECT_NAME
```

9. Deleting non-contributing reactions

After you run a reaction sensitivity analysis with --deleterxns, you can run **fba-delete_noncontributing_reactions** to actually delete the unnecessary reactions from the model. The RxnSensitivity object is automatically linked to a specific model so you will not need to specify the input model in this function. However, you can (and probably should) specify a different ID to use for the model with reactions deleted. Do so with the **--newmodel** flag.

```
$ fba-delete_noncontributing_reactions $RXN_SENSITIVITY_NAME \
      --newmodel $FILTERED_MODEL_NAME
```

10. Gap filling to minimal media

We used the same commands as outlined in **step 5** (gap filling to complete media) except for two things:

A. By default, the gap fill algorithm only tries to achieve growth on "complete" media. You can specify other media using **-m** - you will also probably have to specify a media workspace. We recommend (and have implemented in this workflow) running gap filling on complete media first before trying to achieve growth on any specific media. Doing so greatly simplifies the gap filling problem and also highlights those reactions that would be essential regardless of the chosen media condition (unless new transporters are added).
B. We recommend you **do not** perform iterative gap filling in this step (do not use the --iterativegf flag on minimal media).

You can define your own media conditions with which to perform gap filling by creating a Media object in your workspace using **fba-addmedia**. However, the KBase also has about 700 default media conditions saved in the workspace **KBaseMedia**. To fill gaps in the model and achieve growth on a specific media condition, *fill gaps on complete media first* (since that solution is a basis for all other media conditions) and then call **fba-gapfill** again and use these flags:

```
-m $MEDIA_NAME --mediaws KBaseMedia
```

11. Checking growth on minimal media

To run FBA to a **specific media** (with a Media object in a workspace) use the **-m** flag (and **--mediaws** if the media is not in your current workspace) to the **fba-runfba** command. The default media for KBase are found in the KBaseMedia workspace so use the following to run FBA on one of those media conditions (you can also create your own media and put it in your workspace, in which case use that workspace instead with the—mediaws argument):

```
$ fba-runfba --fba $FBA_ID --media $MEDIA_NAME --mediaws KbaseMedia \
        $MINIMAL_GAPFILLED_MODEL_NAME
```

If you imported your media condition using **fba-addmedia** you can specify that media (and your workspace name) instead.

12. Importing phenotype data

Note that we have already done this for the phenotype data used in the manuscript and saved them in the KBasePhenotypeDatasets workspace. If you only want to use those, you can skip this step. However, you will need to do this to do simulations of your own phenotype data.

The phenotype data is imported from a tab-delimited table with the following headers (the headers must be exactly the same as this, but can be in any order):

4. **media** - Name of the Media object containing the media for which the phenotype was measured
5. **mediaws** - Workspace in which the Media object above is located (often KBaseMedia, or your own workspace)
6. **growth** - 1 for Grows, 0 for Does Not Grow
7. **geneko** - OPTIONAL. If specified, it is a semicolon-delimited list of gene knockouts. The gene IDs must match the IDs from your original genome source (e.g. SEED IDs in form fig|#.#.peg.# where each # is some number).
8. **addtlcpd** - OPTIONAL. If specified, it is a semicolon-delimited list of compounds added to the specified Media condition before measuring the phenotype (use it for example to record the effects of making small changes to media and testing effects on growth).

Example: You did knockouts of "fig|83333.1.peg.1", "*fig|83333.1.peg.2*" and "*fig|83333.1.peg.3*" separately and tried to grow your organism on Carbon-D-Glucose. The Δ*fig|83333.1.peg.1* strain grew but the Δ*fig|83333.1.peg.2* and Δ*fig|83333.1.peg.1* strains did not. The input file would then look like this: (note that the separator between each field is a tab, including in the header).

media mediaws growth geneko

Carbon-D-Glucose	KBaseMedia	1	fig|83333.1.peg.1
Carbon-D-Glucose	KBaseMedia	0	fig|83333.1.peg.2
Carbon-D-Glucose	KbaseMedia	0	fig|83333.1.peg.3

Example 2: You tried a triple knockout of these three genes and it did not grow. You can add a line like this to the above file to account for this:

Carbon-D-Glucose	KbaseMedia	0	fig|83333.1.peg.1;fig|83333.1.peg.2;fig|83333.1.peg.3

Note that it is possible to import other IDs such as locus tags into a genome file and then use them in the phenotype table. Doing so is outside the scope of this tutorial but see **fba-importtranslation** for details.

Once you have set up this table, import it into IRIS using its file import capability and then run:

```
$ fba-importpheno $GENOME_ID $PHENOTYPE_FILE --phenoid $PHENOTYPE_SET_ID
```

13. Phenotype simulations

Run phenotype simulations using the **fba-simpheno** command. In order to run this you will need a phenotype set. Several phenotype sets for the organisms we discussed in the manuscript are available in the KBasePhenotypeDatasets workspace. Otherwise you will need to import your phenotype data as a PhenotypeSet object (**step 12**) first.

We recommend that for knockout simulations you first try to run FBA on the media in which the knockouts were performed (**step 11**). If you get a 0 growth rate, you should run gap filling to that media so that you don't get all negative growth predictions. If you do this, don't use iterative gap filling, but use either likelihood or network-based gap fill algorithms depending on what you have been using to get this far. Once you have a growing model just use **fba-simpheno** to simulate the phenotype.

```
$ fba-simpheno $MODEL_NAME --phenows KBasePhenotypeDatasets $PHENOTYPE_SET_ID \
        --phenosimid $OUTPUT_SIMULATIONS
```

--phenosimid should be specified if you want to give the resulting phenotype simulation set a specific name (recommended). You can then take a look at that object and identify the correct and incorrect growth predictions relative to the available phenotype data.

For biolog simulations you should perform gap filling to achieve growth on a minimal media (such as Carbon-D-Glucose) before running simulations. You should also specify **--alltransporters** in the **fba-simpheno** command so that transporters are automatically added for all compounds in all tested growth conditions before simulation is done. This is necessary because transporters are the hardest to get right, and it is quite likely that the model will be missing transporters that, if present, would allow the cell to grow with the rest of what's in the network. The final command to use becomes:

```
$ fba-simpheno $MODEL_NAME --phenows KBasePhenotypeDatasets $PHENOTYPE_SET_ID \
-- phenosimid $OUTPUT_SIMULATIONS  --alltransporters
```

Figures and tables

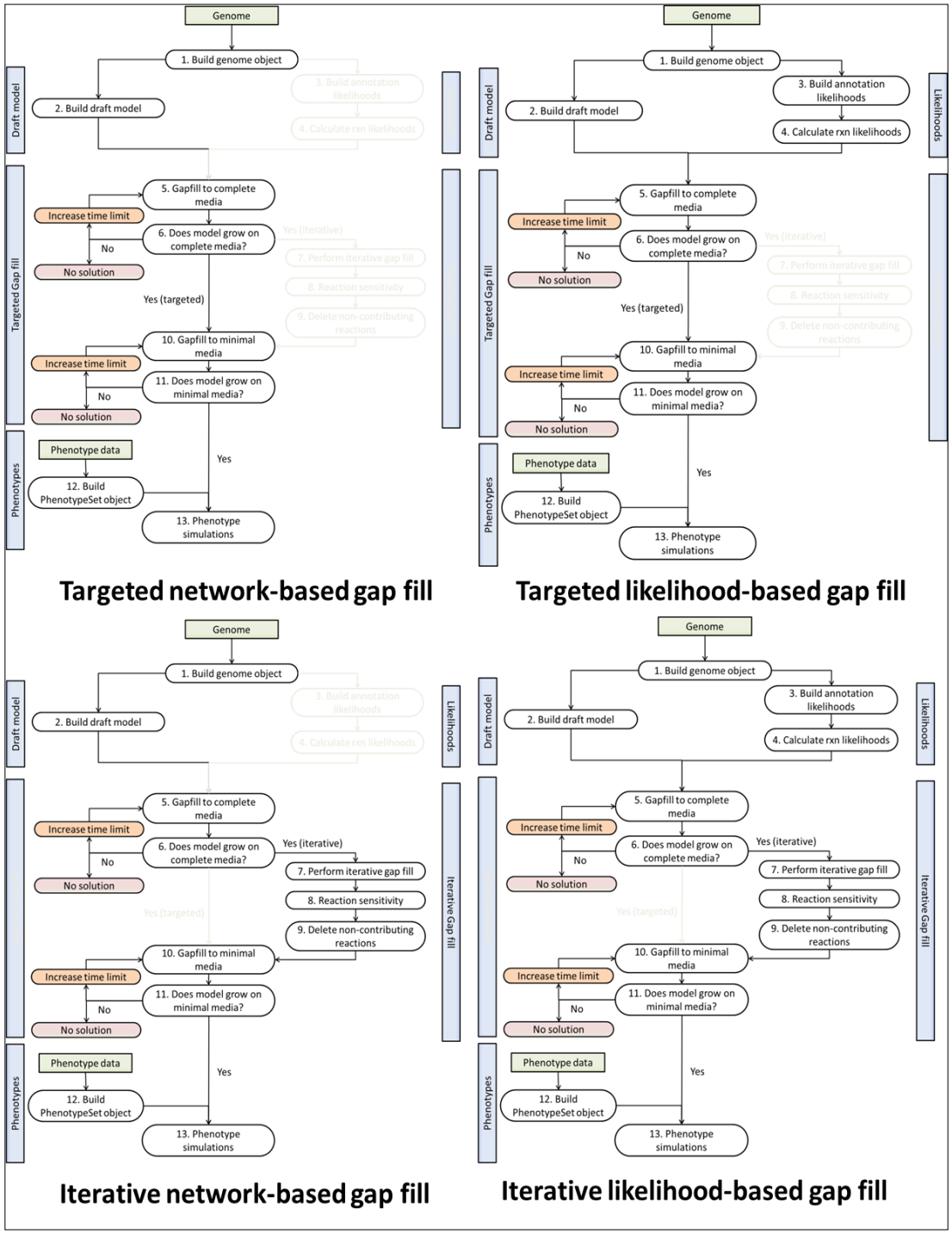

Figure B.1. Gap filling workflows implemented in the KnowledgeBase. Gray boxes indicate steps to skip in a particular workflow.

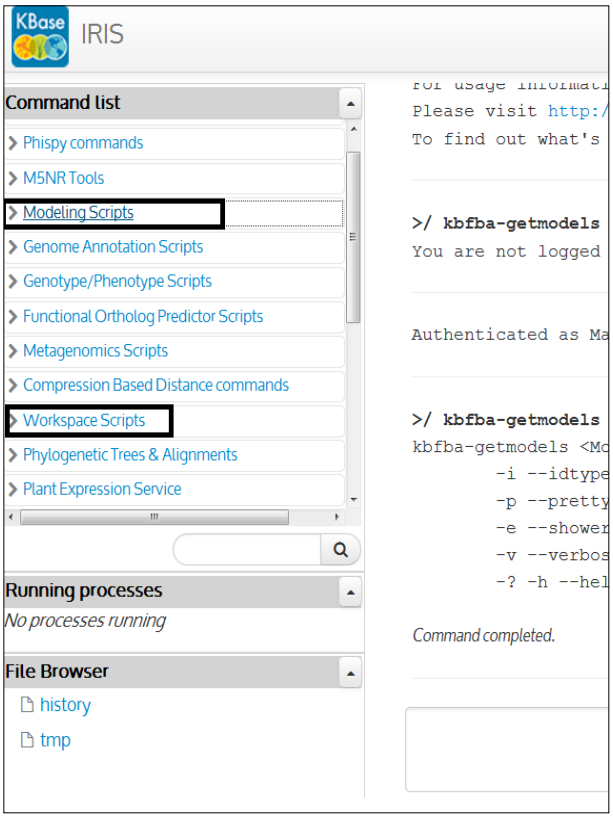

Figure B.2. Partial screenshot for the IRIS web-based command line interface.

Appendix C: Description of the KBASE Client API for likelihood-based gap filling workflows

This tutorial describes how to build metabolic models using the four workflows that we have described in the manuscript. There are actually two ways to run this workflow:

Using the **Client API**, or

Using the **Web-based command line interface**

This tutorial describes a script that uses the client API to perform the workflows. Please see the other tutorial file (Supplemental file 2) for a detailed description of the workflows themselves.

Obtaining a Globus Online account

You will need to create a Globus Online account and a workspace (see Supplemental file 2 for details) before running the workflow script. Do not use the same password as used in other websites in case the password is echoed and logged somewhere, though we try to use getpass() to avoid that.

Obtaining the KBase client API

First you will need to have the following packages installed:

3. Python, version 2.6 or 2.7
    4. The following built-in packages are used by client libraries: urllib2, httplib, urlparse, random, base64, ConfigParser, json
    5. The following built-in packages are used by the workflow script: argparse, subprocess, traceback, sys, time, operator
6. Python packages (get using apt-get or pip or whatever you have to install it):
    7. httplib2

For example in Ubuntu do the following to get httplib2

$ sudo apt-get install python-httplib2

Second, download the "ClientWorkflow.zip" provided with this manuscript.

Finally, add the extracted directory (the one that contains the "biokbase" directory) to your PYTHONPATH.

Running the workflow script

The workflow script has the following syntax:

```
usage: Workflow [-h] [--password PASSWORD] [--genome_source SOURCE]
                [-w WORKSPACE] [--force] [--network] [--prob] [--iterative]
                [--iterativeprob] [--num-solutions NUMSOLUTIONS]
                [--ws-url WSURL] [--fba-url FBAURL] [--pa-url PAURL]
                [--knockout KNOCKOUT] [--knockoutws KNOCKOUTWS]
                [--biologdata BIOLOG] [--biologdataws BIOLOGWS]
                [--positiveTransportersOnly] [--maxtime MAXTIME]
                genome username
```

The required arguments are a genome ID (by default coming from the PubSEED, http://pubseed.theseed.org) and a username. The script asks for a password interactively if it is not provided on the command line.

Alternative genome sources

You can specify that you want your genome to come from the KBase central store instead of the PubSEED by specifying this using --genome_source .

The four workflows

You can specify which workflow to run using the following flags:

C. --network: Run the targeted network-based gap fill workflow (activate biomass only)
D. --prob : Run the targeted likelihood-based gap fill workflow (activate biomass only)
E. --iterative: Run the iterative network-based gap fill workflow
F. --iterativeprob: Run the iterative likelihood-based gap fill workflow

You can also specify that you want to run the biolog or knockout lethality phenotype predictions after gap filling using:

- --biologdata: For biolog data
- --knockout: For knockout data

For biolog data you have the option of fitting to it by adding transporters only for growth-positive substrates using --positiveTransportersOnly. By default, transporters are added for ALL media in the biolog data before running simulations.

If a gap fill job fails due to lack of time you can increase the time limit using --maxtime. The argument is provided in units of seconds.

Note: The servers are prone to random failures (504s etc). If you restart the workflow script with the same arguments as were used before the error, it will start back up where it left off. It is recommended to check the results of the last step first to see if an object is present and if results are in it - you might

need to delete the object (using ws-delete) before starting the workflow again. Also check to see if your job is still running - the workflow might have just failed while checking to see if your job was done. If this happens, wait for the job to finish and then restart the workflow using the same arguments.

Specifying where your data is

All data used in Workflow.py is extracted from and saved in workspaces. By default the Workflow.py looks for everything in the last workspace you were in when logged in. Alternatives to the default can be specified as follows:

C. -w: This specifies where all the results of Workflow.py itself will be saved.
D. --knockoutws: This specifies where knockout data is located, if you are running that part of the workflow.
E. --biologdataws: This specifies where biolog data is located, if you are running that part of the workflow.

In order to run the Workflow, you must have write permissions in the main workspace (-w) and read permission in the knockout/biolog workspaces. I suggest using IRIS (see other tutorial) to create the workspace and manage permissions.

Specifying what servers to use

Every server is specified by a URL. If the URL ever changes you will need to specify the new URL using the URL arguments (or go in and change the default):

--ws-url : Workspace service URL
--fba-url : FBA Modeling service URL
--pa-url: Probabilistic Annotation service URL

Rerunning from scratch

If you want to force the workflow to rebuild every object instead of checking to see if they exist and restarting the workflow from where it left off, use --force.